

Aus dem Walther-Straub-Institut für Pharmakologie und Toxikologie  
Institut der Ludwig-Maximilians-Universität München  
Vorstand: Prof. Dr. med. Thomas Gudermann



***Targeting mitochondrial calcium uptake for the treatment of  
cardiac diseases***

Dissertation  
zum Erwerb des Doktorgrades der Naturwissenschaften  
an der Medizinischen Fakultät der  
Ludwig-Maximilians-Universität zu München

vorgelegt von  
Paulina Sander  
aus  
Stuttgart

2022

---

Mit Genehmigung der Medizinischen Fakultät  
der Universität München

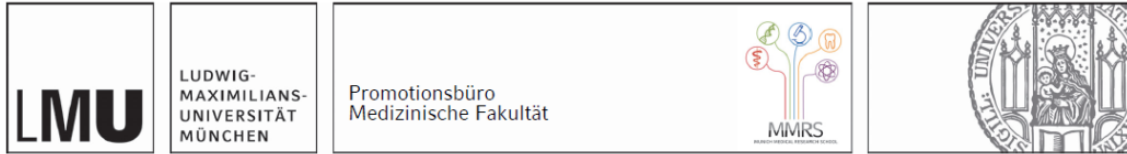
Betreuer: PD Johann Schredelseker PhD

Zweitgutachter: Prof. Dr. Alexander Faußner

Dekan: Prof. Dr. med. Thomas Gudermann

Tag der mündlichen Prüfung: 29.09.2022

## Affidavit



### Eidesstattliche Versicherung

Sander, Paulina

\_\_\_\_\_  
Name, Vorname

Ich erkläre hiermit an Eides statt, dass ich die vorliegende Dissertation mit dem Titel:

Targeting mitochondrial calcium uptake for the treatment of cardiac diseases

selbständig verfasst, mich außer der angegebenen keiner weiteren Hilfsmittel bedient und alle Erkenntnisse, die aus dem Schrifttum ganz oder annähernd übernommen sind, als solche kenntlich gemacht und nach ihrer Herkunft unter Bezeichnung der Fundstelle einzeln nachgewiesen habe.

Ich erkläre des Weiteren, dass die hier vorgelegte Dissertation nicht in gleicher oder in ähnlicher Form bei einer anderen Stelle zur Erlangung eines akademischen Grades eingereicht wurde.

München, 22.02.2022

Paulina Sander

\_\_\_\_\_  
Ort, Datum  
Doktorand

\_\_\_\_\_  
Unterschrift Doktorandin bzw.

# Contents

<b>Affidavit</b> .....	<b>3</b>
<b>Contents</b> .....	<b>4</b>
<b>Abbreviations</b> .....	<b>5</b>
<b>List of Publications</b> .....	<b>6</b>
<b>1 Abstract</b> .....	<b>7</b>
<b>2 Zusammenfassung (Deutsch)</b> .....	<b>8</b>
<b>3 Introduction</b> .....	<b>10</b>
3.1 Alteration of cardiomyocyte Ca <sup>2+</sup> handling in cardiac diseases .....	10
3.1.1 Arrhythmia.....	11
3.1.2 Heart failure .....	12
3.2 Current and experimental therapeutic approaches in cardiac arrhythmia and heart failure .....	12
3.2.1 Potential target structures for novel drug candidates.....	13
3.2.2 Cardiac mitochondrial Ca <sup>2+</sup> as a target in cardiac diseases .....	14
3.2.2.1 Mitochondrial Ca <sup>2+</sup> uptake pathway .....	15
3.2.2.2 Mitochondrial Ca <sup>2+</sup> uptake enhancers .....	16
<b>4 Publications: Short summary &amp; personal contribution</b> .....	<b>19</b>
4.1 Publication I: Novel mitochondrial Ca <sup>2+</sup> uptake enhancers .....	19
4.2 Publication II: Mitochondrial Ca <sup>2+</sup> uptake in heart failure .....	20
4.3 Supplementary review: Mitochondrial Ca <sup>2+</sup> uptake across the outer mitochondrial membrane.....	21
<b>5 References</b> .....	<b>23</b>
<b>6 Publication I</b> .....	<b>30</b>
<b>7 Publication II</b> .....	<b>45</b>
<b>8 Supplementary: Publication III</b> .....	<b>60</b>
<b>Acknowledgement</b> .....	<b>78</b>

## Abbreviations

Ca <sup>2+</sup>	calcium ions
CICR	calcium induced calcium release
CPVT	catecholaminergic polymorphic ventricular tachycardia
CVDs	cardiovascular diseases
ECC	excitation contraction coupling
HF	heart failure
IMM	inner mitochondrial membrane
LCC	L-type Ca <sup>2+</sup> channels
MCU	mitochondrial calcium uniporter
MCUC	mitochondrial calcium uniporter complex
MCUP	mitochondrial Ca <sup>2+</sup> uptake pathway
MiCUps	mitochondrial Ca <sup>2+</sup> uptake enhancers
NCX	sodium calcium exchanger
OMM	outer mitochondrial membrane
RyR	ryanodine receptor
SERCA	sarcoplasmic/endoplasmic reticulum calcium ATPase
SR	sarcoplasmic reticulum
VDAC	voltage dependent anion channel

## List of Publications

The present thesis is a cumulative thesis. For this purpose, the following publications were included:

- **Approved drugs ezetimibe and disulfiram enhance mitochondrial  $\text{Ca}^{2+}$  uptake and suppress cardiac arrhythmogenesis**

**Paulina Sander**, Michael Feng, Maria K. Schweitzer, Fabiola Wilting, Sophie M. Guten-thaler, Daniela M. Arduino, Sandra Fischbach, Lisa Dreizehnter, Alessandra Moretti, Thomas Gudermann, Fabiana Perocchi, Johann Schredelseker

British Journal of Pharmacology, 2021, 178(22):4518-4532

- **Cardiac-specific deletion of voltage dependent anion channel 2 leads to di-lated cardiomyopathy by altering calcium homeostasis**

Thirupura S Shankar, Dinesh K.A. Ramadurai, Kira Steinhorst, Salah Sommakia, Rachit Badolia, Aspasia Thodou Krokidi, Dallen Calder, Sutip Navankasattusas, **Paulina Sander**, Oh Sung Kwon, Aishwarya Aravamudhan, Jing Ling, Andreas Dendorfer, Changmin Xie, Ohyun Kwon, Emily H. Y. Cheng, Kevin J. Whitehead, Thomas Gudermann, Russel S. Richardson, Frank B. Sachse, Johann Schredelseker, Kenneth W. Spitzer, Dipayan Chaudhuri, Stavros G. Drakos

Nature Communications, 2021, 12(1):4583

As an additional component of my scientific work and to put the above publications into the larger scientific context, the following review is included as a supplementary contribution:

- **A Calcium Guard in the Outer Membrane: Is VDAC a Regulated Gatekeeper of Mitochondrial Calcium Uptake?**

**Paulina Sander**, Thomas Gudermann & Johann Schredelseker

International Journal of Molecular Science, 2021, 19;22(2):946

# 1 Abstract

Cardiovascular diseases, such as arrhythmia and heart failure, are the leading cause of death worldwide and a dramatically increasing social and economic burden due to rapidly aging populations. Current treatment options are limited due to the lack of effective treatments and perilous side effects of available drugs. Thus, the development of new therapies for safer and more effective treatment remains a challenge.

Contraction of the heart is initiated by depolarization of the sinus node, followed by propagation of an excitation wave along the heart muscle. Calcium ions ( $\text{Ca}^{2+}$ ) play a central role in cardiac activity by acting as intracellular messengers that convert electrical signals into mechanical activity. Rhythmic oscillations of intracellular  $\text{Ca}^{2+}$  during systole and diastole thus play an important role in the regulation of the heartbeat and abnormalities in this  $\text{Ca}^{2+}$  homeostasis often lead to rhythmic and contractile dysfunction of the heart. A number of intracellular structures maintain this meticulously regulated  $\text{Ca}^{2+}$  balance in cardiomyocytes and have recently gained increasing attention as potential targets for the treatment of cardiac diseases. One component whose impact on cardiac  $\text{Ca}^{2+}$  cycling has only started to be investigated so far are the mitochondria, which are located in close proximity to the sarcoplasmic reticulum, the internal  $\text{Ca}^{2+}$  storage, and are equipped with an efficient machinery to take up  $\text{Ca}^{2+}$ . Previous work in our laboratory has shown that activation of mitochondrial  $\text{Ca}^{2+}$  uptake can prevent arrhythmogenesis in cardiomyocytes and thus serves as a promising pharmacological target structure for cardiovascular disease. However, there is a lack of appropriate agonists for mitochondrial  $\text{Ca}^{2+}$  uptake that can be used for preclinical and clinical studies. Thus in the first part of my thesis (Sander et al. 2021) I characterized novel activators of mitochondrial  $\text{Ca}^{2+}$  uptake, which were identified from a screen of 727 compounds already used in human clinical trials for their potential to enhance mitochondrial  $\text{Ca}^{2+}$  uptake. I identified ezetimibe and disulfiram, two clinically approved drugs as new, highly potent agonists of mitochondrial  $\text{Ca}^{2+}$  uptake. Both effectively suppress arrhythmogenic signals in various  $\text{Ca}^{2+}$ -induced arrhythmia models and are thus promising candidates for future preclinical and clinical studies.

In addition to their antiarrhythmic activity, I analyzed a positive inotropic effect of enhanced mitochondrial  $\text{Ca}^{2+}$  uptake in the second part of this thesis (Shankar et al. 2021): while our collaboration partner demonstrated that cardiac specific knock-out of the voltage-dependent anion channel 2 (VDAC2), a large pore forming channel mediating  $\text{Ca}^{2+}$  flux over the outer mitochondrial membrane, induces heart failure, we show that oppositely pharmacological activation of VDAC2 by its agonist efsevin increases cardiac contractility in a murine heart failure model.

Our results contradict the common perception that VDAC creates holes in the outer mitochondrial membrane which are freely permeable to ions and show that mitochondrial  $\text{Ca}^{2+}$  uptake via VDAC2 plays a crucial role in cardiac function by influencing cellular  $\text{Ca}^{2+}$  signaling. Therefore, in a third part of my thesis I further reviewed this novel hypothesis in the context of current literature, which was published as a review article (Sander, Gudermann, Schredelseker, 2021). Taken together, this thesis provides several lines of evidence that mitochondrial  $\text{Ca}^{2+}$  uptake plays a pivotal role in cellular  $\text{Ca}^{2+}$  dynamics and excitation-contraction coupling and could serve as a promising future therapeutic target for cardiac diseases such as arrhythmia and heart failure.

## 2 Zusammenfassung (Deutsch)

Herz-Kreislauf-Erkrankungen wie Herzrhythmusstörungen und Herzversagen sind weltweit die häufigste Todesursache und stellen aufgrund der rasch alternden Bevölkerung eine dramatisch zunehmende soziale und wirtschaftliche Belastung dar. Die derzeitigen Behandlungsmöglichkeiten sind aufgrund des Mangels an wirksamen Therapien und der gefährlichen Nebenwirkungen der verfügbaren Medikamente begrenzt. Somit bleibt die Entwicklung neuer Therapien für eine sicherere und wirksamere Behandlung eine zentrale Herausforderung der kardiovaskulären Forschung.

Die Kontraktion des Herzens wird durch eine Depolarisation des Sinusknotens eingeleitet, gefolgt von der Ausbreitung einer Erregungswelle entlang des Herzmuskels. Kalziumionen ( $\text{Ca}^{2+}$ ) spielen eine zentrale Rolle bei der Herztätigkeit, da sie als intrazelluläre Botenstoffe elektrische Signale in mechanische Aktivität umwandeln. Rhythmische Oszillationen des intrazellulären Kalziums während der Systole und Diastole spielen daher eine wichtige Rolle bei der Regulierung des Herzschlags, und Anomalien dieser Kalziumhomöostase führen häufig zu rhythmischen und kontraktile Funktionsstörungen des Herzens. Gerade deshalb, stellen die molekularen Komponenten dieses Kalziumnetzwerks interessante Zielstrukturen für die Entwicklung neuartige Medikamente dar. Eine Komponente, deren Einfluss auf den kardialen Kalziumzyklus bisher kaum untersucht wurde, sind die Mitochondrien, die sich in unmittelbarer Nähe zum sarkoplasmatischen Retikulum, dem internen  $\text{Ca}^{2+}$ -Speicher, befinden und mit einer effizienten Maschinerie zur Aufnahme von  $\text{Ca}^{2+}$  ausgestattet sind. Frühere Arbeiten in unserem Labor haben gezeigt, dass die Aktivierung der mitochondrialen  $\text{Ca}^{2+}$ -Aufnahme die Entstehung von Herzrhythmusstörungen in Kardiomyozyten verhindern kann und somit eine vielversprechende pharmakologische Zielstruktur für Herz-Kreislauf-Erkrankungen darstellt. Es mangelt jedoch an geeigneten Agonisten für die mitochondriale  $\text{Ca}^{2+}$ -Aufnahme, die für präklinische und klinische Studien verwendet werden können. Daher habe ich im ersten Teil meiner Dissertation (Sander et al. 2021) neuartige Aktivatoren der mitochondrialen  $\text{Ca}^{2+}$ -Aufnahme charakterisiert, die aus einem Screening von 727 Verbindungen, die bereits in klinischen Studien am Menschen verwendet werden, auf ihr Potenzial zur Verbesserung der mitochondrialen  $\text{Ca}^{2+}$ -Aufnahme hin identifiziert wurden. Ich identifizierte Ezetimib und Disulfiram, zwei klinisch zugelassene Medikamente, als neue, hochwirksame Agonisten der mitochondrialen  $\text{Ca}^{2+}$ -Aufnahme. Beide unterdrücken wirksam arrhythmogene Signale in verschiedenen  $\text{Ca}^{2+}$ -induzierten Arrhythmie-Modellen und stellen daher vielversprechende Kandidaten für zukünftige präklinische und klinische Studien dar.

Zusätzlich zu ihrer antiarrhythmischen Aktivität habe ich im zweiten Teil dieser Arbeit (Shankar et al. 2021) einen positiv inotropen Effekt der verstärkten mitochondrialen  $\text{Ca}^{2+}$ -Aufnahme analysiert: Während unser Kooperationspartner gezeigt hat, dass ein kardialer Knock-out des Voltage-dependent anion channel 2 (VDAC2), einem Porenprotein, das die Kalziumaufnahme über die äußere mitochondriale Membran vermittelt, zu Herzversagen führt, zeigen wir, dass die pharmakologische Aktivierung von VDAC2 durch seinen Agonisten Efsevin die kardiale Kontraktilität in einem murinen Herzinsuffizienzmodell erhöht.

Unsere Ergebnisse widersprechen der gängigen Auffassung, dass VDAC lediglich unselektive Löcher in der äußeren mitochondrialen Membran schafft, die für Ionen frei durchlässig sind, und zeigen, dass die mitochondriale  $\text{Ca}^{2+}$ -Aufnahme über VDAC2 eine entscheidende Rolle für die Herzfunktion spielt, indem sie die zelluläre Kalzium-Signalgebung beeinflusst. In einem dritten Teil meiner Dissertation habe ich diese neuartige Hypothese im Zusammenhang mit der aktuellen Literatur überprüft, was als Übersichtsartikel veröffentlicht wurde (Sander, Gudermann,



Schredelseker, 2021). Insgesamt liefert diese Promotion mehrere Belege dafür, dass die mitochondriale  $\text{Ca}^{2+}$ -Aufnahme eine zentrale Rolle bei der zellulären Kalziumdynamik in Herzmuskelzellen und der elektromechanischen Kopplung spielt und als vielversprechendes künftiges therapeutisches Ziel für Herzerkrankungen wie Herzrhythmusstörungen und Herzinsuffizienz dienen könnte.

### 3 Introduction

Diseases of the heart, such as heart failure and cardiac arrhythmia, represent an increasing social and economic burden, accelerated by a rapidly aging population. Cardiovascular diseases (CVDs) are the leading cause of mortality and morbidity in developed nations [1]. This is partly related to insufficient treatment options and severe side effects of commonly used drugs. Therefore, the development of new therapies for safer and more effective treatment remains a challenge. Since 1883, the year Sydney Ringer observed that  $\text{Ca}^{2+}$  is essential for cardiac contraction, it has gained increasing understanding as an intracellular messenger for the regulation of cardiac rhythmicity and contractility [2]. Moreover, it has emerged that aberrations in  $\text{Ca}^{2+}$  homeostasis play a significant role in the pathogenesis of many cardiovascular diseases. Electrical and mechanical cardiac malfunction, which includes arrhythmogenesis, cardiac decompensation and impaired contractility is closely associated with abnormalities in intracellular  $\text{Ca}^{2+}$  handling [3]. Hence, gaining a mechanistic understanding of changes in cardiac cellular  $\text{Ca}^{2+}$  handling is a critical step towards developing and improving novel treatment strategies for heart diseases: To identify novel targets for therapeutic intervention and early diagnosis, it is important to understand the molecular basis and the pathways of  $\text{Ca}^{2+}$  handling and signalling related to CVDs.

#### 3.1 Alteration of cardiomyocyte $\text{Ca}^{2+}$ handling in cardiac diseases

Cardiomyocyte contraction occurs by a process called excitation-contraction coupling (ECC), in which  $\text{Ca}^{2+}$  connects cardiomyocyte excitation to mechanical activity (**Figure 1**). Upon sarcolemmal depolarization  $\text{Ca}^{2+}$  enters the cell through voltage dependent L-type  $\text{Ca}^{2+}$  channels (LCC) [4]. Incoming  $\text{Ca}^{2+}$  activates juxtaposed ryanodine receptors (RyRs),  $\text{Ca}^{2+}$  channels in the membrane of the sarcoplasmic reticulum (SR), which amplifies the incoming  $\text{Ca}^{2+}$  signal by triggering a stronger release of  $\text{Ca}^{2+}$  in a process called  $\text{Ca}^{2+}$  induced  $\text{Ca}^{2+}$  release [5]. The SR is a specialised endoplasmic reticulum that acts as an internal storage for  $\text{Ca}^{2+}$  and its membrane proteins are highly specialised in the cycling of  $\text{Ca}^{2+}$ . The SR  $\text{Ca}^{2+}$  release is mediated by RyR2 channels, the cardiomyocyte specific isoform of RyR [6], which are localized in clusters in the SR membrane in close proximity (~20 nm) to clusters of LCCs in the sarcolemma [7], an arrangement known as the cardiomyocyte dyad. Combined  $\text{Ca}^{2+}$  influx from LCCs and SR  $\text{Ca}^{2+}$  release raises the free intracellular  $\text{Ca}^{2+}$  level ( $[\text{Ca}^{2+}]_i$ ), which facilitates the binding of  $\text{Ca}^{2+}$  to troponin C, the  $\text{Ca}^{2+}$  sensing protein of the contraction machinery, and thereby initiates contraction of the myofilaments [8]. Following contraction, low diastolic conditions of cytosolic  $\text{Ca}^{2+}$  are restored to enable  $\text{Ca}^{2+}$  dissociation from troponin C to allow myofilament and subsequent muscle relaxation. This requires the closure of the RyR2s and an effective  $\text{Ca}^{2+}$  removal machinery. Small amounts of  $\text{Ca}^{2+}$  are extruded from the cell through the  $\text{Na}^+/\text{Ca}^{2+}$  exchanger (NCX) in the sarcolemma, but the major amount is recirculated into the SR via sarcoplasmic/endoplasmic reticulum  $\text{Ca}^{2+}$  ATPase (SERCA). This interplay of molecular actors ensures intracellular  $\text{Ca}^{2+}$  transients of high  $\text{Ca}^{2+}$  during systole and low  $\text{Ca}^{2+}$  during diastole.  $\text{Ca}^{2+}$  transients have to be tightly regulated for a proper heartbeat and aberrant handling of intracellular  $\text{Ca}^{2+}$  at any of these steps can cause cardiac dysfunction [9].

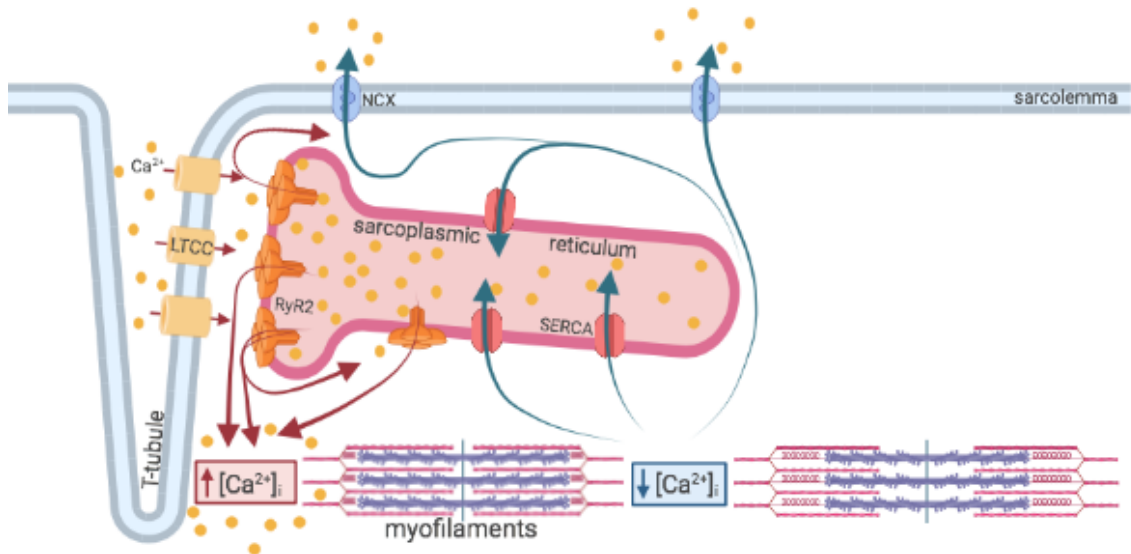


**Figure 1: Excitation-contraction coupling:**  $\text{Ca}^{2+}$  influx via LCCs activates neighboring RyR2s, triggering greater  $\text{Ca}^{2+}$  influx into the cytosol, a process called  $\text{Ca}^{2+}$ -induced  $\text{Ca}^{2+}$  release. The increase in cytosolic  $\text{Ca}^{2+}$  causes contraction of the myofilaments.  $\text{Ca}^{2+}$  must be effectively removed from the cytosol to allow relaxation of the cardiomyocytes. The majority is pumped back into the SR via SERCA, while part is transported out of the cell across the cell membrane via NCX. (Figure was created with Biorender)

### 3.1.1 Arrhythmia

Significant progress has been made in understanding the molecular mechanisms by which aberrant  $\text{Ca}^{2+}$  fluxes mediate different types of cardiac arrhythmias. The discovery of mutations in patients with inherited arrhythmia syndromes has provided the best evidence that defects in various  $\text{Ca}^{2+}$  channels and  $\text{Ca}^{2+}$  transporters, and therefore aberrant cellular  $\text{Ca}^{2+}$  handling, are directly associated with the occurrence of arrhythmia. A growing list of inherited genetic defects leading to fatal cardiac arrhythmia syndromes has been identified, including diseases like catecholaminergic polymorphic ventricular tachycardia (CPVT) and hypertrophic cardiomyopathy (HCM). CPVT patients show ventricular tachycardia induced by  $\beta$ -adrenergic stimulation in the absence of a structural heart disease [10]. Inherited mutations in the RyR2 gene were identified as the most common genetic subtype of CPVT, accounting for approximately 50-60 % of the CPVT cases [11]. Under physiological conditions, in healthy cardiomyocytes, a small amount of incoming  $\text{Ca}^{2+}$  via LCCs activates single clusters of RyR2 channels during systole, which leads to a subsequent increase in local  $\text{Ca}^{2+}$ . This  $\text{Ca}^{2+}$  in turn activates adjacent RyR2 clusters, triggering CICR, thus leading to a global increase in cytosolic  $\text{Ca}^{2+}$  [12]. Due to the opening probability of RyR2 channels, small and unsynchronized SR- $\text{Ca}^{2+}$  release events occur during diastole, so called  $\text{Ca}^{2+}$  sparks [13]. Once these spontaneous, diastolic  $\text{Ca}^{2+}$  sparks activate neighbouring RyR2 clusters, the  $\text{Ca}^{2+}$  signal can propagate across the cell in waves. Taken together, spontaneous  $\text{Ca}^{2+}$  sparks and  $\text{Ca}^{2+}$  waves are referred to as SR  $\text{Ca}^{2+}$  leak [14]. In CPVT this SR  $\text{Ca}^{2+}$  leak is increased due to gain of function mutations in RyR2. The leak is further amplified with increased phosphorylation of RyR2 under sympathetic activity, which can be detected as a higher frequency of diastolic  $\text{Ca}^{2+}$  sparks and waves [13]. Although only 50-60% of CPVT mutations are linked to mutations in the RyR2, all mutations associated with CPVT result in higher diastolic  $\text{Ca}^{2+}$  leak [15]–[18]. The increase in intracellular diastolic  $\text{Ca}^{2+}$  leads to activation of the electrogenic

NCX, which exchanges three sodium ions for one  $\text{Ca}^{2+}$  ion, resulting in a depolarizing inward sodium current [19]. If the threshold for voltage gated  $\text{Na}^+$  channels is reached, spontaneous action potentials occur that can trigger tissue wide depolarisation waves, thus leading to arrhythmia [20], [21]. However, RyR2 destabilization does not only occur in inherited diseases such as CPVT. Recently, a hitherto unknown mechanism of aging has been linked to RyR2 instability. In mice, aging alone, independently of cardiac diseases, results in RyR2 hyperglycation, thus leading to increased SR  $\text{Ca}^{2+}$  leak [22]. Excitation-contraction coupling in general is known to become dysfunctional with age, leading to an increased propensity for cardiac arrhythmias in the elderly population [23]–[25]. However, not only do alterations in RyR2 contribute to arrhythmogenesis, altered  $\text{Ca}^{2+}$  homeostasis at any point of ECC can lead to abnormal automaticity, triggered activity and provide a substrate for arrhythmias [26]. In addition, acquired modifications of various  $\text{Ca}^{2+}$  handling proteins can contribute to the pathogenesis of arrhythmias in patients with a broad spectrum of cardiac diseases, including atrial fibrillation and ventricular tachycardia in heart failure.

### 3.1.2 Heart failure

Heart failure (HF) is a chronic, progressive condition in which the heart is unable to meet the metabolic demands of the body. The causes of heart failure are diverse, varying from genetic predispositions and inherited diseases to acquired risk factors and modifiable environmental causes [27],[28]. Aging itself is the major risk factor for cardiac diseases, so that hypertension, atherosclerosis, and resulting chronic HF reach epidemic proportions in the elderly. An estimated 1 in 5 people will develop HF in their lifetime, the mortality remains high and approximately 50% of patients with HF die within five years from initial diagnosis due to ventricular tachycardia [1],[29]. As for arrhythmia, also in HF dysregulation of intracellular  $\text{Ca}^{2+}$  handling is thought to be a major contributor to disease initiation and progression. Both, contractile dysfunction and the increased susceptibility to ventricular arrhythmias observed in failing hearts are linked to an imbalanced  $\text{Ca}^{2+}$  homeostasis [23],[30]. The main factors that determine the intensity and duration of myocyte contraction are the amount of  $\text{Ca}^{2+}$  that is provided to the cytoplasm during systole and the rate in which the  $\text{Ca}^{2+}$  is delivered and removed [31]. In the failing heart, all these factors are commonly impaired. First, an increase in SR  $\text{Ca}^{2+}$  leak as a consequence of increased RyR2 activity and impaired refractoriness leads to a decreased SR  $\text{Ca}^{2+}$  load and higher diastolic  $\text{Ca}^{2+}$  levels, which is associated with the progression of HF [32]. Second, the SR load is further compromised by a decreased expression of SERCA and a higher activity of the NCX [32]–[34]. Third, the amplitude of the incoming  $\text{Ca}^{2+}$  current via the LCCs is generally decreased in atrial and ventricular cardiomyocytes of failing hearts [12],[13]. Together, these pathogenic mechanisms lead to increased cellular  $\text{Ca}^{2+}$  during diastole and lower  $\text{Ca}^{2+}$  levels during systole, and thus explain the reduced cardiac contractility. Additionally, the increased diastolic  $\text{Ca}^{2+}$  entails an increased prevalence of ventricular tachycardia by enhancing the open probability of RyR2 during diastole and thus favouring ectopic excitations. This mechanism is further enhanced by coping mechanisms of the autonomic nervous system, which increases phosphorylation and thus destabilisation of RyR2s [34][37].

## 3.2 Current and experimental therapeutic approaches in cardiac arrhythmia and heart failure

Both acquired and hereditary cardiac dysfunctions, which includes arrhythmia, decompensation as well as impaired contractility, are tightly linked to aberrations in intracellular  $\text{Ca}^{2+}$  signalling and

Ca<sup>2+</sup> handling proteins [3]. Given the fact that dysregulation of Ca<sup>2+</sup> handling proteins occurs exclusively in pathological and not in physiological hypertrophy, it clearly underlines the central role of abnormal Ca<sup>2+</sup> handling in the pathogenesis of heart failure [38]. Nevertheless, there are no common pharmacological CVD therapies that directly target intracellular Ca<sup>2+</sup> handling. Basic treatment strategy for HF involves reducing the workload on the heart by lowering blood pressure and decreasing heart rate. In line with this, the European Society of Cardiology (ESC) and other institutions recommend antihypertensive agents and  $\beta$ -blockers as first line therapy for HF due to lack of more efficient drugs [39], [40]. In principle, cardiac glycosides can be applied to increase contractile force in HF. The inhibition of sodium-potassium-ATPase (Na<sup>+</sup>/K<sup>+</sup>-ATPase) by cardiac glycosides leads to an increase in cytosolic Na<sup>+</sup>, which in turn reduces the driving force for NCX and thereby its activity and increases cytosolic Ca<sup>2+</sup>. This results in a positive inotropic effect, with an increase in peak contractile force. Despite their positive inotropic effect, the clinical use of cardiac glycosides is limited as their therapeutic index is narrow and side effects of overdosage are severe, as they include cardiac arrhythmia, especially atrial tachycardias and atrioventricular block. Thus, treatment options for patients with HF are very limited as there are no safe therapeutic interventions to increase the contractility of the heart.

Particularly worth mentioning here is that the main cause of death in HF is arrhythmia and approximately 50% of patients with HF die within five years from initial diagnosis due to ventricular tachycardia [1]. This is again related to the limited efficacy and severe side effects of commonly used drugs, in this case antiarrhythmics. The classification of antiarrhythmic drugs according to Vaughan Williams is the most common and is based on the electrophysiological properties of the substances. While class II antiarrhythmics suppress the propagation of ectopic signals indirectly by reducing the adrenergic excitability of the heart by blocking beta receptors, antiarrhythmic drugs of Vaughan-Williams classes I, III, and IV directly target plasma membrane ion channels [41]: Class I antiarrhythmic agents act by blocking the voltage-gated Na<sup>+</sup> channel responsible for action potential depolarization, which causes deceleration of the excitation conduction. Class III agents extend the action potential by blocking repolarizing potassium current. Class IV agents slow down the influx of Ca<sup>2+</sup> by blocking LCCs and thus delaying the formation and conduction of action potentials in pacemaker and AV-nodal cells. Antiarrhythmic drugs of Vaughan-Williams classes I, III, and IV endanger the patient's health, due to their effect on the cardiac action potential. As a result of action potential modulation, they interfere with cardiac excitation conduction and thus are susceptible to pro-arrhythmic effects. In some cases, there was evidence of a higher mortality under medication compared to placebo administration [42] and thus these drugs can not be applied long-term.

### 3.2.1 Potential target structures for novel drug candidates

To improve the efficacy of pharmacological interventions and to develop novel therapies with less side-effects, there is a continuous search for novel therapeutic approaches capable of preventing or reversing the pathophysiology associated with heart failure and arrhythmias. Intracellular Ca<sup>2+</sup> handling is one of main the eye-catchers of the current research arising from the aforementioned points. Therefore, research in this field is currently focusing on Ca<sup>2+</sup> handling proteins of ECC, such as RyR2, SERCA, and NCX, as a novel therapeutic approach for HF and arrhythmias [43]. While some therapeutics targeting Ca<sup>2+</sup> handling proteins are still in early preclinical stages several have entered clinical trials, but beside some positive results there were several drawbacks due to low specificity, off-targets, side effects and limited effects on mortality [29], [44]–[52]. For example, dantrolene was shown to inhibit CPVT related ventricular tachycardia by stabilizing the

closed state of RyR2, this effect was shown in mice and a small cohort of CPVT-1 patients [53]. An early phase I clinical trial is evaluating the intravenous administration of dantrolene on the occurrence of ventricular arrhythmias in patients with structural heart disease, and although this highlights the role of RyR2 as a target in arrhythmias, no results have been published to date [54]. Flecainide, a class I sodium channel blocker, is also capable of inhibiting SR  $\text{Ca}^{2+}$  leak by reducing the duration of RyR2 channel opening, thereby preventing exercise-induced ventricular arrhythmias in two CPVT patients [55]. Istaroxime, which stimulates SERCA and by that increasing SR load and preventing cytosolic  $\text{Ca}^{2+}$  overload, was shown to have a moderate antiarrhythmic effect, but it should be mentioned that it could be pro-arrhythmic due to its  $\text{Na}^+/\text{K}^+$ -ATPase inhibition [56]. NCX blockers show contrasting effects on arrhythmogenesis under different conditions. This can be partly explained by various off target effects of the blockers, which were often shown to inhibit LCC and  $\text{K}^+$  currents [57]. Blockers of the NCX reverse mode were protective against  $\text{Ca}^{2+}$  overload and thus able to suppress arrhythmia [58], but in another model the same blocker enhanced the inducibility of arrhythmias [59].

Current research has indicated that pathogenic remodelling of  $\text{Ca}^{2+}$  signalling varies depending on the underlying heart disease. Therefore it may be necessary to pursue personalised therapeutic approaches to target individual  $\text{Ca}^{2+}$  handling proteins for specific cardiac diseases. Furthermore, it may be necessary to combine the individual therapeutic interventions, for instance, it has been emphasized that RyR2 modulation alone is not sufficient to induce a sustained change in heartbeats due to compensatory readjustments of the SR load [60]. Overall, regardless of the current possibilities it is obvious that there is need for further research in this area and new strategies are needed to treat mishandling of  $\text{Ca}^{2+}$  in HF and arrhythmia.

### 3.2.2 Cardiac mitochondrial $\text{Ca}^{2+}$ as a target in cardiac diseases

The search for new, more efficient strategies for the treatment of  $\text{Ca}^{2+}$ -induced cardiac diseases directed our lab to focus on cardiac mitochondria. In an unbiased screen using zebrafish embryos with fibrillating hearts, Shimizu and coworkers discovered a newly synthesized substance called efsevin that was able to restore rhythmic cardiac contractions [61]. In a subsequent pull-down assay, they identified the pore forming outer mitochondrial membrane protein voltage-dependent anion channel 2 (VDAC2) to be the target of this substance. With this discovery, our research began on how pharmacological alteration of mitochondrial  $\text{Ca}^{2+}$  uptake can prevent  $\text{Ca}^{2+}$ -induced arrhythmias.

Mitochondria occupy up to 30% of the total cell volume in the myocardium. Their metabolic activity has to be synchronized to the energy demand of the cardiomyocytes [62]. In case of higher workload, a gradual and moderate increase in mitochondrial  $\text{Ca}^{2+}$  results in  $\text{Ca}^{2+}$  dependent upregulation of mitochondrial enzyme activity and therefore a change in  $\text{Ca}^{2+}$  signalling couples energy demand to increased ATP production [63]. To facilitate this coupling, mitochondria are equipped with an efficient and regulated machinery for  $\text{Ca}^{2+}$  import, spanning both mitochondrial membranes and forming a selective mitochondrial  $\text{Ca}^{2+}$  uptake pathway (MCUP) [64]–[66]. To ensure that the  $\text{Ca}^{2+}$  signal is delivered efficiently, this complex and the SR form interconnected membranes especially at SR  $\text{Ca}^{2+}$  release sites, thus ensuring a constant interaction between those two organelles [67], [68]. Although their main purpose is the generation of cellular energy in form of ATP they are also one component of cardiac  $\text{Ca}^{2+}$  handling that is still rather elusive and often overlooked [69]. In addition to the slow and gradual uptake of  $\text{Ca}^{2+}$  into mitochondria needed for energy-demand matching, the tight connection of those two organelles further enables

mitochondrial  $\text{Ca}^{2+}$  uptake that is fast enough to shape  $\text{Ca}^{2+}$  transients on a beat-to-beat basis, modulating local intracellular  $\text{Ca}^{2+}$  fluxes and thereby regulating contractile activity [68], [70]–[73].

### 3.2.2.1 Mitochondrial $\text{Ca}^{2+}$ uptake pathway

$\text{Ca}^{2+}$  has to pass two membranes on its way into the mitochondrion, and several mechanisms have been described for mitochondrial  $\text{Ca}^{2+}$  uptake.

The outer mitochondrial membrane (OMM) is highly occupied by voltage dependent anion channels (VDACs), which are often described as unselective pores, due to their large diameter of approximately 15 Å and permeability to large metabolites, such as ATP. Therefore, it is often assumed that they are freely permeable to  $\text{Ca}^{2+}$  and that the selectivity and regulation for mitochondrial  $\text{Ca}^{2+}$  uptake takes place at the inner mitochondrial membrane (IMM). However, several observations challenge this idea and suggest a regulatory role of VDACs for mitochondrial  $\text{Ca}^{2+}$  uptake. Consistent with this theory are observations that VDAC is coupled to  $\text{Ca}^{2+}$  release domains of ER/SRs via anchoring proteins [74], [75]. Furthermore, the calcium selectivity of the channel depends on its intrinsic open state and can be altered by interactions with protein partners, metabolites or small synthetic molecules [61], [76]–[78]. In our review, we discuss the theory that VDAC serves as a physiological regulator of mitochondrial  $\text{Ca}^{2+}$  uptake in the OMM [79].

In the IMM, the mitochondrial  $\text{Ca}^{2+}$  uniporter (MCU) is the best established and most characterized pathway for  $\text{Ca}^{2+}$  entry. Although its biophysical properties were first described in the 1960s [80], MCUs molecular identity remained elusive until 2011 when two groups revealed the molecular machinery [65], [66]. After this discovery, research on mitochondrial  $\text{Ca}^{2+}$  uptake experienced a new era, as more specific research tools were now available, such as genetically modified mice [81]. Starting from this discovery, numerous regulatory subunits of the MCU complex (MCUC) have been identified and intensively studied [82]. The pore-forming subunits MCU, the heteromer-forming negative regulator MCUB and the essential MCU regulator EMRE span the inner mitochondrial membrane. The auxiliary regulatory  $\text{Ca}^{2+}$  sensing subunits MICU1-3 modulate the opening state of the MCU complex [65], [83]–[85].

Although the selectivity and conductance for  $\text{Ca}^{2+}$  by MCUC is remarkably high, it must be noted that the complex itself is activated by  $\text{Ca}^{2+}$  with a very low affinity ( $\text{EC}_{50} \approx 10 \mu\text{M}$ ). Since global cytosolic  $\text{Ca}^{2+}$  in cardiomyocytes increases from ~100 nM under resting conditions to ~1  $\mu\text{M}$  with each heartbeat, this would limit  $\text{Ca}^{2+}$  uptake from the cytosol via MCUC [86]. However, a mechanism known as  $\text{Ca}^{2+}$  microdomains has been identified in which  $\text{Ca}^{2+}$  concentration can increase locally to 10-20  $\mu\text{M}$  around  $\text{Ca}^{2+}$  release sites, thereby activating MCUC [87], [88]. Microdomains are spatially restricted regions of high  $\text{Ca}^{2+}$  concentrations that can occur at points where  $\text{Ca}^{2+}$  enters the cytosol, either at the cell membrane or at internal  $\text{Ca}^{2+}$  stores [89]. In order to activate the MCUC by  $\text{Ca}^{2+}$  microdomains, a direct shuttling route from the  $\text{Ca}^{2+}$  release sites via the OMM to MCUC at the IMM is necessary.

As mentioned before in cardiomyocytes mitochondria and SR form interconnected membranes especially at SR  $\text{Ca}^{2+}$  release sites, thus ensuring a constant interaction between those two organelles [67], [68]. VDACs isoform 2 is directly tethered to RyR2s, the  $\text{Ca}^{2+}$  release sites of the SR, which allows direct shuttling of  $\text{Ca}^{2+}$  from the SR into mitochondria [90]–[92]. This connection is further stabilized by different proteins, such as the anchoring protein GRP75 [74], [93]. The connection between the mitochondrial membranes then occurs through the physical coupling of VDAC and MCU [94]. In summary, the connection of SR and mitochondria forms an optimal  $\text{Ca}^{2+}$

transport route, consisting of RyR2, VDAC2, MCUC and further stabilizing proteins, sufficient to influence cardiac contractile activity.

### 3.2.2.2 Mitochondrial Ca<sup>2+</sup> uptake enhancers

Our lab's focus on mitochondrial Ca<sup>2+</sup> uptake in the context of cardiac diseases began with a screening of various compounds for their effects on the rhythmicity of the heart. In this previous study Shimizu and co-workers identified the new compound efsevin, which restores rhythmic cardiac contractions in the otherwise fibrillating heart of a zebrafish arrhythmia model [61]. In a subsequent pull down assay, they identified VDAC2 as the molecular target of efsevin. Further studies revealed that efsevin binds within the pore and facilitates the transition of VDAC2 to a less anion-selective state, thereby enhancing Ca<sup>2+</sup> flux [78]. With this data, the central hypothesis was formulated, that pharmacological activation of mitochondrial Ca<sup>2+</sup> uptake buffers a part of the Ca<sup>2+</sup> released by diastolic Ca<sup>2+</sup> sparks into the mitochondria, thereby limiting the spark temporarily and spatially. This in turn prevents the spark from spreading further and activating neighbouring RyR2 clusters, and thus Ca<sup>2+</sup> waves, and thereby explains the antiarrhythmic effect (see **Figure 2**). Indeed, Schweitzer et al were able to show that in murine cardiomyocytes, when exposed to efsevin, potentially arrhythmogenic diastolic Ca<sup>2+</sup> sparks are temporally and spatially limited and the formation of Ca<sup>2+</sup> waves was diminished [61]. To prove the general validity of this hypothesis, efsevin and another activator of the MCUP, Kaempferol [95], were tested for their ability to prevent arrhythmias. Both mitochondrial Ca<sup>2+</sup> uptake enhancers (MiCUpS) were able to suppress the generation of Ca<sup>2+</sup> waves and thus arrhythmic, spontaneous action potentials in murine and human CPVT cells [76]. Furthermore, both suppressed episodes of ventricular tachycardia *in vivo* [76]. Kaempferol, in contrast to efsevin, does not activate VDAC2 but MCU, which proves that general increase of mitochondrial Ca<sup>2+</sup> uptake at the inner or outer membrane leads to antiarrhythmic effects.

These results show that MiCUpS efficiently suppressed ventricular tachycardia in a murine CPVT model [76]. Although CPVT is a rare inheritable heart disease, its arrhythmogenesis is attributable to increased diastolic Ca<sup>2+</sup>, as is the case in other cardiac diseases. Consequently, MiCUpS may not only be effective in the treatment of this relatively rare disease, but may also be supportive in the treatment of other CVDs associated with Ca<sup>2+</sup>.



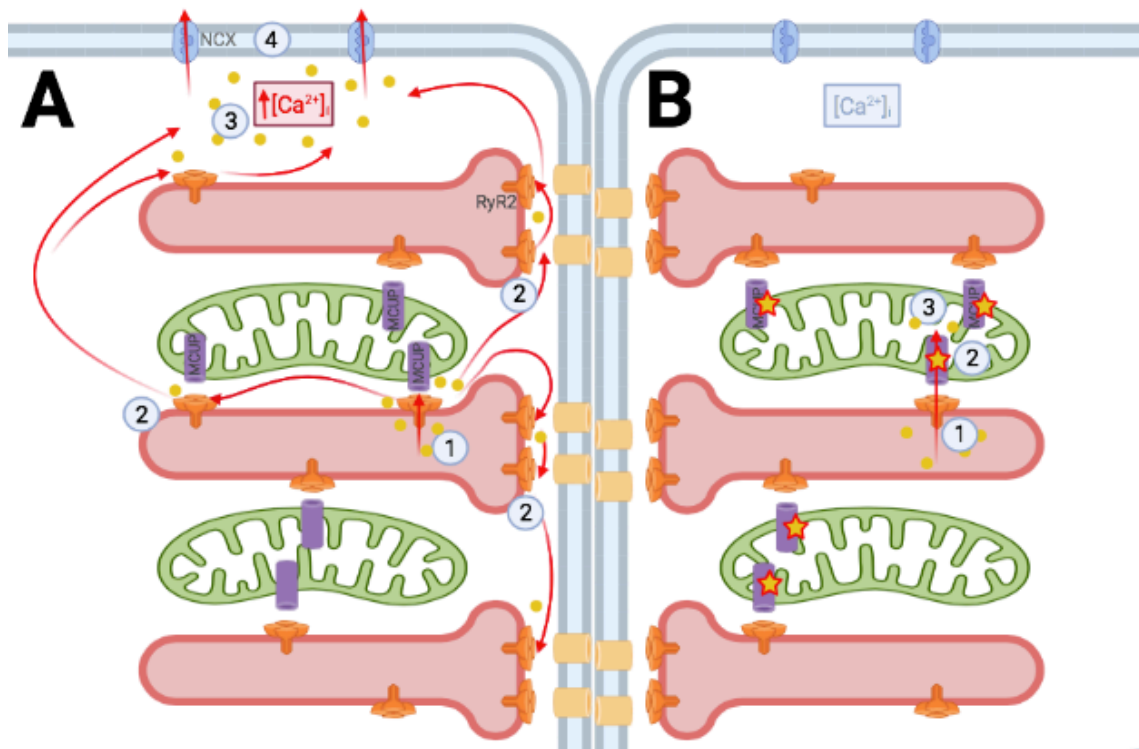


**Figure 2: MiCUp mediated arrhythmia suppression.** **[A]** Ca<sup>2+</sup> flux without MiCUPS (1) spontaneous, diastolic Ca<sup>2+</sup> release into the cytosol via leaky RyR2 (2) saltatory expansion of a Ca<sup>2+</sup> wave by activation of neighboring RyR2 (3) increase of diastolic cytosolic [Ca<sup>2+</sup>]<sub>i</sub> (4) activation of electrogenic NCX **[B]** Ca<sup>2+</sup> flux with MiCUPS (1) spontaneous, diastolic Ca<sup>2+</sup> release into the cytosol via leaky RyR2 (2) Ca<sup>2+</sup> uptake via activated MCUP (VDAC2/MCUC) (indicated by stars) (3) buffering of Ca<sup>2+</sup> into mitochondria, saltatory expansion of the Ca<sup>2+</sup> wave is interrupted, no change in diastolic [Ca<sup>2+</sup>]<sub>i</sub>. (Figure was created with Biorender)

Interestingly, despite the increase in mitochondrial Ca<sup>2+</sup> uptake over a period of several days, no evidence of serious adverse effects, such as apoptosis, was observed, neither in cellular nor animal models [61], [76], making mitochondrial Ca<sup>2+</sup> uptake enhancers excellent candidates for further preclinical and clinical studies. However, both substances are highly experimental. The basic pharmacokinetic and pharmacodynamic parameters are still largely unknown. Analysis of the dose-response curve of mitochondrial Ca<sup>2+</sup> uptake for efsevin and kaempferol in permeabilized cardiomyocytes shows an EC<sub>50</sub> of 2-5 μM for both substances, which is a major drawback for use as a drug in human therapy due to the dramatically increased potential for off-target effects. Numerous other targets have been described for kaempferol besides the MCUP [96] and although VDAC2 was identified as primary target of efsevin no further data on other targets are available yet.

In conclusion, mitochondrial Ca<sup>2+</sup> uptake represents a promising new target structure to treat arrhythmias associated with alterations in intracellular Ca<sup>2+</sup> handling. Considering the Ca<sup>2+</sup> handling of the cell, it may also be a decisive advantage of MiCUPS - besides the most obvious one, that they do not affect the excitation of the cell, like most of the common antiarrhythmics- that they do not interfere with the direct EC-coupling, such as modulators of the Ca<sup>2+</sup> storage proteins RyR2 and SERCA. However, further progress in establishing this therapy requires substantially more effective MiCUPS, with better described pharmacodynamics and -kinetics and a significantly lower EC<sub>50</sub>.

I have dedicated the research in the context of my doctoral thesis to the search for new, safer and more efficient MiCUpS and to the question of whether the increase in mitochondrial  $\text{Ca}^{2+}$  uptake can also serve as a therapeutic approach for other  $\text{Ca}^{2+}$ -induced heart diseases. Above all, there was always the underlying question of how mitochondrial  $\text{Ca}^{2+}$  uptake can be modified physiologically, pathophysiologically and pharmacologically. In the following chapter I will describe how I addressed these questions and will highlight my contribution to the individual publications. While the first publication deals with the search for more efficient MiCUpS, the second explores the potential to treat not only arrhythmias but also heart failure by increasing mitochondrial  $\text{Ca}^{2+}$  uptake. Complementing my research, I have attached our review in which we challenge the commonly accepted view and present a novel concept of how mitochondrial  $\text{Ca}^{2+}$  uptake is regulated.

## 4 Publications: Short summary & personal contribution

### 4.1 Publication I: Novel mitochondrial Ca<sup>2+</sup> uptake enhancers

#### ***Approved drugs ezetimibe and disulfiram enhance mitochondrial Ca<sup>2+</sup> uptake and suppress cardiac arrhythmogenesis***

*Paulina Sander, Michael Feng, Maria K. Schweitzer, Fabiola Wilting, Sophie M. Gutenthaler, Daniela M. Arduino, Sandra Fischbach, Lisa Dreizehnter, Alessandra Moretti, Thomas Gudermann, Fabiana Perocchi, Johann Schredelseker*

*British Journal of Pharmacology, 2021, 178(22):4518-4532*

Due to severe side effects of common antiarrhythmic drugs the treatment of cardiac arrhythmia still remains challenging. Our group recently demonstrated that mitochondrial Ca<sup>2+</sup> uptake represents a promising new target for safer pharmacological intervention in Ca<sup>2+</sup> induced arrhythmias [76]. Nevertheless, druggable agonists of the MCUP suitable for further preclinical and clinical studies are missing. With the aim to bridge this gap between basic research and clinical treatment we conceptualized this study. In a first selective step we used a HeLa based high throughput screen for novel potential MiCUPs, in which we particularly used a library of substances with a background in medical use to circumvent the lack of toxicology and pharmacology/-kinetics data. In a collaborative approach with the laboratory of Dr. Fabiana Perocchi, we adapted a screening platform first established for mitochondrial Ca<sup>2+</sup> uptake blockers to screen a chemical library of 727 compounds [97]. Three substances, namely disulfiram, ezetimibe and honokiol, increased Ca<sup>2+</sup> uptake in mitochondria. Since this basic screen of compounds was in non-excitabile HeLa cells, which differ a lot in mitochondrial abundance and in the composition of MCUP [98], [99], I first tested these hits in cardiomyocytes and determined their efficacy to suppress arrhythmias. Although most components of the MCUP are ubiquitously expressed, a tissue selectivity exists that is determined by the composition, subcellular localization and protein interactions of the MCUP subunits [85], [100], [101]. As mentioned before we propose that the cardiac specific Ca<sup>2+</sup> transfer between the SR and the mitochondria via RyR2, VDAC2, and MCU is the molecular prerequisite for the antiarrhythmic effect of MiCUPs [61], [76], [78]. To test if the substances are agonists of this specific MCUP I used HL-1 cardiomyocytes and performed an assay in which I specifically analyzed local Ca<sup>2+</sup> transfer from the SR to the mitochondria. Just two of the three hits from the initial HeLa based screen were able to significantly enhance mitochondrial Ca<sup>2+</sup> uptake in HL-1 cardiomyocytes, indicating that there is indeed a difference in MCUP in excitable and non-excitabile cells. Consequently, I evaluated the antiarrhythmic potential of the two newly identified MiCUPs in two translational models of Ca<sup>2+</sup> induced arrhythmia. I tested the two MiCUPs *in vivo* for their potential to reverse the fibrillating heartbeat in a zebrafish arrhythmia model of Ca<sup>2+</sup> overload [61], [102], where both restored rhythmic cardiac contractions. In order to demonstrate the efficacy in a human-relevant model, I isolated ventricular cardiomyocytes of a CPVT mouse model [103] and investigated the impact of ezetimibe and disulfiram on arrhythmogenic signals. Both substances significantly reduced both diastolic and systolic arrhythmogenic Ca<sup>2+</sup> signals. To ensure that the effective target of the suppression of arrhythmogenic signals in CPVT

cardiomyocytes is indeed enhanced mitochondrial  $\text{Ca}^{2+}$  uptake in crossbred CPVT mice with mice lacking the pore forming unit of MCU [81]. Strikingly, in isolated cardiomyocytes of these mice both substances failed to suppress arrhythmogenic signals, indicating that enhanced mitochondrial  $\text{Ca}^{2+}$  uptake via MCUP is solely attributable for the antiarrhythmic effects.

In this study, I characterised two EMA and FDA approved compounds as potential antiarrhythmic agents that have not previously been linked to mitochondrial  $\text{Ca}^{2+}$  uptake or treatment of cardiac arrhythmias. While both compounds were very effective in suppressing arrhythmogenesis, disulfiram showed side effects in all models tested. Zebrafish embryos exhibited severe malformations and cardiomyocytes showed increased cytosolic baseline  $\text{Ca}^{2+}$  levels and spontaneous activity. In summary, this means that disulfiram, while effective, should be used with caution in preclinical and clinical applications. Both, ezetimibe and disulfiram efficiently suppressed arrhythmogenesis with a significant higher affinity to the MCUP compared to the previously described agonists efsevin and kaempferol, thus making them promising candidates for future preclinical and clinical studies, taking our hypothesis a big step forward from basic research to therapeutic application. Especially since the identification of clinically approved drugs opens the door for repurposing studies. Compared to the existing MiCUPS kaempferol and efsevin, which are of limited medicinal use, disulfiram and ezetimibe could serve as lead compounds for the development of innovative therapeutic approaches in the fight against  $\text{Ca}^{2+}$ -induced CVDs.

## 4.2 Publication II: Mitochondrial $\text{Ca}^{2+}$ uptake in heart failure

### ***Cardiac-specific deletion of voltage dependent anion channel 2 leads to dilated cardiomyopathy by altering calcium homeostasis***

*Thirupura S Shankar, Dinesh K.A. Ramadurai, Kira Steinhorst, Salah Sommakia, Rachit Bado-  
lia, Aspasia Thodou Krokidi, Dallen Calder, Sutip Navankasattusas, **Paulina Sander**, Oh Sung  
Kwon, Aishwarya Aravamudhan, Jing Ling, Andreas Dendorfer, Changmin Xie, Ohyun Kwon,  
Emily H. Y. Cheng, Kevin J. Whitehead, Thomas Gudermann, Russel S. Richardson, Frank B.  
Sachse, Johann Schredelseker, Kenneth W. Spitzer, Dipayan Chaudhuri, Stavros G. Drakos*

*Nature Communications, 2021, 12(1):4583*

The impact of mitochondrial  $\text{Ca}^{2+}$  uptake on cardiomyocyte  $\text{Ca}^{2+}$  handling is, as mentioned before, often underestimated. Even more when it comes to  $\text{Ca}^{2+}$  handling across the outer mitochondrial membrane (OMM). Due to the high abundance of large VDAC porins in the OMM, the membrane is still widely thought to be freely permeable for  $\text{Ca}^{2+}$  ions without any regulatory processes. In this paper we challenge this common hypothesis, by showing the ground-breaking results of cardiac ventricular myocyte specific knock down of VDAC2. Although global knockdown of VDAC2 has been shown to be embryonically lethal in 2003 [77] and it is known that there is a cardiac specific intense crosstalk between SR and mitochondria via RyR2 and VDAC2 [68], there are no further studies investigating the effects of cardiac VDAC2-KO in animal models. Our results indicate that cardiac specific loss of VDAC2 alters both mitochondrial and intracellular  $\text{Ca}^{2+}$  signalling, resulting in a severe impairment of cardiac excitation-contraction coupling. On the other hand, activation of mitochondrial  $\text{Ca}^{2+}$  uptake with the VDAC2 agonist efsevin elevated  $\text{Ca}^{2+}$  transients, thereby increasing the contraction force in a mouse model of pressure-overload induced heart failure, highlighting the importance of mitochondrial  $\text{Ca}^{2+}$  uptake via VDAC2 and the resulting

potential for therapeutic advances in combating HF through pharmacological regulation of intracellular  $\text{Ca}^{2+}$  fluxes.

In this study I performed control and TAC (transverse aortic constriction) surgery, to induce pressure overload cardiac hypertrophy and HF in mice [104], [105]. I isolated murine ventricular cardiomyocytes and examined the effect of the VDAC2 agonist efsevin on cytosolic  $\text{Ca}^{2+}$  transients in wildtype mice. I have demonstrated that the increased mitochondrial  $\text{Ca}^{2+}$  uptake under efsevin leads to an elevation of  $\text{Ca}^{2+}$  transients, illustrating a potential positive inotropic effect. With this data we highlight, that enhancing mitochondrial  $\text{Ca}^{2+}$  uptake with MiCUPS is not only sufficient to suppress arrhythmia, they are also effective in increasing  $\text{Ca}^{2+}$  transient amplitude and thus the contractility in hearts with HF. With this study we show for the first time how crucial mitochondrial  $\text{Ca}^{2+}$  uptake via VDAC2 is for the physiology of the heart and offer a completely new potential therapeutic approach for HF, a disease for which there is to date no adequate medical treatment.

### 4.3 Supplementary review: Mitochondrial $\text{Ca}^{2+}$ uptake across the outer mitochondrial membrane

#### *A Calcium Guard in the Outer Membrane: Is VDAC a Regulated Gatekeeper of Mitochondrial Calcium Uptake?*

*Paulina Sander, Thomas Gudermann & Johann Schredelseker*

*International Journal of molecular science, 2021, 19:22(2):946*

The question we were confronted with, every time we presented our research on VDAC2, was whether and how mitochondrial  $\text{Ca}^{2+}$  could be regulated at the OMM. The experimental work presented in this thesis highlights the importance of mitochondrial  $\text{Ca}^{2+}$  uptake for cardiac physiology. Previous work from our lab [61], [76], [78] and the work presented in publication 2 challenges the idea that regulation of mitochondrial  $\text{Ca}^{2+}$  uptake is solely regulated by the MCU complex and puts VDAC2 in the outer mitochondrial membrane in focus as a regulated  $\text{Ca}^{2+}$  channel. We therefore set out to perform a thorough literature analysis and to combine information in support or disagreement of this hypothesis in a review article. For this, I focused on the parts about regulation at the cellular level in agreement with my experimental expertise. In particular, I addressed the questions which physiological and pathophysiological relevance OMM  $\text{Ca}^{2+}$  flux regulation has and how it can be regulated by VDAC expression levels, interaction with protein partners or specific subcellular localization in  $\text{Ca}^{2+}$  microdomains. In the end, we present a novel concept in which the regulation of  $\text{Ca}^{2+}$  flux across the OMM is placed in a larger context that incorporates otherwise often overlooked concepts such as intrinsic channel regulation as well as the source of  $\text{Ca}^{2+}$  that is taken up by mitochondria. We hypothesize that VDAC-mediated mitochondrial  $\text{Ca}^{2+}$  uptake is not only a critical component in decoding cellular  $\text{Ca}^{2+}$  signals to elicit various physiological responses but is also capable of shaping cytosolic  $\text{Ca}^{2+}$  signals in cardiomyocytes. In contrast to the generally accepted view that MCUC is the sole regulator of mitochondrial  $\text{Ca}^{2+}$  uptake, our hypothesis underline that regulation also occurs via VDAC isoforms 1-3 in the outer membrane and is regulated at multiple levels, from expression, to protein partners and finally to the intrinsic properties of VDAC, which can adopt multiple conductance states [79].

Together with the substantiated hypothesis of our review, our work provides the basis that it is not MCU alone but a macromolecular complex between VDAC in the OMM and MCU in the IMM that regulates mitochondrial  $\text{Ca}^{2+}$  uptake, which in turn can be adjusted by further processes. With this work, we have changed the view on the regulation of mitochondrial  $\text{Ca}^{2+}$  uptake and clarified

that future studies should be cautious when investigating mitochondrial  $\text{Ca}^{2+}$  uptake, assuming that the OMM is freely permeable to  $\text{Ca}^{2+}$ . Not only does this contradict the complexity of mitochondrial  $\text{Ca}^{2+}$  uptake, but it can also lead to falsified results due to choosing the wrong  $\text{Ca}^{2+}$  source or not respecting the regulation by the OMM and VDAC.

## 5 References

- [1] E. E. J. Benjamin *et al.*, "2019 Heart Disease and Stroke Statistical Update Fact Sheet: Older Americans & Cardiovascular Diseases," *Circulation*, vol. 139, no. 10, 2019.
- [2] S. Ringer, "A further Contribution regarding the influence of the different Constituents of the Blood on the Contraction of the Heart," *J. Physiol.*, vol. 4, no. 1, 1883.
- [3] Q. Lou, A. Janardhan, and I. R. Efimov, "Remodeling of calcium handling in human heart failure," *Adv. Exp. Med. Biol.*, vol. 740, 2012.
- [4] D. J. Beuckelmann and W. G. Wier, "Mechanism of release of calcium from sarcoplasmic reticulum of guinea-pig cardiac cells.," *J. Physiol.*, vol. 405, pp. 233–55, Nov. 1988.
- [5] M. ENDO, M. TANAKA, and Y. OGAWA, "Calcium Induced Release of Calcium from the Sarcoplasmic Reticulum of Skinned Skeletal Muscle Fibres," *Nature*, vol. 228, no. 5266, pp. 34–36, Oct. 1970.
- [6] A. Kushnir and A. R. Marks, "The ryanodine receptor in cardiac physiology and disease.," *Adv. Pharmacol.*, vol. 59, pp. 1–30, 2010.
- [7] J. L. Greenstein and R. L. Winslow, "Integrative systems models of cardiac excitation-contraction coupling.," *Circ. Res.*, vol. 108, no. 1, pp. 70–84, Jan. 2011.
- [8] D. M. Bers, "Cardiac excitation–contraction coupling," *Nature*, vol. 415, no. 6868, pp. 198–205, Jan. 2002.
- [9] "Cardiomyopathy of overload: A major determinant of prognosis in congestive heart failure," *J. Cardiothorac. Anesth.*, vol. 4, no. 4, 1990.
- [10] N. Liu and S. G. Priori, "Disruption of calcium homeostasis and arrhythmogenesis induced by mutations in the cardiac ryanodine receptor and calsequestrin," *Cardiovasc. Res.*, vol. 77, no. 2, pp. 293–301, Sep. 2007.
- [11] S. G. Priori *et al.*, "Mutations in the cardiac ryanodine receptor gene (hRyR2) underlie catecholaminergic polymorphic ventricular tachycardia.," *Circulation*, vol. 103, no. 2, pp. 196–200, Jan. 2001.
- [12] A. Fabiato, "Time and calcium dependence of activation and inactivation of calcium-induced release of calcium from the sarcoplasmic reticulum of a skinned canine cardiac purkinje cell," *J. Gen. Physiol.*, vol. 85, no. 2, 1985.
- [13] H. Cheng, M. R. Lederer, W. J. Lederer, and M. B. Cannell, "Calcium sparks and [Ca<sup>2+</sup>]<sub>i</sub> waves in cardiac myocytes," *Am. J. Physiol. - Cell Physiol.*, vol. 270, no. 1 39-1, 1996.
- [14] R. A. Bassani and D. M. Bers, "Rate of diastolic Ca release from the sarcoplasmic reticulum of intact rabbit and rat ventricular myocytes," *Biophys. J.*, vol. 68, no. 5, 1995.
- [15] N. Roux-buisson *et al.*, "Absence of triadin, a protein of the calcium release complex, is responsible for cardiac arrhythmia with sudden death in human," *Hum. Mol. Genet.*, vol. 21, no. 12, 2012.
- [16] B. Gray *et al.*, "A novel heterozygous mutation in cardiac calsequestrin causes autosomal dominant catecholaminergic polymorphic ventricular tachycardia," *Heart Rhythm*, vol. 13, no. 8, 2016.
- [17] M. Nyegaard *et al.*, "Mutations in calmodulin cause ventricular tachycardia and sudden cardiac death," *Am. J. Hum. Genet.*, vol. 91, no. 4, 2012.
- [18] H. D. Devalla *et al.*, "TECRL, a new life-threatening inherited arrhythmia gene associated with overlapping clinical features of both LQTS and CPVT," *EMBO Mol. Med.*, vol. 8, no. 12, 2016.
- [19] D. G. Allen, D. A. Eisner, and C. H. Orchard, "Characterization of oscillations of intracellular calcium concentration in ferret ventricular muscle.," *J. Physiol.*, vol. 352, pp. 113–28, Jul. 1984.
- [20] G. L. Aistrup *et al.*, "Pacing-induced heterogeneities in intracellular Ca<sup>2+</sup> signaling, cardiac alternans, and ventricular arrhythmias in intact rat heart," *Circ. Res.*, vol. 99, no. 7, 2006.
- [21] J. A. Wasserstrom *et al.*, "Variability in timing of spontaneous calcium release in the intact

- rat heart is determined by the time course of sarcoplasmic reticulum calcium load," *Circ. Res.*, vol. 107, no. 9, 2010.
- [22] M. Ruiz-Meana *et al.*, "Ryanodine Receptor Glycation Favors Mitochondrial Damage in the Senescent Heart," *Circulation*, vol. 139, no. 7, 2019.
- [23] A. M. Janczewski and E. G. Lakatta, "Modulation of sarcoplasmic reticulum Ca<sup>2+</sup> cycling in systolic and diastolic heart failure associated with aging," *Heart Failure Reviews*, vol. 15, no. 5. 2010.
- [24] H. A. Feridooni, K. M. Dibb, and S. E. Howlett, "How cardiomyocyte excitation, calcium release and contraction become altered with age," *Journal of Molecular and Cellular Cardiology*, vol. 83. 2015.
- [25] S. Hamilton and D. Terentyev, "Altered Intracellular Calcium Homeostasis and Arrhythmogenesis in the Aged Heart," *International journal of molecular sciences*, vol. 20, no. 10. 2019.
- [26] A. P. Landstrom, D. Dobrev, and X. H. T. Wehrens, "Calcium Signaling and Cardiac Arrhythmias," *Circulation Research*, vol. 120, no. 12. 2017.
- [27] W. B. KANNEL, T. R. DAWBER, A. KAGAN, N. REVOTSKIE, and J. STOKES, "Factors of risk in the development of coronary heart disease--six year follow-up experience. The Framingham Study.," *Ann. Intern. Med.*, vol. 55, 1961.
- [28] U. N. Khot *et al.*, "Prevalence of Conventional Risk Factors in Patients with Coronary Heart Disease," *J. Am. Med. Assoc.*, vol. 290, no. 7, 2003.
- [29] C. W. Yancy *et al.*, "2013 ACCF/AHA Guideline for the Management of Heart Failure," *Circulation*, vol. 128, no. 16, 2013.
- [30] S. E. Lehnart, X. H. T. Wehrens, A. Kushnir, and A. R. Marks, "Cardiac ryanodine receptor function and regulation in heart disease," in *Annals of the New York Academy of Sciences*, 2004, vol. 1015.
- [31] D. T. Yue, E. Marban, and W. Gil Wier, "Relationship between force and intracellular [Ca<sup>2+</sup>] in tetanized mammalian heart muscle," *J. Gen. Physiol.*, vol. 87, no. 2, 1986.
- [32] A. E. Belevych, P. B. Radwański, C. A. Carnes, and S. Györke, "'Ryanopathy': Causes and manifestations of RyR2 dysfunction in heart failure," *Cardiovascular Research*, vol. 98, no. 2. 2013.
- [33] K. F. Frank, B. Böck, K. Brixius, E. G. Kranias, and R. H. G. Schwinger, "Modulation of SERCA: Implications for the failing human heart," *Basic Research in Cardiology, Supplement*, vol. 97, no. 1. 2002.
- [34] T. R. Shannon, S. M. Pogwizd, and D. M. Bers, "Elevated sarcoplasmic reticulum Ca<sup>2+</sup> leak in intact ventricular myocytes from rabbits in heart failure," *Circ. Res.*, vol. 93, no. 7, 2003.
- [35] R. C. Bond, S. M. Bryant, J. J. Watson, J. C. Hancox, C. H. Orchard, and A. F. James, "Reduced density and altered regulation of rat atrial L-type Ca<sup>2+</sup> current in heart failure," *Am. J. Physiol. - Hear. Circ. Physiol.*, vol. 312, no. 3, 2017.
- [36] S. M. Bryant, C. H. T. Kong, J. Watson, M. B. Cannell, A. F. James, and C. H. Orchard, "Altered distribution of I<sub>Ca</sub> impairs Ca release at the t-tubules of ventricular myocytes from failing hearts," *J. Mol. Cell. Cardiol.*, vol. 86, 2015.
- [37] B. Hegyi *et al.*, "Enhanced Depolarization Drive in Failing Rabbit Ventricular Myocytes: Calcium-Dependent and  $\beta$ -Adrenergic Effects on Late Sodium, L-Type Calcium, and Sodium-Calcium Exchange Currents," *Circ. Arrhythmia Electrophysiol.*, vol. 12, no. 3, 2019.
- [38] M. Nakamura and J. Sadoshima, "Mechanisms of physiological and pathological cardiac hypertrophy," *Nature Reviews Cardiology*, vol. 15, no. 7. 2018.
- [39] P. Ponikowski *et al.*, "2016 ESC Guidelines for the diagnosis and treatment of acute and chronic heart failure: The Task Force for the diagnosis and treatment of acute and chronic heart failure of the European Society of Cardiology (ESC). Developed with the special contribution of the Heart Failure Association (HFA) of the ESC," *Eur. J. Heart Fail.*, vol.



- 18, no. 8, 2016.
- [40] "Diagnosis and management of adults with chronic heart failure: summary of updated NICE guidance," *BMJ*, 2018.
- [41] D. D. Hayes, "Vaughan Williams classification of antiarrhythmic drugs," *Nursing (Lond)*., vol. 48, no. 11, 2018.
- [42] D. S. Echt *et al.*, "Mortality and Morbidity in Patients Receiving Encainide, Flecainide, or Placebo: The Cardiac Arrhythmia Suppression Trial," *N. Engl. J. Med.*, vol. 324, no. 12, 1991.
- [43] A. Njegic, C. Wilson, and E. J. Cartwright, "Targeting Ca<sup>2+</sup> Handling Proteins for the Treatment of Heart Failure and Arrhythmias," *Frontiers in Physiology*, vol. 11, 2020.
- [44] H. K. Hammond *et al.*, "Intracoronary gene transfer of adenylyl cyclase 6 in patients with heart failure: A randomized clinical trial," *JAMA Cardiol.*, vol. 1, no. 2, 2016.
- [45] D. Cowart, R. P. Venuti, K. Lynch, J. T. Guptill, R. J. Noveck, and S. Y. Foo, "A Phase 1 Randomized Study of Single Intravenous Infusions of the Novel Nitroxyl Donor BMS-986231 in Healthy Volunteers," *J. Clin. Pharmacol.*, vol. 59, no. 5, 2019.
- [46] C. Hayward, N. R. Banner, A. Morley-Smith, A. R. Lyon, and S. E. Harding, "The Current and Future Landscape of SERCA Gene Therapy for Heart Failure: A Clinical Perspective," *Human Gene Therapy*, vol. 26, no. 5, 2015.
- [47] J. S. Hulot, K. Ishikawa, and R. J. Hajjar, "Gene therapy for the treatment of heart failure: Promise postponed," *Eur. Heart J.*, vol. 37, no. 21, 2016.
- [48] B. Greenberg *et al.*, "Calcium upregulation by percutaneous administration of gene therapy in patients with cardiac disease (CUPID 2): A randomised, multinational, double-blind, placebo-controlled, phase 2b trial," *Lancet*, vol. 387, no. 10024, 2016.
- [49] M. Ferrandi *et al.*, "Istaroxime stimulates SERCA2a and accelerates calcium cycling in heart failure by relieving phospholamban inhibition," *Br. J. Pharmacol.*, vol. 169, no. 8, 2013.
- [50] J. K. Ghali *et al.*, "A Phase 1-2 Dose-Escalating Study Evaluating the Safety and Tolerability of Istaroxime and Specific Effects on Electrocardiographic and Hemodynamic Parameters in Patients with Chronic Heart Failure with Reduced Systolic Function," *Am. J. Cardiol.*, vol. 99, no. 2 SUPPL., 2007.
- [51] J. I. Goldhaber and M. A. Hamilton, "Role of inotropic agents in the treatment of heart failure," *Circulation*, vol. 121, no. 14, 2010.
- [52] N. M. Ashpole *et al.*, "Calcium/calmodulin-dependent protein kinase II (CaMKII) inhibition induces neurotoxicity via dysregulation of glutamate/calcium signaling and hyperexcitability," *J. Biol. Chem.*, vol. 287, no. 11, 2012.
- [53] S. Kobayashi *et al.*, "Dantrolene, a therapeutic agent for malignant hyperthermia, inhibits catecholaminergic polymorphic ventricular tachycardia in a RyR2R2474S/+ knock-in mouse model," *Circ. J.*, vol. 74, no. 12, 2010.
- [54] S. Kobayashi *et al.*, "A multicenter, randomized, double-blind, controlled study to evaluate the efficacy and safety of dantrolene on ventricular arrhythmia as well as mortality and morbidity in patients with chronic heart failure (SHO-IN trial): rationale and design," *J. Cardiol.*, vol. 75, no. 4, 2020.
- [55] H. Watanabe *et al.*, "Flecainide prevents catecholaminergic polymorphic ventricular tachycardia in mice and humans," *Nat. Med.*, vol. 15, no. 4, 2009.
- [56] A. Bossu, A. Kostense, H. D. M. Beekman, M. J. C. Houtman, M. A. G. van der Heyden, and M. A. Vos, "Istaroxime, a positive inotropic agent devoid of proarrhythmic properties in sensitive chronic atrioventricular block dogs," *Pharmacol. Res.*, vol. 133, 2018.
- [57] H. Tanaka, K. Nishimaru, T. Aikawa, W. Hirayama, Y. Tanaka, and K. Shigenobu, "Effect of SEA0400, a novel inhibitor of sodium-calcium exchanger, on myocardial ionic currents," *Br. J. Pharmacol.*, vol. 135, no. 5, 2002.
- [58] M. Mukai, H. Terada, S. Sugiyama, H. Satoh, and H. Hayashi, "Effects of a selective inhibitor of Na<sup>+</sup>/Ca<sup>2+</sup> exchange, KB-R7943, on reoxygenation-induced injuries in guinea

- pig papillary muscles," *J. Cardiovasc. Pharmacol.*, vol. 35, no. 1, 2000.
- [59] P. C. Chang, H. T. Wo, H. L. Lee, M. S. Wen, and C. C. Chou, "Paradoxical effects of KB-R7943 on arrhythmogenicity in a chronic myocardial infarction rabbit model," *J. Cardiol.*, vol. 66, no. 1, 2015.
- [60] D. A. Eisner, A. W. Trafford, M. E. Díaz, C. L. Overend, and S. C. O'Neill, "The control of Ca release from the cardiac sarcoplasmic reticulum: Regulation versus autoregulation," *Cardiovascular Research*, vol. 38, no. 3, 1998.
- [61] H. Shimizu *et al.*, "Mitochondrial Ca<sup>2+</sup> uptake by the voltage-dependent anion channel 2 regulates cardiac rhythmicity," *Elife*, vol. 4, Jan. 2015.
- [62] D. F. Wilson, K. Nishiki, and M. Erecińska, "Energy metabolism in muscle and its regulation during individual contraction-relaxation cycles," *Trends Biochem. Sci.*, vol. 6, pp. 16–19, Jan. 1981.
- [63] M. R. Duchen, "Contributions of mitochondria to animal physiology: from homeostatic sensor to calcium signalling and cell death," *J. Physiol.*, pp. 1–17, Apr. 1999.
- [64] Y. Kirichok, G. Krapivinsky, and D. E. Clapham, "The mitochondrial calcium uniporter is a highly selective ion channel," *Nature*, vol. 427, no. 6972, pp. 360–364, Jan. 2004.
- [65] J. M. Baughman *et al.*, "Integrative genomics identifies MCU as an essential component of the mitochondrial calcium uniporter," *Nature*, vol. 476, no. 7360, pp. 341–345, Jun. 2011.
- [66] D. De Stefani, A. Raffaello, E. Teardo, I. Szabò, and R. Rizzuto, "A forty-kilodalton protein of the inner membrane is the mitochondrial calcium uniporter," *Nature*, vol. 476, no. 7360, pp. 336–340, Jun. 2011.
- [67] G. Csordás, A. P. Thomas, and G. Hajnóczky, "Calcium signal transmission between ryanodine receptors and mitochondria in cardiac muscle," *Trends in Cardiovascular Medicine*, vol. 11, no. 7, 2001.
- [68] G. W. Dorn and C. Maack, "SR and mitochondria: Calcium cross-talk between kissing cousins," *J. Mol. Cell. Cardiol.*, vol. 55, pp. 42–49, 2013.
- [69] E. Barth, G. Stämmler, B. Speiser, and J. Schaper, "Ultrastructural quantitation of mitochondria and myofilaments in cardiac muscle from 10 different animal species including man," *J. Mol. Cell. Cardiol.*, vol. 24, no. 7, pp. 669–81, Jul. 1992.
- [70] V. K. Sharma, V. Ramesh, C. Franzini-Armstrong, and S.-S. Sheu, "Transport of Ca<sup>2+</sup> from Sarcoplasmic Reticulum to Mitochondria in Rat Ventricular Myocytes," *J. Bioenerg. Biomembr.*, vol. 32, no. 1, pp. 97–104, 2000.
- [71] E. N. Dedkova and L. A. Blatter, "Calcium signaling in cardiac mitochondria," *J. Mol. Cell. Cardiol.*, vol. 58, pp. 125–33, May 2013.
- [72] E. A. Rog-Zielinska, C. M. Johnston, E. T. O'Toole, M. Morphey, A. Hoenger, and P. Kohl, "Electron tomography of rabbit cardiomyocyte three-dimensional ultrastructure," *Prog. Biophys. Mol. Biol.*, vol. 121, no. 2, 2016.
- [73] V. Robert *et al.*, "Beat-to-beat oscillations of mitochondrial [Ca<sup>2+</sup>] in cardiac cells," *EMBO J.*, vol. 20, no. 17, 2001.
- [74] G. Szabadkai *et al.*, "Chaperone-mediated coupling of endoplasmic reticulum and mitochondrial Ca<sup>2+</sup> channels," *J. Cell Biol.*, vol. 175, no. 6, 2006.
- [75] C. K. Min *et al.*, "Coupling of ryanodine receptor 2 and voltage-dependent anion channel 2 is essential for Ca<sup>2+</sup> transfer from the sarcoplasmic reticulum to the mitochondria in the heart," *Biochem. J.*, vol. 447, no. 3, pp. 371–379, Nov. 2012.
- [76] M. K. Schweitzer *et al.*, "Suppression of Arrhythmia by Enhancing Mitochondrial Ca<sup>2+</sup> Uptake in Catecholaminergic Ventricular Tachycardia Models," *JACC Basic to Transl. Sci.*, vol. 2, no. 6, 2017.
- [77] E. H. Y. Cheng, T. V. Sheiko, J. K. Fisher, W. J. Craigen, and S. J. Korsmeyer, "VDAC2 inhibits BAK activation and mitochondrial apoptosis," *Science (80-. )*, vol. 301, no. 5632, 2003.

- [78] F. Wilting *et al.*, "The antiarrhythmic compound efsevin directly modulates voltage-dependent anion channel 2 by binding to its inner wall and enhancing mitochondrial Ca<sup>2+</sup> uptake," *Br. J. Pharmacol.*, vol. 177, no. 13, 2020.
- [79] P. Sander, T. Gudermann, and J. Schredelseker, "A calcium guard in the outer membrane: Is vdac a regulated gatekeeper of mitochondrial calcium uptake?," *International Journal of Molecular Sciences*, vol. 22, no. 2, 2021.
- [80] H. F. DELUCA and G. W. ENGSTROM, "Calcium uptake by rat kidney mitochondria.," *Proc. Natl. Acad. Sci. U. S. A.*, vol. 47, pp. 1744–50, Nov. 1961.
- [81] X. Pan *et al.*, "The physiological role of mitochondrial calcium revealed by mice lacking the mitochondrial calcium uniporter.," *Nat. Cell Biol.*, vol. 15, no. 12, pp. 1464–72, Dec. 2013.
- [82] S. Feno, R. Rizzuto, A. Raffaello, and D. Vecellio Reane, "The molecular complexity of the Mitochondrial Calcium Uniporter," *Cell Calcium*, vol. 93, 2021.
- [83] Y. Sancak *et al.*, "EMRE Is an Essential Component of the Mitochondrial Calcium Uniporter Complex," *Science (80-. )*, vol. 342, no. 6164, pp. 1379–1382, Dec. 2013.
- [84] F. Perocchi *et al.*, "MICU1 encodes a mitochondrial EF hand protein required for Ca<sup>2+</sup> uptake," *Nature*, vol. 467, no. 7313, pp. 291–296, Sep. 2010.
- [85] M. Patron, V. Granatiero, J. Espino, R. Rizzuto, and D. De Stefani, "MICU3 is a tissue-specific enhancer of mitochondrial calcium uptake," *Cell Death Differ.*, vol. 26, no. 1, 2019.
- [86] Y. Kirichok, G. Krapivinsky, and D. E. Clapham, "The mitochondrial calcium uniporter is a highly selective ion channel," *Nature*, vol. 427, no. 6972, pp. 360–364, Jan. 2004.
- [87] R. Rizzuto, M. Brini, M. Murgia, and T. Pozzan, "Microdomains with high Ca<sup>2+</sup> close to IP<sub>3</sub>-sensitive channels that are sensed by neighboring mitochondria.," *Science*, vol. 262, no. 5134, pp. 744–7, Oct. 1993.
- [88] G. S. B. Williams, L. Boyman, A. C. Chikando, R. J. Khairallah, and W. J. Lederer, "Mitochondrial calcium uptake.," *Proc. Natl. Acad. Sci. U. S. A.*, vol. 110, no. 26, pp. 10479–86, Jun. 2013.
- [89] M. J. Berridge, "Calcium microdomains: Organization and function," *Cell Calcium*, vol. 40, no. 5–6, 2006.
- [90] C. K. Min *et al.*, "Coupling of ryanodine receptor 2 and voltage-dependent anion channel 2 is essential for Ca<sup>2+</sup> transfer from the sarcoplasmic reticulum to the mitochondria in the heart," *Biochem. J.*, vol. 447, no. 3, 2012.
- [91] S. De la Fuente and S. S. Sheu, "SR-mitochondria communication in adult cardiomyocytes: A close relationship where the Ca<sup>2+</sup> has a lot to say," *Archives of Biochemistry and Biophysics*, vol. 663, 2019.
- [92] S. De La Fuente *et al.*, "Spatial Separation of Mitochondrial Calcium Uptake and Extrusion for Energy-Efficient Mitochondrial Calcium Signaling in the Heart," *Cell Rep.*, vol. 24, no. 12, 2018.
- [93] H. Xu *et al.*, "IP<sub>3</sub>R-Grp75-VDAC1-MCU calcium regulation axis antagonists protect podocytes from apoptosis and decrease proteinuria in an Adriamycin nephropathy rat model," *BMC Nephrol.*, vol. 19, no. 1, 2018.
- [94] Y. Liao, Y. Hao, H. Chen, Q. He, Z. Yuan, and J. Cheng, "Mitochondrial calcium uniporter protein MCU is involved in oxidative stress-induced cell death," *Protein Cell*, vol. 6, no. 6, 2015.
- [95] M. Montero *et al.*, "Direct activation of the mitochondrial calcium uniporter by natural plant flavonoids," *Biochem. J.*, vol. 384, no. 1, 2004.
- [96] K. P. Devi *et al.*, "Kaempferol and inflammation: From chemistry to medicine," *Pharmacological Research*, vol. 99, 2015.
- [97] D. M. Arduino *et al.*, "Systematic Identification of MCU Modulators by Orthogonal Interspecies Chemical Screening," *Mol. Cell*, vol. 67, no. 4, 2017.
- [98] M. Chen, Y. Wang, T. Hou, H. Zhang, A. Qu, and X. Wang, "Differential mitochondrial

- calcium responses in different cell types detected with a mitochondrial calcium fluorescent indicator, mito-GCaMP2," *Acta Biochim. Biophys. Sin. (Shanghai)*, vol. 43, no. 10, 2011.
- [99] C. Mammucari, A. Raffaello, D. Vecellio Reane, G. Gherardi, A. De Mario, and R. Rizzuto, "Mitochondrial calcium uptake in organ physiology: from molecular mechanism to animal models," *Pflugers Archiv European Journal of Physiology*, vol. 470, no. 8. 2018.
- [100] F. Fieni, S. B. Lee, Y. N. Jan, and Y. Kirichok, "Activity of the mitochondrial calcium uniporter varies greatly between tissues," *Nat. Commun.*, vol. 3, 2012.
- [101] A. Raffaello *et al.*, "The mitochondrial calcium uniporter is a multimer that can include a dominant-negative pore-forming subunit," *EMBO J.*, vol. 32, no. 17, pp. 2362–2376, Jul. 2013.
- [102] A. D. Langenbacher *et al.*, "Mutation in sodium-calcium exchanger 1 (NCX1) causes cardiac fibrillation in zebrafish," *Proc. Natl. Acad. Sci. U. S. A.*, vol. 102, no. 49, pp. 17699–704, Dec. 2005.
- [103] M. Cerrone *et al.*, "Bidirectional Ventricular Tachycardia and Fibrillation Elicited in a Knock-In Mouse Model Carrier of a Mutation in the Cardiac Ryanodine Receptor," *Circ. Res.*, vol. 96, no. 10, pp. e77–e82, May 2005.
- [104] H. A. Rockman *et al.*, "Segregation of atrial-specific and inducible expression of an atrial natriuretic factor transgene in an in vivo murine model of cardiac hypertrophy," *Proc. Natl. Acad. Sci. U. S. A.*, vol. 88, no. 18, 1991.
- [105] A. C. deAlmeida, R. J. van Oort, and X. H. T. Wehrens, "Transverse aortic constriction in mice," *J. Vis. Exp.*, no. 38, 2010.



## 6 Publication I

Received: 26 November 2020 | Revised: 21 June 2021 | Accepted: 30 June 2021

DOI: 10.1111/bph.15630

### RESEARCH ARTICLE



# Approved drugs ezetimibe and disulfiram enhance mitochondrial $\text{Ca}^{2+}$ uptake and suppress cardiac arrhythmogenesis

Paulina Sander<sup>1</sup> | Michael Feng<sup>2</sup> | Maria K. Schweitzer<sup>1</sup> | Fabiola Wilting<sup>1</sup> |  
 Sophie M. Gutenthaler<sup>1</sup> | Daniela M. Arduino<sup>2</sup> | Sandra Fischbach<sup>1</sup> |  
 Lisa Dreizehnter<sup>3</sup> | Alessandra Moretti<sup>3,4</sup> | Thomas Gudermann<sup>1,4</sup> |  
 Fabiana Perocchi<sup>2,5</sup> | Johann Schredelseker<sup>1,4</sup>

<sup>1</sup>Walther Straub Institute of Pharmacology and Toxicology, Faculty of Medicine, LMU Munich, Munich, Germany

<sup>2</sup>Institute for Diabetes and Obesity, Helmholtz Diabetes Center (HDC), Helmholtz Zentrum München, Neuherberg, Germany

<sup>3</sup>I. Department of Medicine, Cardiology, Klinikum rechts der Isar, Technische Universität München, Munich, Germany

<sup>4</sup>Partner Site Munich Heart Alliance (MHA), Deutsches Zentrum für Herz-Kreislauf-Forschung (DZHK), Munich, Germany

<sup>5</sup>Munich Cluster for Systems Neurology, Munich, Germany

#### Correspondence

Johann Schredelseker, Walther Straub Institute of Pharmacology and Toxicology, Faculty of Medicine, LMU Munich, Nussbaumstr. 26, D-80336, Munich, Germany. Email: johann.schredelseker@lmu.de

#### Funding information

Deutsche Forschungsgemeinschaft, Grant/Award Numbers: SCHR 1471/1-1, TRR 152; Helmholtz-Gemeinschaft, Grant/Award Number: Initiative and Network Fund ExNet-0041-Phase2-3; Munich Center for Systems Neurology, Grant/Award Numbers: SyNergy EXC 2145, SyNergy EXC 2145/ID 390857198; Initiative and Network Fund of the Helmholtz Association, Grant/Award Number: ExNet-0041-Phase2-3; Bert L & N Kuggie Vallee Foundation

**Background and Purpose:** Treatment of cardiac arrhythmia remains challenging due to severe side effects of common anti-arrhythmic drugs. We previously demonstrated that mitochondrial  $\text{Ca}^{2+}$  uptake in cardiomyocytes represents a promising new candidate structure for safer drug therapy. However, druggable agonists of mitochondrial  $\text{Ca}^{2+}$  uptake suitable for preclinical and clinical studies are still missing.

**Experimental Approach:** Here we screened 727 compounds with a history of use in human clinical trials in a three-step screening approach. As a primary screening platform we used a permeabilized HeLa cell-based mitochondrial  $\text{Ca}^{2+}$  uptake assay. Hits were validated in cultured HL-1 cardiomyocytes and finally tested for anti-arrhythmic efficacy in three translational models: a  $\text{Ca}^{2+}$  overload zebrafish model and cardiomyocytes of both a mouse model for catecholaminergic polymorphic ventricular tachycardia (CPVT) and induced pluripotent stem cell derived cardiomyocytes from a CPVT patient.

**Key Results:** We identified two candidate compounds, the clinically approved drugs ezetimibe and disulfiram, which stimulate SR-mitochondria  $\text{Ca}^{2+}$  transfer at nanomolar concentrations. This is significantly lower compared to the previously described mitochondrial  $\text{Ca}^{2+}$  uptake enhancers (MiCUp) efsevin, a gating modifier of the voltage-dependent anion channel 2, and kaempferol, an agonist of the mitochondrial  $\text{Ca}^{2+}$  uniporter. Both substances restored rhythmic cardiac contractions in a zebrafish cardiac arrhythmia model and significantly suppressed arrhythmogenesis in freshly isolated ventricular cardiomyocytes from a CPVT mouse model as well as induced pluripotent stem cell derived cardiomyocytes from a CPVT patient.

**Abbreviations:** AEQ<sub>mt</sub>, mitochondrial matrix-targeted aequorin; CPVT, catecholaminergic polymorphic ventricular tachycardia; MiCUp, mitochondrial  $\text{Ca}^{2+}$  uptake enhancer; NCC, NIH Clinical Collection; RyR, ryanodine receptor; SR, sarcoplasmic reticulum; *tre*, *tremblor*; VDACC2, voltage-dependent anion channel 2.

This is an open access article under the terms of the Creative Commons Attribution License, which permits use, distribution and reproduction in any medium, provided the original work is properly cited.

© 2021 The Authors. *British Journal of Pharmacology* published by John Wiley & Sons Ltd on behalf of British Pharmacological Society.

**Conclusion and Implications:** Taken together we identified ezetimibe and disulfiram as novel MiCUPS and efficient suppressors of arrhythmogenesis and as such as, promising candidates for future preclinical and clinical studies.

**KEYWORDS**

anti-arrhythmic, arrhythmia, CPVT, MCU, mitochondrial  $\text{Ca}^{2+}$  uptake pathway, mitochondrial  $\text{Ca}^{2+}$  uptake enhancers, mitochondria

## 1 | INTRODUCTION

While mortality and morbidity rates related to cardiovascular diseases are generally declining, arrhythmia-related incidents are still on the rise (Benjamin et al., 2018). This is in part related to limited effectiveness and major side effects of common anti-arrhythmic drugs. Anti-arrhythmic drugs of Vaughan Williams class I, III and IV act by targeting plasma membrane ion channels and suppressing propagation of ectopic signals. However, due to their effects on the cardiac action potential and thus cardiac conduction speed, they are prone to proarrhythmic side effects. Therefore, novel therapeutic strategies that suppress the initiation of arrhythmogenic signals inside cardiomyocytes are currently in focus of the search for novel and safer anti-arrhythmic therapies.

We have recently demonstrated a critical role of mitochondrial  $\text{Ca}^{2+}$  uptake for the regulation of cardiac rhythmicity (Shimizu et al., 2015). The cardiac contraction cycle is initiated by influx of extracellular  $\text{Ca}^{2+}$  into cardiomyocytes and subsequent  $\text{Ca}^{2+}$  release predominantly from the sarcoplasmic reticulum (SR) to initiate muscle contraction (Bers, 2002, 2008). Mitochondria are located in close proximity to the SR (Rog-Zielinska et al., 2016) and can rapidly take up  $\text{Ca}^{2+}$  on a beat-to-beat interval (Robert et al., 2001) through a selective mitochondrial  $\text{Ca}^{2+}$  uptake pathway consisting of pore proteins in both mitochondrial membranes and several positive and negative regulators (Baughman et al., 2011; De Stefani et al., 2011; Kirichok et al., 2004; Waldeck-Weiermair et al., 2013). In cardiomyocytes, the mitochondrial  $\text{Ca}^{2+}$  uptake pathway is directly tethered to the  $\text{Ca}^{2+}$  release sites of the SR. Within the  $\text{Ca}^{2+}$  microdomain around the  $\text{Ca}^{2+}$  release sites of the SR, the local cytosolic  $\text{Ca}^{2+}$  concentration reaches values high enough to activate the mitochondrial  $\text{Ca}^{2+}$  uptake pathway allowing for rapid and direct shuttling of  $\text{Ca}^{2+}$  from the SR into mitochondria (De la Fuente et al., 2016; De la Fuente & Sheu, 2019). Under pathological conditions, erratic  $\text{Ca}^{2+}$  release of single  $\text{Ca}^{2+}$  release sites in form of  $\text{Ca}^{2+}$  sparks followed by  $\text{Ca}^{2+}$  waves during diastole leads to spontaneous contractions and arrhythmia (Allen et al., 1984). Pharmacological activation of mitochondrial- $\text{Ca}^{2+}$  uptake locally buffers these events and thereby suppresses arrhythmogenic signals in cardiomyocytes, while systolic events remain unaltered (Shimizu et al., 2015). Indeed, treatment with agonists of mitochondrial- $\text{Ca}^{2+}$  uptake suppressed episodes of arrhythmia in a murine model for catecholaminergic polymorphic ventricular tachycardia (CPVT) (Schweitzer et al., 2017). Interestingly,

### What is already known

- Cardiac arrhythmia results from imbalances in cellular  $\text{Ca}^{2+}$  homeostasis.
- Activation of mitochondrial  $\text{Ca}^{2+}$  uptake suppresses arrhythmogenic  $\text{Ca}^{2+}$  signals during diastole.

### What does this study add

- The two clinically approved drugs, ezetimibe and disulfiram activate mitochondrial  $\text{Ca}^{2+}$  uptake.
- Both efficiently suppress arrhythmogenesis in translational models in a nanomolar range.

### What is the clinical significance

- The results strengthen mitochondrial  $\text{Ca}^{2+}$  uptake as a pharmacological target.
- The identification of clinically approved drugs allows for repurposing studies.

despite enhancing mitochondrial  $\text{Ca}^{2+}$  uptake over several days, no signs of severe adverse effects, for example, apoptosis, were observed neither in cellular nor in animal models (Schweitzer et al., 2017; Shimizu et al., 2015). Modulation of mitochondrial- $\text{Ca}^{2+}$  uptake could thus serve as novel pharmacological strategy for the treatment of human cardiac arrhythmias.

This can be accomplished by agonists of either the voltage-dependent anion channel 2 (VDAC2) in the outer mitochondrial membrane or the mitochondrial  $\text{Ca}^{2+}$  uniporter in the inner mitochondrial membrane. Two such compounds, the VDAC2 gating modulator **efsevin** (Shimizu et al., 2015; Wilting et al., 2020) and the mitochondrial  $\text{Ca}^{2+}$  uniporter agonist **kaempferol** (Montero et al., 2004), were found to be effective in reducing arrhythmia, thus providing a proof of concept that mitochondrial  $\text{Ca}^{2+}$  uptake enhancers (MiCUPS) represent, in this respect, a pharmacologically highly relevant class of molecules. However, both drugs are so far only used experimentally and are currently too poorly characterized to have clinical potential.

Furthermore, both are effective at concentrations around 10–20  $\mu\text{M}$  at the *in vitro* target site, making them poor candidates for clinical use.

Here, we applied a three-step protocol to identify novel MiCUpS. First, we screened a chemical library consisting of 727 compounds with a history of use in human clinical trials for novel mitochondrial  $\text{Ca}^{2+}$  uptake enhancers using an established screening platform for mitochondrial  $\text{Ca}^{2+}$  uptake modifiers (Arduino et al., 2017). We identified three hits, the FDA- and EMA-approved drugs, **ezetimibe** and **disulfiram**, and the natural compound **honokiol**, which significantly increased mitochondrial- $\text{Ca}^{2+}$  uptake in permeabilized HeLa cells. To transfer these results to a cardiac system, we measured SR-mitochondria  $\text{Ca}^{2+}$  transfer in a standardized cultured cardiomyocyte assay (Schweitzer et al., 2017; Wilting et al., 2020) and found that two of them, ezetimibe and disulfiram, enhanced SR-mitochondria  $\text{Ca}^{2+}$  transfer at significantly lower concentrations than efsevin and kaempferol. Finally, we performed efficacy testing in translational arrhythmia models (Schweitzer et al., 2017; Shimizu et al., 2015) and found that both substances suppress cardiac fibrillation in zebrafish embryos and arrhythmogenic  $\text{Ca}^{2+}$  signals in murine and human cardiomyocytes carrying mutations associated with CPVT. Altogether, we identified two highly interesting candidates for further preclinical and clinical testing of MiCUp-based anti-arrhythmic therapy.

## 2 | METHODS

### 2.1 | Primary drug screen in permeabilized HeLa cells

Drug screening was performed as described previously (Arduino et al., 2017). Briefly, HeLa cells (ATCC, RRID:CVCL\_0030) stably expressing a mitochondrial matrix-targeted aequorin ( $\text{AEQ}_{\text{mt}}$ ) were grown in Dulbecco's modified Eagle's medium with high-glucose, 10% FBS and 100  $\mu\text{g}\cdot\text{mL}^{-1}$  geneticin (Life Technologies). On the day of the experiment, active aequorin was reconstituted from apoaequorin in the mitochondrial matrix by incubating cells with 3- $\mu\text{M}$  coelenterazine derivative *n* (Biotium) for 3 h at room temperature. Then,  $\text{Ca}^{2+}$  was depleted from intracellular stores by incubation with 200-nM **thapsigargin** (VWR) for 20 min, and cells were permeabilized with 60- $\mu\text{M}$  digitonin for 5 min. Experiments were performed in an intracellular-like buffer containing (in mM) 140 KCl, 1  $\text{KH}_2\text{PO}_4/\text{K}_2\text{HPO}_4$ , 1  $\text{MgCl}_2$ , 20 HEPES, 1  $\text{Na}^+$ -pyruvate, 1 ATP/ $\text{MgCl}_2$ , 2  $\text{Na}^+$ -succinate and 0.1 EGTA as a  $\text{Ca}^{2+}$  chelator (pH 7.2 with KOH) at a density of  $\sim 70,000$  cells/well in a white 96-well compound plate. The NIH Clinical Collection (NCC) library, consisting of 727 compounds (10  $\mu\text{M}$ , in 0.1% [v/v] DMSO) was screened in biological duplicates. DMSO (0.1%) was used as a vehicle control and Ru360 (10  $\mu\text{M}$ , VWR), a classical inhibitor of mitochondrial  $\text{Ca}^{2+}$  uniporter, was used as an experimental control to prove that aequorin luminescence is selective for mitochondrial  $\text{Ca}^{2+}$  uniporter (MCU)-mediated mitochondrial  $\text{Ca}^{2+}$  uptake. Permeabilized cells were incubated in the presence of compounds for 5 min at room temperature and  $\text{Ca}^{2+}$ -stimulated light

signals upon a bolus application of 4- $\mu\text{M}$  free  $\text{Ca}^{2+}$  was recorded at 469 nm every 0.1 s with a luminescence counter (MicroBeta<sup>2</sup> LumiJET Microplate Counter, PerkinElmer). Drug screens were analysed as described previously (Arduino et al., 2017). Briefly, after smoothing the dynamics of mitochondrial- $\text{Ca}^{2+}$ -dependent luminescence obtained for each compound using a cubic spline function as described previously (Arduino et al., 2017), both peak (maximal amplitude of the luminescence signal) and uptake rate (left slope) were automatically determined. Based on these parameters a score ( $S_{\text{drug}}$ ) was assigned to each compound as shown in Figure 1.

### 2.2 | Mitochondrial $\text{Na}^+/\text{Ca}^{2+}$ exchanger-mediated $\text{Ca}^{2+}$ extrusion assay

HeLa cells were harvested in an external medium containing (in mM): 145 NaCl, 5 KCl, 1  $\text{MgCl}_2$ , 10 glucose, 10 HEPES and 0.5 EGTA (pH 7.4/NaOH), treated with 200-nM thapsigargin (VWR) for 10 min and resuspended in an intracellular-like buffer containing (in mM) 140 KCl, 3  $\text{KH}_2\text{PO}_4$ , 2.5  $\text{MgCl}_2$ , 10 HEPES, 0.05 EGTA, 5 Malate, 5 Pyruvate, 5 Succinate, pH 7.4 with KOH. After permeabilization with 60- $\mu\text{M}$  digitonin for 3 min, cells were resuspended in intracellular-like buffer with 0.1- $\mu\text{M}$  calcium green-5N (Thermo Fischer), seeded into a black 96-well plate at a density of  $\sim 1$  million cells/well and incubated for 5 min with compounds or vehicle (0.1% DMSO) before measurements. Calcium Green-5N fluorescence was monitored at Ex506/Em531 every 8 s at room temperature using a CLARIOstar microplate reader (BMG Labtech Perkin-Elmer Envision) and injected with  $\text{CaCl}_2$  (100  $\mu\text{M}$ ). After 3 min, the mitochondrial  $\text{Ca}^{2+}$  uniporter inhibitor Ru360 (10  $\mu\text{M}$ , VWR) was added to each well together with either vehicle or the mitochondrial  $\text{Na}^+/\text{Ca}^{2+}$  exchanger inhibitor CGP-37157 (10  $\mu\text{M}$ , VWR). Afterwards, 60-mM NaCl was injected and mitochondrial  $\text{Na}^+/\text{Ca}^{2+}$  exchanger-dependent  $\text{Ca}^{2+}$  efflux was recorded.

### 2.3 | SR-mitochondria $\text{Ca}^{2+}$ transfer

$\text{Ca}^{2+}$  transfer from the SR into mitochondria was measured as described in Schweitzer et al. (2017). In brief, HL-1 cardiomyocytes (RRID:CVCL\_0303, received as a gift from Dr. William Claycomb, Louisiana State University) (Claycomb et al., 1998) were plated in a 96-well plate randomly assigned to experimental groups of equal group size, loaded with 4- $\mu\text{M}$  Rhod-2, AM (Thermo Fisher) and permeabilized with 25- $\mu\text{M}$  digitonin in internal solution (in mM: 1 BAPTA (VWR), 20 HEPES, 100 L-aspartic acid potassium salt, 40 KCl, 0.5  $\text{MgCl}_2$ , 2 maleic acid, 2 glutamic acid, 5 pyruvic acid, 0.5  $\text{KH}_2\text{PO}_4$ , 5  $\text{MgATP}$  and 0.47  $\text{CaCl}_2$ , [pH = 7.2 with Trizma base]). Fluorescence at Ex = 540  $\pm$  9 nm and Em = 580  $\pm$  20 nm was recorded on an Infinite<sup>®</sup> 200 PRO multimode reader (Tecan, Maennedorf, Switzerland). After 22 s, caffeine was injected to a final concentration of 10 mM. To exclude signals that are not related to  $\text{Ca}^{2+}$  mobilizations, all experiments included a control well with **ruthenium red**, as a blocker



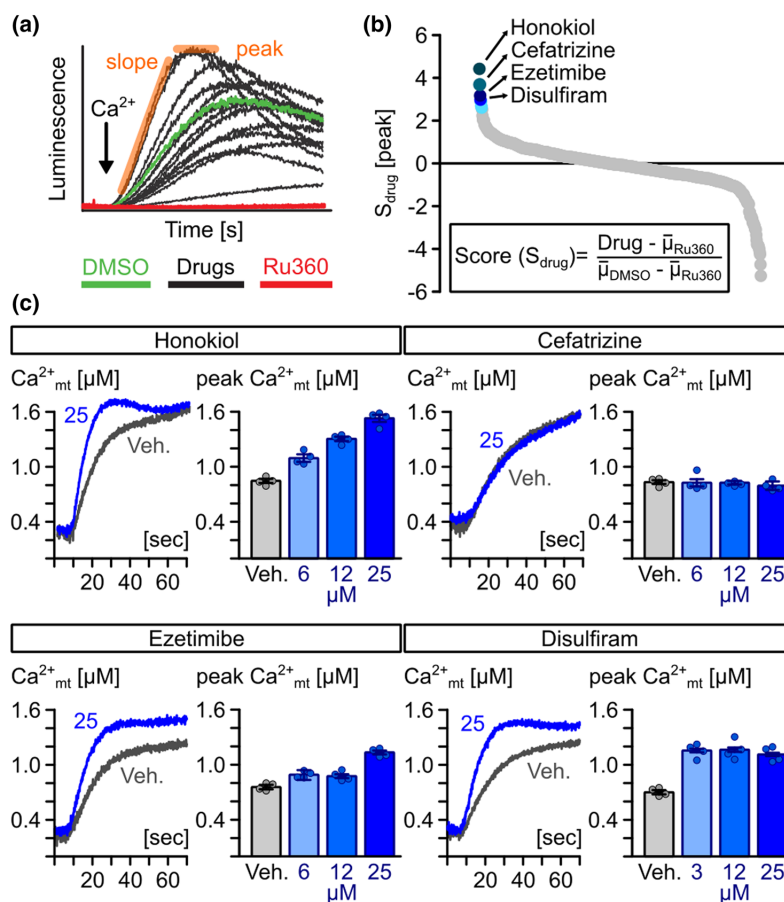


**FIGURE 1** Identification of novel MiCups by chemical screening. (a) Example of Ca<sup>2+</sup>-dependent, mitochondrial aequorin kinetics in digitonin-permeabilized HeLa cells upon the addition of 4-µM free Ca<sup>2+</sup> (black arrow) in the presence of candidate drugs (10 µM), experimental (10-µM Ru360) and vehicle controls (0.1% [v/v] DMSO). (b) Ranking of compounds based on  $S_{drug}$  scores. (c) Representative traces of averaged mitochondrial Ca<sup>2+</sup> kinetics and quantification of mitochondrial (mt)-Ca<sup>2+</sup> uptake rate in mitochondria of permeabilized HeLa cells treated with different concentrations of honokiol, cefatrizine, ezetimibe and disulfiram and 0.1% (v/v) DMSO (vehicle; Veh.) (n = 4)

for SR-mitochondria Ca<sup>2+</sup> transfer (ryanodine receptor/RyR, VDAC and mitochondrial Ca<sup>2+</sup> uniporter), and only experiments in which SR-mitochondria Ca<sup>2+</sup> transfer was blocked by ruthenium red were included in the analysis. Cells were visually inspected after measurement and only recordings from wells where cells were still attached and morphologically intact were used for analysis. EC50 values were calculated using Quest Graph™ EC50 Calculator (AAT Bioquest, Inc.) at <https://www.aatbio.com/tools/ec50-calculator>.

## 2.4 | Cytosolic Ca<sup>2+</sup> measurements on HL-1 cardiomyocytes

For the measurement of Ca<sup>2+</sup> release, HL-1 cells were plated in a 96-well plate loaded with 5-µM fura-2, AM (Thermo Fisher) or 1 h at 37°C, before washing with external solution (in mM: 140 NaCl, 6 KCl, 2 CaCl<sub>2</sub>, 1 MgCl<sub>2</sub>, 10 glucose, 20 HEPES, pH = 7.4 with NaOH). After 30 min incubation to allow for total de-esterification of the dye, cells were washed, randomly assigned to experimental groups, and measured in an Infinite® 200 PRO multimode reader (Tecan, Maennedorf, Switzerland) at Ex = 340 ± 9 nm and 380 ± 9 nm and Em = 510

± 20 nm. Test compounds were added 5 min prior to the experiment. Caffeine to a final concentration of 10 mM was added 22 s after start of the recording.

## 2.5 | Isolation of ventricular cardiomyocytes from RyR2<sup>R4496C/WT</sup> mice

Mice from strain RyR2<sup>tm15gp</sup> (RRID: MGI:3653876) mimic the human CPVT phenotype (Cerrone et al., 2005) and were used as models for human cardiac arrhythmia. Mice were bred in the animal facility of the Walther Straub Institute of Pharmacology and Toxicology at LMU Munich, which is approved by the Bavarian animal welfare committee. Mice were kept in groups of 5–6 animals in ventilated plastic cages with wood shavings (Blue Line, Tecniplast, Buguggiate, Italy). Ventricular cardiomyocytes of 8–16 weeks old male and female mice were isolated by retrograde perfusion through the aorta as described previously (O'Connell et al., 2007; Schweitzer et al., 2017). After cervical dislocation, the heart was excised and placed on a Langendorff mode perfusion system. Tissue was digested by perfusion with Liberase™ TM at a final concentration of 0.075 ml·ml<sup>-1</sup> for 6 min. After

mechanical separation of the ventricles by trituration, cardiomyocytes were consecutively transferred into Tyrode's solution with 0.1, 0.5 and finally 1-mM  $\text{CaCl}_2$  to reintroduce physiological  $\text{Ca}^{2+}$  concentrations. Only excitable, rod-shaped, quiescent cells were used for experiments. All animal procedures had local approval and conformed to the guidelines from Directive 2010/63/EU on the protection of animals used for scientific purposes.

## 2.6 | Human iPSC cardiomyocytes

Human iPSCs from a 60-year-old male donor presenting with a severe form of CPVT were generated as described previously (Moretti et al., 2010). Spontaneously beating areas were explanted after 2–5 months and enzymatically dissociated into single cardiomyocytes. Single cells were plated on fibronectin-coated glass bottom dishes (MatTek, Ashland, MA, USA) and used for experiments at approximately 7 days after dissociation (Schweitzer et al., 2017). Individual dishes were randomly assigned to experimental groups. Human iPSC generation was performed under a human research subject protocol approved by the institutional review boards and the ethic committee of the Klinikum rechts der Isar, Technical University of Munich, which strictly complied with the Helsinki Declaration regarding donor source. Written informed consent was obtained from the affected patient and healthy volunteer.

## 2.7 | Confocal $\text{Ca}^{2+}$ imaging

$\text{Ca}^{2+}$  waves were analysed by confocal microscopy as described previously (Schweitzer et al., 2017). In brief, cardiomyocytes were loaded with 1- $\mu\text{M}$  Fluo-4, AM (Thermo Fisher), and  $\text{Ca}^{2+}$  transients were elicited by electric field stimulation using a S48 square pulse Stimulator (Grass Technologies, Warwick, RI, USA) on an inverted confocal microscope (Leica TCS SP5 or Zeiss LSM 880). Line scan series were generated along the long axis of a myocyte. After reaching steady state pulsing was stopped and cells were analysed for the occurrence of spontaneous diastolic  $\text{Ca}^{2+}$  waves. Every experiment contained a group with isoprenaline and only preparations that were sensitive to stimulation with isoprenaline were used for drug testing. Depending to the quality of the preparation and the yield of cells, the remaining cells were randomly attributed to experimental groups. All groups were measured in random order to avoid the influence of a decrease in the quality of cells over time and were stopped when cell quality decreased as indicated by a hyperexcitability or insensitivity to external stimuli.

## 2.8 | Zebrafish husbandry and phenotype rescue experiments

Zebrafish of the mutant line Tg (*myl7:eGFP*)/*tremblor* (*tre*<sup>tc318d</sup>, RRID:ZFIN\_ZDB-GENO-150505-3) were used as a model for  $\text{Ca}^{2+}$ -induced cardiac arrhythmia (Shimizu et al., 2015) and were

maintained and bred in the animal facility of the Walther Straub Institute of Pharmacology and Toxicology at LMU Munich, which is approved by the Bavarian animal welfare committee. Fish are kept in groups of approximately 10 adult fish in modified mouse cages in a stand-alone zebrafish rack (PP Module, Aqua Schwarz, Göttingen, Germany) under constant surveillance of water quality. Embryos collected from heterozygous *tre* crosses were kept in E3 buffer (in mM: 5 NaCl, 0.33  $\text{MgSO}_4$ , 0.17 KCl, 0.33  $\text{CaCl}_2$ ) and randomly distributed into equal groups of 50–20 embryos exposed to test substances starting at 6 h post fertilization (hpf). Depending on the size of clutches 2–4 groups could be tested in one experiment. Embryos were dechorionated with 30  $\mu\text{g}\cdot\text{mL}^{-1}$  protease from *Streptomyces griseus* at 26 hpf and cardiac function was analysed at 30 hpf by visual examination of the embryonic hearts under a fluorescence stereomicroscope (Euromex DZ5040). Only groups with homogeneous, synchronized development of all embryos were analysed. All animal procedures had local approval and conformed to the guidelines from Directive 2010/63/EU on the protection of animals used for scientific purposes.

## 2.9 | Data and Statistical analysis

Data and statistical analysis complied with the recommendations of the *British Journal of Pharmacology* on experimental design and analysis in pharmacology (Curtis et al., 2018). Because effects and effective concentrations of compounds were not predictable and, in an effort, to reduce animal use, a sample size estimation was not performed and experiments were evaluated after each single experiment. Data are presented as mean  $\pm$  SEM without outlier removal. *N* values represent biological replicates. Normality of data was determined by Shapiro-Wilk test. Tests for statistical significance were conducted as indicated and were ANOVA for comparison of groups with normal distribution of data and Kruskal-Wallis test with Dunn's post hoc test for multigroup comparison. (\**P* < 0.05).

## 2.10 | Materials

Test substances ezetimibe and disulfiram were purchased from Molekula (Germany). All other laboratory chemicals were purchased from Sigma-Aldrich (Germany) or Carl Roth GmbH (Germany) unless noted otherwise in the methods section. Laboratory devices are specified in the respective methods sections.

## 2.11 | Nomenclature of targets and ligands

Key protein targets and ligands in this article are hyperlinked to corresponding entries in the IUPHAR/BPS Guide to PHARMACOLOGY <http://www.guidetopharmacology.org>, the common portal for data from the IUPHAR/BPS Guide to PHARMACOLOGY (Harding et al., 2018).

### 3 | RESULTS

#### 3.1 | Screening for novel mitochondrial $\text{Ca}^{2+}$ uptake enhancers

Since pharmacological enhancement of mitochondrial- $\text{Ca}^{2+}$  uptake can prevent arrhythmogenesis in cardiomyocytes (Schweitzer et al., 2017; Shimizu et al., 2015), but agonists of mitochondrial- $\text{Ca}^{2+}$  uptake are still scarce and experimental, we set out screen for novel, potent MiCUPS for preclinical and clinical testing. As a first step, we took advantage of a previously established and validated mitochondrial- $\text{Ca}^{2+}$  uptake assay. In a previous study, we have developed a permeabilized HeLa cell-based screening approach for the identification of small molecule inhibitors of mt- $\text{Ca}^{2+}$  uptake and have successfully identified specific mitochondrial  $\text{Ca}^{2+}$  uniporter blockers (Arduino et al., 2017). Here, we applied this screening approach for the identification of enhancers and screened the NCC consisting of 727 compounds with a history of use in human clinical trials. Drug effects on luminescence-based mitochondrial- $\text{Ca}^{2+}$  dynamics were quantified by scoring each drug at  $10\ \mu\text{M}$  ( $S_{\text{drug}}$ ) based on its effect on the aequorin-luminescence peak when compared to vehicle (DMSO) and experimental (Ru360) controls (Figure 1a). Compounds were then ranked by their score and the highest scores were selected as MiCUPS (Figure 1b, Supporting Information). The top four hits were further investigated: those included the bioactive biphenolic phytochemical honokiol, the antimicrobial cephalosporine cefatrizine, the cholesterol uptake inhibitor ezetimibe and disulfiram, a drug used to treat chronic

alcoholism. Their effect was further validated by analysis of the dose dependency of the mitochondrial- $\text{Ca}^{2+}$  uptake over a wider range of concentrations (Figure 1c). This revealed dose-dependent enhancement for honokiol, ezetimibe and disulfiram starting at 3–6  $\mu\text{M}$  but not for cefatrizine, which was thus considered a false positive hit from the primary screen. We next confirmed that hits from our screen are indeed enhancers of mitochondrial  $\text{Ca}^{2+}$  uptake rather than blockers of mitochondrial  $\text{Ca}^{2+}$  extrusion, which would likewise lead to enhanced mitochondrial  $\text{Ca}^{2+}$  accumulation. Therefore, we measured mitochondrial  $\text{Na}^+/\text{Ca}^{2+}$  exchanger-mediated mitochondrial  $\text{Ca}^{2+}$  extrusion in permeabilized HeLa cells: unlike the established NCLX blocker **CGP-37157**, neither of our three candidate drugs affected mitochondrial  $\text{Na}^+/\text{Ca}^{2+}$  exchanger activity (Figure 2).

#### 3.2 | Ezetimibe and disulfiram enhance SR-mitochondria $\text{Ca}^{2+}$ transfer in cardiomyocytes

Significant differences were described for mitochondrial  $\text{Ca}^{2+}$  uptake between non-excitable cells like HeLa cells and cardiomyocytes (Chen et al., 2011; Mammucari et al., 2018). In particular, in cardiomyocytes a specialized mechanism of SR-mitochondria  $\text{Ca}^{2+}$  transfer was recently described involving a tight coupling between the ryanodine receptor 2 (RyR2), VDAC2 and mitochondrial  $\text{Ca}^{2+}$  uniporter to allow for rapid transfer of  $\text{Ca}^{2+}$  from the SR into mitochondria (De la Fuente et al., 2016; Min et al., 2012). Because this direct SR-mitochondria  $\text{Ca}^{2+}$  transfer was proposed to be the

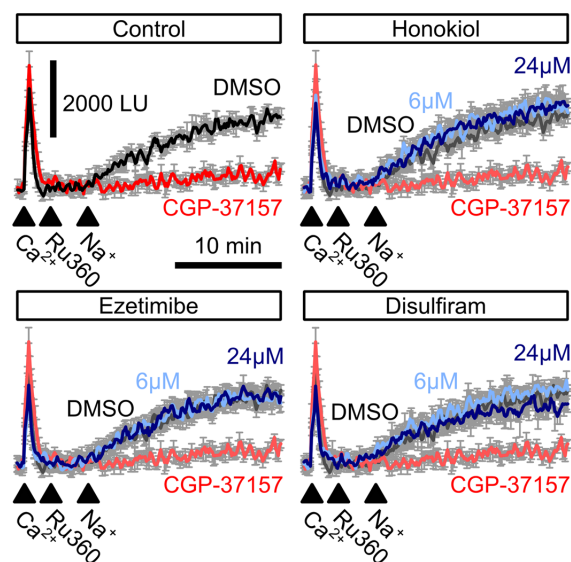


**FIGURE 2** Mitochondrial  $\text{Na}^+/\text{Ca}^{2+}$  exchanger-mediated mitochondrial  $\text{Ca}^{2+}$  extrusion. Free  $\text{Ca}^{2+}$  in the supernatant of permeabilized HeLa cells was recorded using Calcium Green-5N before and after injection of  $100\text{-}\mu\text{M}$   $\text{Ca}^{2+}$  (first arrowhead) followed by a block of mitochondrial  $\text{Ca}^{2+}$  uniporter using Ru360 (second arrowhead). Addition of  $60\text{-mM}$   $\text{Na}^+$  (third arrowhead) induced mitochondrial  $\text{Na}^+/\text{Ca}^{2+}$  exchanger-mediated  $\text{Ca}^{2+}$  extrusion (control, black trace) which could be blocked by the mitochondrial  $\text{Na}^+/\text{Ca}^{2+}$  exchanger blocker CGP-37157 (control, red trace). Neither ezetimibe, nor disulfiram or honokiol affected NCLX activity ( $n = 4$ )

molecular prerequisite for the anti-arrhythmic effect of MiCUPS (Schweitzer et al., 2017; Shimizu et al., 2015; Wilting et al., 2020), we tested the potential of the newly identified MiCUPS ezetimibe, disulfiram and honokiol to specifically enhance SR-mitochondria  $\text{Ca}^{2+}$  transfer in cardiomyocytes. To this aim, we used a plate-reader-based assay on permeabilized HL-1 cardiomyocytes. In contrast to the HeLa-based assay, in this assay  $\text{Ca}^{2+}$  mobilization is triggered by the addition of caffeine in the presence of the fast chelator BAPTA to limit cytosolic  $\text{Ca}^{2+}$  diffusion to the low micrometre range. This assay allows for standardized comparison of multiple conditions (Schweitzer et al., 2017; Wilting et al., 2020) to generate dose-response relationships and was previously successfully used to

investigate the role of VDAC2 in promoting SR-mitochondria  $\text{Ca}^{2+}$  transfer (Min et al., 2012; Wilting et al., 2020). Rapid mitochondrial uptake of  $\text{Ca}^{2+}$  released from the SR by a caffeine pulse was significantly enhanced by ezetimibe and disulfiram, while no significant effect of honokiol could be observed (Figure 3a,b). Strikingly, analysis of dose-response curves revealed that the two active substances, ezetimibe and disulfiram, enhanced mitochondrial- $\text{Ca}^{2+}$  uptake at markedly lower concentrations compared to the established MiCUPS, the mitochondrial  $\text{Ca}^{2+}$  uniporter activator kaempferol (Montero et al., 2004) and the VDAC2 modifier efsevin (Wilting et al., 2020). To exclude a putative false-positive result due to a potential effect of ezetimibe and/or disulfiram on SR  $\text{Ca}^{2+}$  release, we next measured

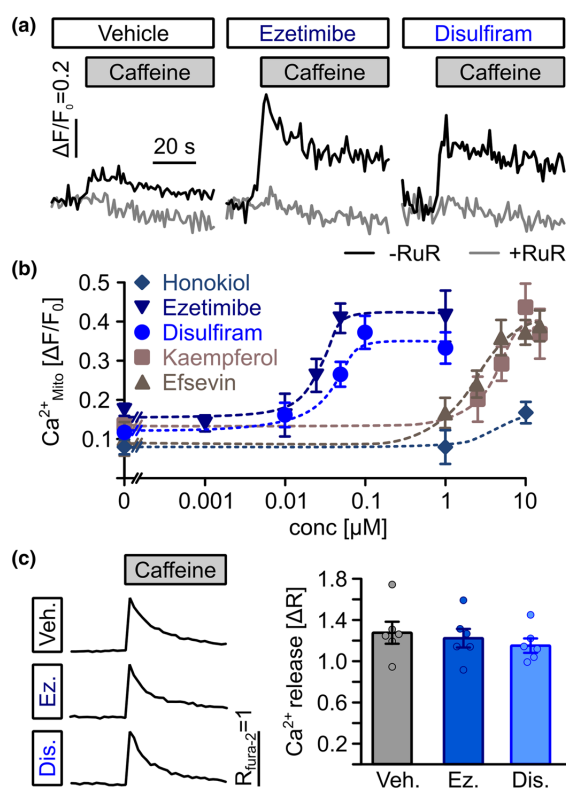


**FIGURE 3** Direct transfer of  $\text{Ca}^{2+}$  from the sarcoplasmic reticulum into mitochondria in cardiomyocytes. (a) Representative recordings of mitochondrial (mt)- $\text{Ca}^{2+}$  uptake (black line) in permeabilized HL-1 cardiomyocytes. Superfusion with 10-mM caffeine induced uptake of  $\text{Ca}^{2+}$  released from the SR into mitochondria, which was enhanced by 1- $\mu\text{M}$  ezetimibe and 1- $\mu\text{M}$  disulfiram. Ruthenium red as a blocker of RyR, VDAC and mitochondrial  $\text{Ca}^{2+}$  uniporter was used to block SR-mitochondria  $\text{Ca}^{2+}$  transfer as a negative control. (b) Ezetimibe and disulfiram enhanced SR-mitochondria (Mito)  $\text{Ca}^{2+}$  transfer dose dependently from  $0.17 \pm 0.01$  ( $n = 26$  biological replicates from nine experiments) in vehicle-treated control cells to maximum values of  $\Delta F/F_0 = 0.41 \pm 0.04$  at 50 nM for ezetimibe ( $n = 19$  replicates from seven experiments) and from  $0.15 \pm 0.01$  ( $n = 20$  replicates from seven experiments) to  $0.37 \pm 0.04$  at 100 nM for disulfiram ( $n = 9$  replicates from nine individual experiments) and at significantly lower concentrations than the established MiCUPS kaempferol and efsevin (ezetimibe:  $\text{EC}_{50} = 25.5$  nM, disulfiram:  $\text{EC}_{50} = 36.8$  nM, kaempferol:  $\text{EC}_{50} = 3.7$   $\mu\text{M}$ , efsevin:  $\text{EC}_{50} = 2.9$   $\mu\text{M}$ ), while no significant effect of honokiol could be observed. (c) Ezetimibe (Ez) and disulfiram (Dis) did not alter SR  $\text{Ca}^{2+}$  release as assessed by fura-2 fluorescence in intact HL-1 cardiomyocytes after addition of 10-mM caffeine. The baseline fura-2 fluorescence ratio ( $R_{340\text{nm}/380\text{nm}}$ ) was  $0.75 \pm 0.03$  for vehicle-treated cells,  $0.72 \pm 0.03$  for cells treated with 1- $\mu\text{M}$  ezetimibe and  $0.79 \pm 0.03$  for cells treated with 1- $\mu\text{M}$  disulfiram. Release of  $\text{Ca}^{2+}$  from the SR induced a change in fluorescence ( $\Delta R$ ) of  $1.07 \pm 0.09$  for vehicle-treated cells,  $1.02 \pm 0.08$  for cells treated with 1- $\mu\text{M}$  ezetimibe and  $0.96 \pm 0.06$  for cells treated with 1- $\mu\text{M}$  disulfiram ( $n = 34$  replicates from six experiments, ANOVA)

cytosolic  $\text{Ca}^{2+}$  levels in intact ezetimibe- and disulfiram-treated HL-1 cardiomyocytes using fura-2 and analysed basal  $\text{Ca}^{2+}$  levels and  $\text{Ca}^{2+}$  release after superfusion with 10-mM caffeine (Figure 3c). We observed no significant change for either baseline fura-2 fluorescence ratio ( $R_{340\text{nm}/380\text{nm}}$ ) or release of  $\text{Ca}^{2+}$  from the SR ( $\Delta R$ ) (Figure 3c). In conclusion, the above data indicates that both, ezetimibe and disulfiram, specifically enhance mitochondrial- $\text{Ca}^{2+}$  uptake in HL-1 cardiomyocytes without affecting baseline cytosolic  $\text{Ca}^{2+}$  levels or SR  $\text{Ca}^{2+}$  release and have significantly lower  $\text{EC}_{50}$  values than the established MiCUp kaempferol and efsevin.

### 3.3 | Ezetimibe and disulfiram suppress arrhythmia in a zebrafish model of $\text{Ca}^{2+}$ -overload induced arrhythmia

Consequently, we set out to evaluate the potency of the newly identified MiCUpS identified in our screening approach to suppress arrhythmia in translational models. Prior to application of MiCUpS to these models, we confirmed that both substances, ezetimibe and disulfiram, effectively enhance mitochondrial  $\text{Ca}^{2+}$  uptake also in intact HeLa cells at concentrations comparable to those effective in permeabilized cells (Figure S1). While we found enhanced mitochondrial- $\text{Ca}^{2+}$

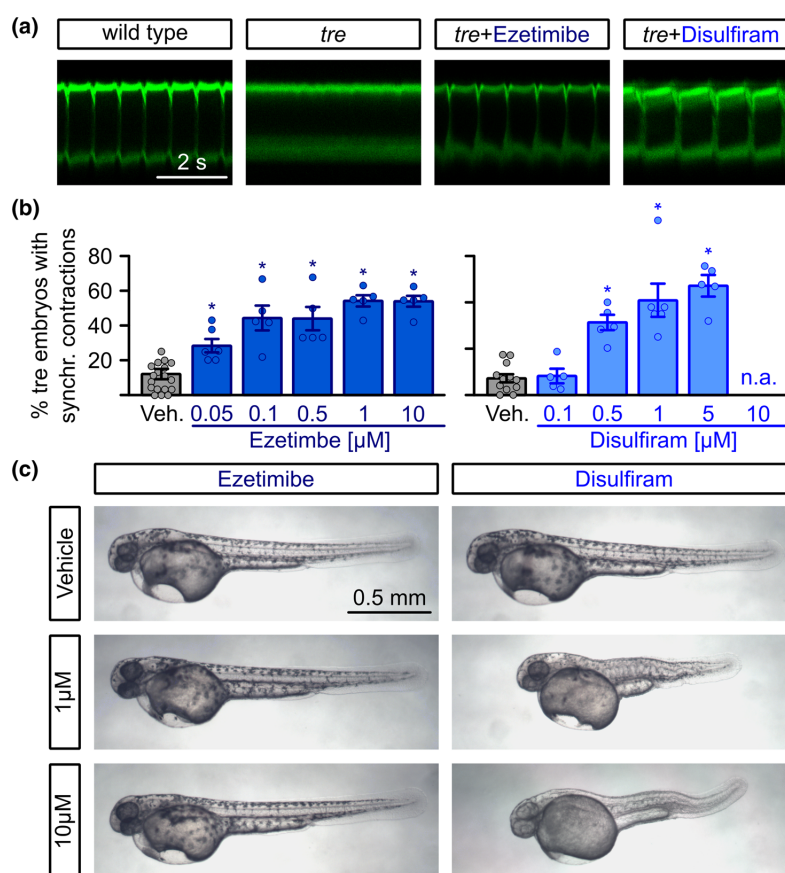


**FIGURE 4** Restoration of rhythmic cardiac contractions in the zebrafish arrhythmia model *tremblor*. (a) Representative confocal linescan recordings through atria of beating GFP-labelled hearts from living zebrafish embryos (TG (myl7:eGFP)) at 1 day after fertilization. Rhythmic cardiac contractions can be observed in wild-type but not *tremblor* (*tre*) embryos. Treatment of *tre* embryos with 1  $\mu\text{M}$  ezetimibe or 1  $\mu\text{M}$  disulfiram restored rhythmic cardiac contractions. (b) Quantification of the percentage of *tre* embryos with synchronized contractions revealed a rescue of the *tre* phenotype from 11.1 ± 2.04% embryos with synchronized contractions in the vehicle control ( $n = 1289$  embryos in 15 individual experiments) to 28.39 ± 3.9% of *tre* embryos at 0.05  $\mu\text{M}$  ( $n = 155$  embryos in six individual experiments), 44.07 ± 7.21% ( $n = 448$  embryos in five individual experiments) after addition of 0.1  $\mu\text{M}$  and a maximum of 53.85 ± 3.38% at 1  $\mu\text{M}$  ezetimibe ( $n = 354$  embryos in five individual experiments). While 0.1  $\mu\text{M}$  disulfiram did not induce a significant effect ( $n = 507$  embryos in five individual experiments), 1  $\mu\text{M}$  disulfiram enhanced the percentage of embryos with synchronized contractions from 9.66 ± 2.31% ( $n = 1133$  embryos from 12 individual experiments) to 54.27 ± 9.48% at 1  $\mu\text{M}$  ( $n = 371$  embryos from five individual experiments) and to 62.83 ± 5.6% at 5  $\mu\text{M}$  ( $n = 418$  embryos from five individual experiments) (Kruskal–Wallis test). (c) Treatment of zebrafish embryos with ezetimibe did not alter gross morphology of embryos, while disulfiram induced severe malformations of the body and a lack of pigmentation

uptake for both substances at 3–6  $\mu\text{M}$ , higher concentrations of disulfiram showed a decrease in mitochondrial- $\text{Ca}^{2+}$  uptake indicating cellular toxicity, while higher concentrations of ezetimibe further enhanced mitochondrial- $\text{Ca}^{2+}$  uptake. We then took advantage of a previously established *in vivo* arrhythmia model in which we recently demonstrated that zebrafish embryos of the transgenic line *tremblor* (*tre<sup>tc318</sup>*), lacking a cardiac isoform of the  $\text{Na}^+/\text{Ca}^{2+}$  exchanger, display  $\text{Ca}^{2+}$  overload-induced cardiac arrhythmia (Langenbacher et al., 2005; Shimizu et al., 2015). In contrast to wild-type embryos, which consistently show rhythmic cardiac contractions at day 1 of development. Homozygous *tre* embryos display a hypercontracted heart that shows only chaotic contractions within the myocardium (Langenbacher et al., 2005). This phenotype can be rescued by treatment with efsevin (Shimizu et al., 2015). We therefore tested the newly identified MiCups ezetimibe and disulfiram for their potential to restore

rhythmic cardiac contractions in this model (Figure 4a). Addition of 0.05- $\mu\text{M}$  ezetimibe restored rhythmic cardiac contractions in roughly one quarter of *tre* embryos and approximately 60% of *tre* embryos at concentrations above 1  $\mu\text{M}$  (Figure 4b), while only a tenth of control embryos treated with vehicle showed synchronized contractions. In agreement with the dose-response curves in HL-1 cardiomyocytes slightly higher concentrations of disulfiram were needed to obtain a similar phenotype rescue in *tre* embryos, where 0.1  $\mu\text{M}$  disulfiram did not induce a significant effect but again approximately one half to 60% of all *tre* embryos were rescued at concentrations above 0.5  $\mu\text{M}$ . Although not all embryos treated with ezetimibe or disulfiram showed rhythmic contractions, this rescue efficiency is comparable to the rescue efficiency initially described with 10  $\mu\text{M}$  efsevin (Shimizu et al., 2015). Interestingly however, zebrafish embryos treated with disulfiram showed signs of intoxication such as a lack of pigmentation

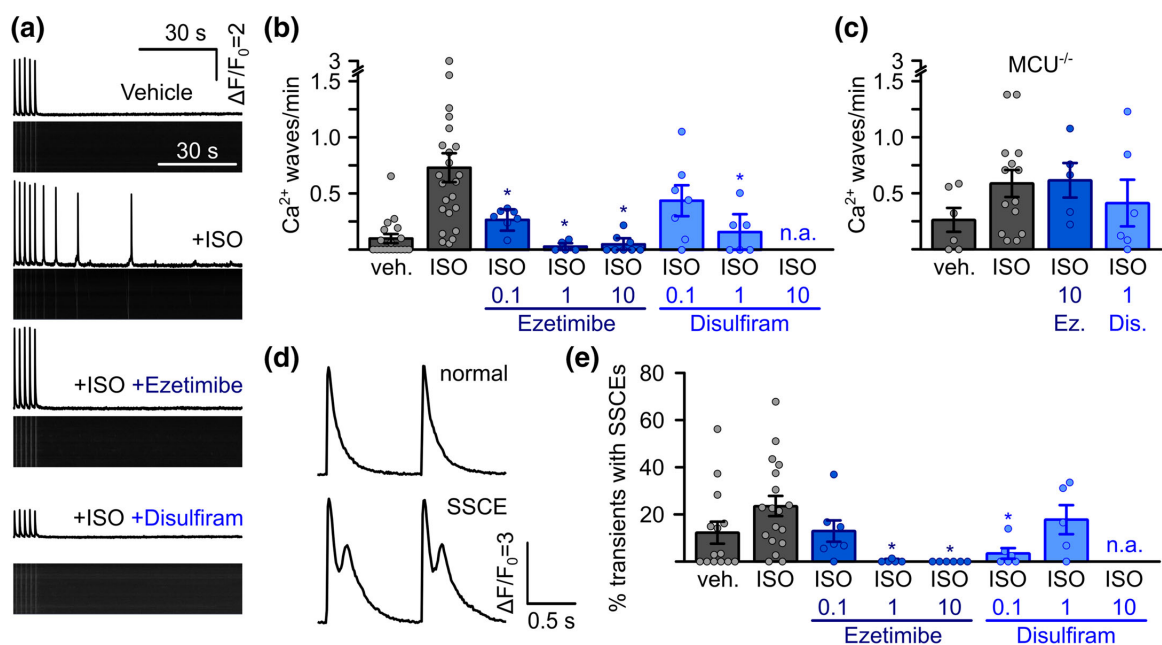


**FIGURE 5** Suppression of arrhythmogenesis in freshly isolated murine  $\text{RyR2}^{\text{C4496R/WT}}$  cardiomyocytes by ezetimibe and disulfiram.

(a) Representative confocal linescan recordings of intracellular  $\text{Ca}^{2+}$  in freshly isolated ventricular cardiomyocytes from  $\text{RyR2}^{\text{C4496R/WT}}$  mice. Cells were continuously pulsed at 0.5 Hz and spontaneous  $\text{Ca}^{2+}$  waves were analysed during 1.5 min after pulsing was stopped. Addition of isoprenaline (ISO) induced spontaneous  $\text{Ca}^{2+}$  waves which could be blocked by the addition of ezetimibe or disulfiram. (b) Quantitative analysis of the experiments in (a). Addition of ISO raised the propensity for spontaneous  $\text{Ca}^{2+}$  waves from  $0.10 \pm 0.04$  waves per minute ( $n = 143$  cells from 18 mice) to  $0.73 \pm 0.13$  ( $n = 222$  cells from 24 mice) in  $\text{RyR2}^{\text{C4496R/WT}}$  mice. Addition of MiCups lowered waves to  $0.27 \pm 0.06$  under 0.1  $\mu\text{M}$  ezetimibe ( $n = 64$  cells from seven mice),  $0.032 \pm 0.02$  under 1  $\mu\text{M}$  ezetimibe ( $n = 35$  cells from five mice) and, finally,  $0.05 \pm 0.03$  under 10  $\mu\text{M}$  ezetimibe ( $n = 80$  cells from eight mice) and to  $0.44 \pm 0.14$  under 0.1 ( $n = 49$  cells from seven mice) and  $0.15 \pm 0.08$  under 1 ( $n = 35$  cells from six mice) for disulfiram (Kruskal–Wallis test). (c) Disruption of mitochondrial  $\text{Ca}^{2+}$  uptake by genetic ablation of mitochondrial  $\text{Ca}^{2+}$  uniporter (MCU) in  $\text{MCU}^{-/-}/\text{RyR2}^{\text{C4496R/WT}}$  mice abolished the effect of ezetimibe (Ez) and disulfiram (Dis) indicated by comparable values of  $0.61 \pm 0.15$  ( $n = 42$  cells from five mice,  $P > 0.05$  Kruskal–Wallis-test) for ISO + 10  $\mu\text{M}$  ezetimibe and  $0.39 \pm 0.20$  ( $n = 47$  cells from six mice,  $P > 0.05$ , Kruskal–Wallis-test) for ISO + 1  $\mu\text{M}$  disulfiram compared to  $0.59 \pm 0.12$  ( $n = 107$  from 14 mice) under ISO alone. (d) Representative recording from electrically induced systolic  $\text{Ca}^{2+}$  transients showing normal transients (upper trace) and transients with secondary systolic  $\text{Ca}^{2+}$  elevations (SSCEs). (e) SSCEs were observed in  $12.4 \pm 4.7\%$  ( $n = 121$  cells from 14 mice) of all transients in the vehicle control and rose to  $23.3 \pm 4.4\%$  after addition of ISO ( $n = 134$  cells from 18 mice). Addition of ezetimibe dose-dependently suppressed SSCEs to a minimum of 0.0% under 10  $\mu\text{M}$  ezetimibe ( $n = 53$  cells from six mice). Disulfiram decreased SSCEs to  $3.4 \pm 2.2\%$  at 0.1  $\mu\text{M}$  ( $n = 42$  cells from six mice), while cells treated with 1  $\mu\text{M}$  showed SSCEs in  $17.5 \pm 6.5\%$  of all transients ( $n = 32$  cells from five mice, Kruskal–Wallis test). n.a. = not analysable.

and a disturbed morphology, which was not observed in ezetimibe-treated embryos (Figure 4c). Taken together, low micromolar concentrations of both drugs can efficiently restore rhythmic cardiac contractions in *tr*e embryos but disulfiram appears to have toxic effects at effective concentrations above 1  $\mu$ M.

### 3.4 | Ezetimibe and disulfiram suppress arrhythmogenesis in cardiomyocytes of a murine tachycardia model

We next tested both compounds for their anti-arrhythmic potential in freshly isolated cardiomyocytes of a murine model for catecholaminergic polymorphic ventricular tachycardia (CPVT) (Cerrone et al., 2005). Consistent with the phenotype of CPVT, cardiomyocytes from RyR2<sup>R4496C/WT</sup> mice develop spontaneous Ca<sup>2+</sup> waves during diastole when stimulated with catecholamines (Figure 5a) (Schweitzer et al., 2017; Sedej et al., 2010). This effect excels RyR2<sup>R4496C/WT</sup> cardiomyocytes as a valuable model for *ex vivo* testing, since a putative reduction of these waves induced by test compounds can not only be directly compared to the disease state (i.e. after catecholamine stimulation) but also to the pretrigger control in the same set of cells. Ca<sup>2+</sup> waves originate from the spontaneous release of Ca<sup>2+</sup> through mutated RyR2s and represent the origin of ectopic cardiac excitations that cause arrhythmia (Allen et al., 1984). Both MiCups dose-dependently reduced the number of isoprenaline (ISO)-induced

Ca<sup>2+</sup> waves to levels comparable to unstimulated control cells (Figure 5b). Interestingly, and comparable to our zebrafish data, disulfiram displayed toxic effects at higher concentrations (10  $\mu$ M) reflected by an elevation of basal cytosolic Ca<sup>2+</sup> levels. Cells treated with 10- $\mu$ M disulfiram showed very high fluo-4 fluorescence (51.5  $\pm$  4.8FU compared to 15.3  $\pm$  0.5FU under isoprenaline alone) and extensive spontaneous activity, which prevented further analysis (Figure S2).

To confirm that this striking effect in CPVT cardiomyocytes is solely attributable to the enhanced mitochondrial-Ca<sup>2+</sup> uptake induced by the two MiCups, we crossbred RyR2<sup>R4496C</sup> mice with *MCU*<sup>-/-</sup> mice, which lack the central pore forming subunit of the mitochondrial Ca<sup>2+</sup> uniporter complex (Pan et al., 2013). In freshly isolated RyR2<sup>R4496C/WT</sup>/*MCU*<sup>-/-</sup> cardiomyocytes, we again observed an induction of diastolic Ca<sup>2+</sup> waves upon isoprenaline treatment compared to untreated control cells. Strikingly, application of the highest effective doses, 10  $\mu$ M ezetimibe and 1  $\mu$ M disulfiram, failed to reduce Ca<sup>2+</sup> waves in both cases (Figure 5c), indicating that mitochondrial Ca<sup>2+</sup> uptake is the effective target of ezetimibe and disulfiram.

Apart from diastolic Ca<sup>2+</sup> waves, systolic Ca<sup>2+</sup> activity was suggested as a potential trigger for arrhythmia in CPVT (Némec et al., 2010; Némec et al., 2016). We therefore also analysed systolic Ca<sup>2+</sup> transients of our recordings for the occurrence of secondary systolic Ca<sup>2+</sup>-elevations (SSCEs) and found that a significantly higher portion of transients recorded from cells treated with isoprenaline showed secondary systolic Ca<sup>2+</sup>-elevations than transients recorded

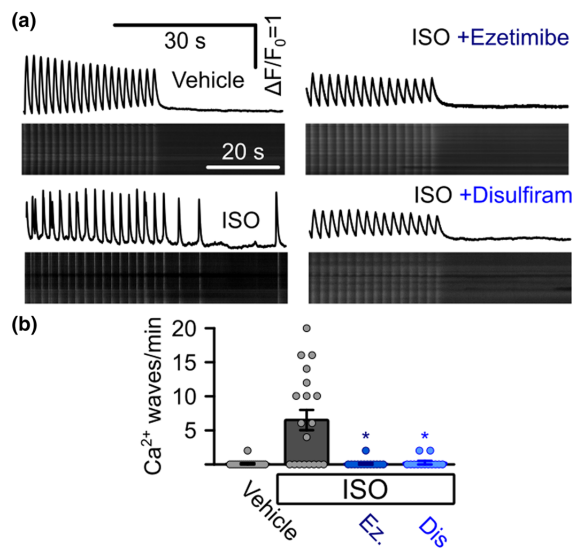


**FIGURE 6** Suppression of arrhythmic Ca<sup>2+</sup> signals in iPSC-derived cardiomyocytes from a catecholaminergic polymorphic ventricular tachycardia (CPVT) patient. (a) Representative confocal linescan recordings of intracellular Ca<sup>2+</sup> in iPSC-derived cardiomyocytes from a CPVT patient. Cells were continuously pulsed at 0.5 Hz and spontaneous Ca<sup>2+</sup> waves were analysed after pulsing was stopped. Addition of isoprenaline (ISO) induced spontaneous Ca<sup>2+</sup> waves which could be blocked by the addition of ezetimibe or disulfiram. (b) Quantitative analysis of the experiments in (a). Addition of ISO induced the occurrence of waves in CPVT cells (0 waves per minute for vehicle control,  $n = 11$  cells,  $5.87 \pm 1.80$  under ISO,  $n = 16$ , Kruskal–Wallis test), which could be suppressed by the addition of ezetimibe (Ez) or disulfiram (Dis) ( $0.10 \pm 0.07$  waves per minute for ezetimibe,  $n = 13$  cells,  $0.05 \pm 0.05$  waves per minute for disulfiram,  $n = 13$ , Kruskal–Wallis test, data from four independent enzymatic dissociations of 19 individual beating cell clusters)

from vehicle-treated control cells. Strikingly, both, ezetimibe and disulfiram, significantly reduced secondary systolic  $\text{Ca}^{2+}$ -elevations (Figure 5d,e). A clear dose-dependence was observed for ezetimibe; however, higher concentrations of disulfiram induced higher spontaneous  $\text{Ca}^{2+}$  activity, which might again be attributed to the enhanced baseline  $\text{Ca}^{2+}$  observed under disulfiram (Figure S2).

### 3.5 | Ezetimibe and disulfiram suppress arrhythmogenesis in human iPSC-derived CPVT cardiomyocytes

Finally, we tested both substances for their ability to suppress arrhythmogenic  $\text{Ca}^{2+}$  waves in human cells to estimate the translatability of our data and the potential of ezetimibe and disulfiram to serve as candidates for a human therapy (Figure 6). To this aim, we used iPSC-derived cardiomyocytes from a CPVT patient. Comparable to murine CPVT cardiomyocytes and in line with the CPVT phenotype, these cells did not display spontaneous diastolic  $\text{Ca}^{2+}$  waves under unstimulated control conditions while addition of isoprenaline (ISO) induced prominent  $\text{Ca}^{2+}$  waves (Figure 6a,b). Strikingly, addition of ezetimibe and disulfiram reduced  $\text{Ca}^{2+}$  waves to control conditions.

## 4 | DISCUSSION

### 4.1 | Mitochondrial $\text{Ca}^{2+}$ uptake enhancer screen

We have previously demonstrated that the VDAC2 agonist efsevin as well as the mitochondrial  $\text{Ca}^{2+}$  uniporter agonist kaempferol potently suppress arrhythmia in murine and human models of CPVT (Schweitzer et al., 2017; Shimizu et al., 2015). However, in regard of a clinical application of these substances, it is of note that both enhance SR-mitochondria  $\text{Ca}^{2+}$  transfer with an  $\text{EC}_{50}$  of around 5  $\mu\text{M}$ , a concentration that is likely to favour off-target effects. Furthermore, data concerning efsevin's bioavailability, pharmacodynamics, stability and toxicity are largely missing. Though kaempferol was used in clinical studies before, it was only used at a low dose as a nutritional supplement and was shown to bind multiple targets including the NF- $\kappa\text{B}$  (Kadioglu et al., 2015), the fibroblast growth factor (Lee et al., 2018) and other signalling pathways (Kim et al., 2015; Wu et al., 2017; Yao et al., 2014). Thus, though our previous findings established the mitochondrial  $\text{Ca}^{2+}$  uptake pathway as a promising candidate target for future preclinical and clinical development of a human anti-arrhythmic therapy, efsevin and kaempferol represent poor candidates for this purpose and novel substances for further testing are needed. While several studies have already identified effective blockers of the mitochondrial  $\text{Ca}^{2+}$  uniporter complex (Arduino & Perocchi, 2018; Di Marco et al., 2020; Kon et al., 2017; Nathan et al., 2017; Woods & Wilson, 2020), agonists still remain scarce.

We therefore set up a three-step protocol to identify novel MiCUps with anti-arrhythmic effects: primary screening was performed in a previously validated HeLa-cell based assay that allows

screening of large compound libraries in a system that is cost efficient and automatable. Further target validation was performed in HL-1 cells allowing for testing of multiple candidate substances at multiple concentrations on cardiac myocytes. Finally, only candidates passing steps one and two were further evaluated for their anti-arrhythmic potential in translational animal models thereby reducing animal usage.

Using this approach, we screened the NCC consisting of 727 compounds with a history of use in human clinical trials to identify novel specific enhancers of mitochondrial- $\text{Ca}^{2+}$  uptake. Three compounds, honokiol, disulfiram and ezetimibe, were selected as hits based on their stimulatory effect on mt- $\text{Ca}^{2+}$  uptake without blocking mitochondrial  $\text{Ca}^{2+}$  extrusion in primary drug screens as well as dose-dependent measurements in permeabilized HeLa cells. We then further tested these compounds for their ability to selectively enhance the transfer of  $\text{Ca}^{2+}$  from the SR into mitochondria in cardiomyocytes as the mechanism proposed to be the molecular prerequisite for the anti-arrhythmic effect of MiCUps (Schweitzer et al., 2017; Shimizu et al., 2015; Wilting et al., 2020). Interestingly, honokiol, which displayed the most pronounced effects in HeLa cells, was inactive in this system, while ezetimibe and disulfiram consistently enhanced mitochondrial- $\text{Ca}^{2+}$  uptake. This might be attributable to differences in the mitochondrial  $\text{Ca}^{2+}$  uptake pathway between non-excitabile and excitable cells and highlights the importance of re-evaluation of hits from our primary screening platform in cardiac cells. After passing both assays, ezetimibe and disulfiram were then further tested for their anti-arrhythmogenic potential in translational models and both were shown to indeed suppress arrhythmogenesis.

Taken together, we successfully identified two novel, potent MiCUps by applying a combination of a HeLa-based chemical screening followed by cardiomyocyte-specific target validation and final testing in arrhythmia models. With this protocol, we identified ezetimibe and disulfiram as novel candidates for the use in further preclinical and eventually clinical tests on the efficacy of MiCUps for the treatment of cardiac arrhythmia, but also as valuable compounds for further basic research on the mitochondrial  $\text{Ca}^{2+}$  uptake pathway and preclinical research for other indications. In this respect enhancing mitochondrial  $\text{Ca}^{2+}$  uptake was recently suggested to be beneficial to facilitate cerebral blood flow after traumatic brain injury (Murugan et al., 2016) and to promote metabolism/secretion coupling in type 2 diabetes (Bermont et al., 2020).

### 4.2 | Cardiac selectivity of novel mitochondrial $\text{Ca}^{2+}$ uptake enhancers

In this and previous studies, we successfully applied MiCUps on different models from cell cultures to *in vivo* systems, but never observed gross effects, for example, apoptosis, on other tissues than the heart (Schweitzer et al., 2017; Shimizu et al., 2015). Though these experiments never exceeded treatment times of several days to weeks, these data suggest MiCUps as promising candidates for the treatment of cardiac diseases. It has been proposed that, although most components of the mitochondrial  $\text{Ca}^{2+}$  uptake pathway are



ubiquitously expressed throughout the organism, tissue selectivity of mitochondrial  $\text{Ca}^{2+}$  uptake is determined by composition and subcellular localization of individual components and channel subunits. Here, we observed differences in drug effects and effective doses between cardiomyocytes and non-excitable HeLa cells, which might be at least one explanation for their specificity. Honokiol was active in HeLa cells but did not show activity in HL-1 cardiomyocytes. Furthermore, the concentrations of ezetimibe and disulfiram needed to activate mitochondrial- $\text{Ca}^{2+}$  uptake significantly vary between the two systems. A possible explanation could be differences in tissue-specific mitochondrial  $\text{Ca}^{2+}$  uniporter activity (Fieni et al., 2012), mitochondrial  $\text{Ca}^{2+}$  uptake pathway composition (Patron et al., 2019; Raffaello et al., 2013), or physiological adaptation (Lambert et al., 2019). Since the target protein of the identified MiCUPS within the mitochondrial  $\text{Ca}^{2+}$  uptake pathway remains elusive, it is conceivable that the mitochondrial  $\text{Ca}^{2+}$  uptake pathway in cardiac cells lacks the component required for honokiol binding or that this component is only present at a very low level. Vice versa, it is possible that the specific mitochondrial  $\text{Ca}^{2+}$  uptake pathway composition that is present in cardiomyocytes is a better target for ezetimibe and disulfiram. Alternatively, different subcellular localizations of mitochondrial  $\text{Ca}^{2+}$  uptake pathway components in the two cell types might account for the observed differences. By using caffeine as a trigger and BAPTA in the intracellular solution, we specifically analyse local transfer of  $\text{Ca}^{2+}$  from the SR into mitochondria in HL-1 cardiomyocytes. In contrast, global addition of  $4\text{-}\mu\text{M}$   $\text{Ca}^{2+}$  was used as a trigger in HeLa cells. Since both channels of the mitochondrial  $\text{Ca}^{2+}$  uptake pathway, VDAC2 and the mitochondrial  $\text{Ca}^{2+}$  uniporter preferentially accumulate in areas of the mitochondrion which interact with the SR (De la Fuente et al., 2016, 2018; Min et al., 2012; Sander et al., 2021) and the concentration of  $\text{Ca}^{2+}$  released from the SR reaches concentrations of up to 1 mM in close vicinity to the  $\text{Ca}^{2+}$  release sites, this could explain why lower concentrations of ezetimibe and disulfiram are active in cardiomyocytes. Finally, the existence of two different mitochondrial  $\text{Ca}^{2+}$  uniporter subpopulations with distinct subunit composition and  $\text{Ca}^{2+}$  sensitivity, one in the SR-mitochondria interface and one outside these junctions could account for the system-dependent activities. Such subpopulations could be established to differentiate between local and global  $\text{Ca}^{2+}$  signals. In this scenario, honokiol might only target the latter population, while ezetimibe and disulfiram are more selective for the SR-associated population.

The discussed differences in composition and localization of the different mitochondrial  $\text{Ca}^{2+}$  uptake pathway components could thus explain the observed cardio-selectivity of MiCUPS. Therefore, MiCUPS could act as specific enhancers of mitochondrial- $\text{Ca}^{2+}$  uptake in the heart, while being relatively inert in other tissues. However, future studies are needed to evaluate this hypothesis and to specifically investigate effects of MiCUPS on other tissues. It is of note that we used MiCUPS for acute treatment and it is thus feasible that changes in mitochondrial- $\text{Ca}^{2+}$  uptake have an immediate effect on cardiomyocytes but not in other cell types. Still, even subtle differences in mitochondrial- $\text{Ca}^{2+}$  uptake might interfere with cellular  $\text{Ca}^{2+}$  homeostasis when they persist chronically and might

induce long-term effects in other organs. Thus, additional investigations on other cell types and in particular long-term studies are needed. The identified substances from this study might serve as tools to address these questions.

### 4.3 | Novel mitochondrial $\text{Ca}^{2+}$ uptake enhancers for preclinical and clinical testing

We identified two compounds, ezetimibe and disulfiram, which enhance mitochondrial- $\text{Ca}^{2+}$  uptake at significantly lower concentrations than efsevin and kaempferol and could thus serve as candidate drugs for preclinical and eventually clinical trials on the efficacy of MiCUPS for the treatment of cardiac arrhythmia. In contrast to common anti-arrhythmic drugs, which target ion channels in the cell membrane and thereby modulate the cardiac action potential to suppress propagation of ectopic signals, MiCUPS act intracellularly by inhibiting the generation of arrhythmogenic triggers such as early and late afterdepolarizations. Due to this mechanism of action, which does not directly interfere with ionic currents of the systolic cardiac action potential, MiCUPS are expected to be less prone to proarrhythmic side effects than commonly used anti-arrhythmic drugs of Vaughan Williams class I and III, which retard and prolong systolic cardiac action potentials. Both, ezetimibe and disulfiram, are FDA and EMA approved and currently in use. Ezetimibe is used as a blocker of the **Niemann-Pick C1-like intracellular cholesterol transporter 1 (NPC1L1/SLC65A2)** (Garcia-Calvo et al., 2005) protein in epithelial cells of the small intestine to reduce uptake of cholesterol. It is used for the prevention and treatment of cardiovascular disease. Although ezetimibe is well tolerated, it is however not first-line therapy, due to a lower efficiency compared to the commonly used statins. Ezetimibe is membrane permeable (Alhayali et al., 2018) and orally bioavailable, and plasma concentrations reach a maximum approximately 2 h after intake. It is enterohepatically metabolized (Kosoglou et al., 2005). However, approximately 80%–90% of ezetimibe is rapidly metabolized into ezetimibe-glucuronide (Kosoglou et al., 2005). Though both forms were shown to be active inhibitors of NPC1L1, we found that ezetimibe glucuronide is less effective to reduce  $\text{Ca}^{2+}$  waves in  $\text{RyR2}^{\text{R4496C/WT}}$  cardiomyocytes (Figure S3). Thus, although plasma concentrations of approximately 300 nm for both forms were described after a 10 mg per 10 days oral intake (Ezzet et al., 2001), which would be well in the effective range in our studies, further experiments in preclinical models need to evaluate effective *in vivo* doses.

Disulfiram is an inhibitor of acetaldehyde dehydrogenase and is used for the treatment of alcohol abuse, but serious side effects limit the use of the drug. Also in our experiments, disulfiram induced severe malformations in zebrafish and showed signs of cellular toxicity in intact HeLa cells and cardiomyocytes at higher concentrations. It is of note however that disulfiram is administered to zebrafish embryos at a very sensitive step of development while it is envisioned to serve as an anti-arrhythmic drug for adult subjects. Furthermore, the disulfiram concentration needed for efficient rescue in zebrafish was significantly higher compared to concentrations applied in cellular models which

might be explained by differences in the differentiation state of cardiomyocytes in the distinct models or a limited uptake into zebrafish embryos through the embryonic skin. However, also in cardiomyocytes, we observed enhanced  $\text{Ca}^{2+}$  activity during diastole upon treatment with higher doses disulfiram. This might at least in part be explained by a direct destabilizing effect of disulfiram on the RyR2 during diastole, which would be in agreement with a recently identified modulatory effect of disulfiram on the skeletal muscle isoform RyR1 (Rebeck et al., 2017). Furthermore, disulfiram was shown to influence the permeability of the inner mitochondrial membrane and to release  $\text{Ca}^{2+}$  from mitochondria at higher concentrations (Balakirev & Zimmer, 2001; Chávez et al., 1989) which is in line with our results from intact cells. Although these results speak against the use of disulfiram as an anti-arrhythmic agent in clinical use, on the other hand and consistent with our findings, previous preclinical studies already demonstrated an anti-arrhythmic potential of disulfiram in different animal models (Fossa et al., 1982; Fossa & Carlson, 1983). These effects might now be explained by activation of mitochondrial- $\text{Ca}^{2+}$  uptake. It is of note however that these reports also observed a negative inotropic effect of disulfiram at higher concentrations which might be explained by the unspecific binding to RyR2 or other unspecific effects as the ones outlined above. Taken together, further investigations on drug efficacy and safety are definitely needed for the use of disulfiram.

Summarizing our results, we have identified two novel mitochondrial  $\text{Ca}^{2+}$  uptake enhancers that are already in clinical use. However, before clinical tests for the treatment of human arrhythmia can be performed with these substances, follow-up studies comprising *in vivo* studies with different dosing and administration regimes are needed to determine effective doses and time points of administration to evaluate the potential of MiCUPs to be used as preventive therapy to reduce the risk for arrhythmias or to stop an acute episode of arrhythmia, respectively.

#### ACKNOWLEDGEMENTS

The authors thank Brigitte Mayerhofer and Shuyue Zhang for technical assistance. This work was supported by the Deutsche Forschungsgesellschaft DFG (SCHR 1471/1-1 to J. S and TRR 152 to A.M. and T.G.); the Munich Center for Systems Neurology (grant number SyNergy EXC 2145/ID 390857198 to F.P.); the Bert L & N Kuggie Vallee Foundation (F.P. and D.M.A.); and the Initiative and Network Fund of the Helmholtz Association (grant number ExNet-0041-Phase2-3 ("SyNergy-HMGU") to F.P.).

#### AUTHOR CONTRIBUTIONS

P.S., F.P. and J.S. conceptualized the study. P.S., M.F., M.K.S., F.W., S.M.G., D.M.A., S.F. and L.D., performed experiments. P.S., M.F., M.K.S., F.W., S.M.G., D.M.A., S.F., F.P. and J.S. analysed data. A.M., T.G., F.P. and J.S. provided funding and infrastructure. P.S. and J.S. wrote the manuscript. All authors commented on the manuscript.

#### CONFLICT OF INTEREST

The authors declare that they have no conflict of interest.

#### DECLARATION OF TRANSPARENCY AND SCIENTIFIC RIGOUR

This Declaration acknowledges that this paper adheres to the principles for transparent reporting and scientific rigour of preclinical research as stated in the *British Pharmacological Journal* guidelines for [Design and Analysis](#) and [Animal Experimentation](#), and as recommended by funding agencies, publishers and other organizations engaged with supporting research.

#### DATA AVAILABILITY STATEMENT

The data underlying this article are available in the article and in its supporting information. Raw data are available upon request from the corresponding author.

#### ETHICS APPROVAL STATEMENT

All human and animal studies have been approved by the appropriate ethics committee and have therefore been performed in accordance with the ethical standards laid down in the 1964 Declaration of Helsinki and its later amendments.

#### ORCID

Paulina Sander  <https://orcid.org/0000-0002-2384-3954>

Sophie M. Gutenthaler  <https://orcid.org/0000-0002-8412-3328>

Thomas Gudermann  <https://orcid.org/0000-0002-0323-7965>

Fabiana Perocchi  <https://orcid.org/0000-0002-1102-6500>

Johann Schredelseker  <https://orcid.org/0000-0002-6657-0466>

#### REFERENCES

- Alhayali, A., Selo, M. A., Ehrhardt, C., & Velaga, S. (2018). Investigation of supersaturation and *in vitro* permeation of the poorly water soluble drug ezetimibe. *European Journal of Pharmaceutical Sciences*, 117, 147–153. <https://doi.org/10.1016/j.ejps.2018.01.047>
- Allen, D. G., Eisner, D. A., & Orchard, C. H. (1984). Characterization of oscillations of intracellular calcium concentration in ferret ventricular muscle. *The Journal of Physiology*, 352, 113–128. <https://doi.org/10.1113/jphysiol.1984.sp015281>
- Arduino, D. M., & Perocchi, F. (2018). Pharmacological modulation of mitochondrial calcium homeostasis. *The Journal of Physiology*, 596, 2717–2733. <https://doi.org/10.1113/JP274959>
- Arduino, D. M., Wettmarshausen, J., Vais, H., Navas-Navarro, P., Cheng, Y., Leimpek, A., Ma, Z., Delrio-Lorenzo, A., Giordano, A., Garcia-Perez, C., & Médard, G. (2017). Systematic identification of MCU modulators by orthogonal interspecies chemical screening. *Molecular Cell*, 67, 711–723. e7
- Balakirev, M. Y., & Zimmer, G. (2001). Mitochondrial injury by disulfiram: Two different mechanisms of the mitochondrial permeability transition. *Chemico-Biological Interactions*, 138, 299–311. [https://doi.org/10.1016/S0009-2797\(01\)00283-6](https://doi.org/10.1016/S0009-2797(01)00283-6)
- Baughman, J. M., Perocchi, F., Girgis, H. S., Plovanich, M., Belcher-Timme, C. A., Sancak, Y., Bao, X. R., Strittmatter, L., Goldberger, O., Bogorad, R. L., Kotliansky, V., & Mootha, V. K. (2011). Integrative genomics identifies MCU as an essential component of the mitochondrial calcium uniporter. *Nature*, 476, 341–345. <https://doi.org/10.1038/nature10234>
- Benjamin, E. J., Virani, S. S., Callaway, C. W., Chamberlain, A. M., Chang, A. R., Cheng, S., Chiuve, S. E., Cushman, M., Delling, F. N., Deo, R., de Ferranti, S. D., Ferguson, J. F., Fornage, M., Gillespie, C., Isasi, C. R., Jiménez, M. C., Jordan, L. C., Judd, S. E., Lackland, D., ...

- American Heart Association Council on Epidemiology and Prevention Statistics Committee and Stroke Statistics Subcommittee. (2018). Heart disease and stroke statistics—2018 update: A report from the American Heart Association. *Circulation*, 137, e67–e492. <https://doi.org/10.1161/CIR.0000000000000558>
- Bermont, F., Hermant, A., Benninga, R., Chabert, C., Jacot, G., Santo-Domingo, J., Kraus, M. R. C., Feige, J. N., & de Marchi, U. (2020). Targeting mitochondrial calcium uptake with the natural flavonoid kaempferol, to promote metabolism/secretion coupling in pancreatic  $\beta$ -cells. *Nutrients*, 12, 538. <https://doi.org/10.3390/nu12020538>
- Bers, D. M. (2002). Cardiac excitation-contraction coupling. *Nature*, 415, 198–205. <https://doi.org/10.1038/415198a>
- Bers, D. M. (2008). Calcium cycling and signaling in cardiac myocytes. *Annual Review of Physiology*, 70, 23–49. <https://doi.org/10.1146/annurev.physiol.70.113006.100455>
- Cerrone, M., Colombi, B., Santoro, M., di Barletta, M. R., Scelsi, M., Villani, L., Napolitano, C., & Priori, S. G. (2005). Bidirectional ventricular tachycardia and fibrillation elicited in a knock-in mouse model carrier of a mutation in the cardiac ryanodine receptor. *Circulation Research*, 96, e77–e82. <https://doi.org/10.1161/01.RES.0000169067.51055.72>
- Chávez, E., Zazueta, C., & Bravo, C. (1989). Extensive  $\text{Ca}^{2+}$  release from energized mitochondria induced by disulfiram. *Journal of Bioenergetics and Biomembranes*, 21, 335–345. <https://doi.org/10.1007/BF00762725>
- Chen, M., Wang, Y., Hou, T., Zhang, H., Qu, A., & Wang, X. (2011). Differential mitochondrial calcium responses in different cell types detected with a mitochondrial calcium fluorescent indicator, mito-GCaMP2. *Acta Biochimica et Biophysica Sinica Shanghai*, 43, 822–830. <https://doi.org/10.1093/abbs/gmr075>
- Claycomb, W. C., Lanson, N. A., Stallworth, B. S., Egeland, D. B., Delcarpio, J. B., Bahinski, A., & Izzo, N. J. (1998). HL-1 cells: A cardiac muscle cell line that contracts and retains phenotypic characteristics of the adult cardiomyocyte. *Proceedings of the National Academy of Sciences of the United States of America*, 95, 2979–2984. <https://doi.org/10.1073/pnas.95.6.2979>
- Curtis, M. J., Alexander, S., Cirino, G., Docherty, J. R., George, C. H., Giembycz, M. A., ... Ahluwalia, A. (2018). Experimental design and analysis and their reporting II: Updated and simplified guidance for authors and peer reviewers. *British Journal of Pharmacology*, 175(7), 987–993. <https://doi.org/10.1111/bph.14153>
- De la Fuente, S., Fernandez-Sanz, C., Vail, C., Agra, E. J., Holmstrom, K., Sun, J., Mishra, J., Williams, D., Finkel, T., Murphy, E., & Joseph, S. K. (2016). Strategic positioning and biased activity of the mitochondrial calcium uniporter in cardiac muscle. *The Journal of Biological Chemistry*, 291, 23343–23362.
- De la Fuente, S., Lambert, J. P., Nichtova, Z., Fernandez Sanz, C., Elrod, J. W., Sheu, S.-S., & Csordás, G. (2018). Spatial separation of mitochondrial calcium uptake and extrusion for energy-efficient mitochondrial calcium signaling in the heart. *Cell Reports*, 24, 3099–3107. e4
- De la Fuente, S., & Sheu, S.-S. (2019). SR-mitochondria communication in adult cardiomyocytes: A close relationship where the  $\text{Ca}^{2+}$  has a lot to say. *Archives of Biochemistry and Biophysics*, 663, 259–268. <https://doi.org/10.1016/j.abb.2019.01.026>
- De Stefani, D., Raffaello, A., Teardo, E., Szabó, I., & Rizzuto, R. (2011). A forty-kilodalton protein of the inner membrane is the mitochondrial calcium uniporter. *Nature*, 476, 336–340. <https://doi.org/10.1038/nature10230>
- Di Marco, G., Vallese, F., Jourde, B., Bergsdorf, C., Sturlese, M., De Mario, A., Techer-Etienne, V., Haasen, D., Oberhauser, B., Schleegeer, S., & Minetti, G. (2020). A high-throughput screening identifies MICU1 targeting compounds. *Cell Reports*, 30, 2321–2331. e6
- Ezzet, F., Krishna, G., Wexler, D. B., Statkevich, P., Kosoglou, T., & Batra, V. K. (2001). A population pharmacokinetic model that describes multiple peaks due to enterohepatic recirculation of ezetimibe. *Clinical Therapeutics*, 23, 871–885. [https://doi.org/10.1016/S0149-2918\(01\)80075-8](https://doi.org/10.1016/S0149-2918(01)80075-8)
- Fieni, F., Lee, S. B., Jan, Y. N., & Kirichok, Y. (2012). Activity of the mitochondrial calcium uniporter varies greatly between tissues. *Nature Communications*, 3, 1317. <https://doi.org/10.1038/ncomms2325>
- Fossa, A. A., & Carlson, G. P. (1983). Antiarrhythmic effect of disulfiram in various cardiotoxic models. *Pharmacology*, 26, 164–171. <https://doi.org/10.1159/000137798>
- Fossa, A. A., White, J. F., & Carlson, G. P. (1982). Antiarrhythmic effects of disulfiram on epinephrine-induced cardiac arrhythmias in rabbits exposed to trichloroethylene. *Toxicology and Applied Pharmacology*, 66, 109–117. [https://doi.org/10.1016/0041-008X\(82\)90065-5](https://doi.org/10.1016/0041-008X(82)90065-5)
- García-Calvo, M., Lisnock, J., Bull, H. G., Hawes, B. E., Burnett, D. A., Braun, M. P., Crona, J. H., Davis, H. R., Dean, D. C., Detmers, P. A., Graziano, M. P., Hughes, M., MacIntyre, D. E., Ogawa, A., O'Neill, K. A., Iyer, S. P. N., Shevell, D. E., Smith, M. M., Tang, Y. S., ... Thornberry, N. A. (2005). The target of ezetimibe is Niemann-Pick C1-like 1 (NPC1L1). *Proceedings of the National Academy of Sciences*, 102, 8132–8137.
- Harding, S. D., Sharman, J. L., Faccenda, E., Southan, C., Pawson, A. J., Ireland, S., Gray, A. J. G., Bruce, L., Alexander, S. P. H., Anderton, S., Bryant, C., Davenport, A. P., Doerig, C., Fabbro, D., Levi-Schaffer, F., Spedding, M., Davies, J. A. (2018). The IUPHAR/BPS Guide to PHARMACOLOGY in 2018: updates and expansion to encompass the new guide to IMMUNOPHARMACOLOGY. *Nucleic Acids Research*, 46(D1), D1091–D1106. <https://doi.org/10.1093/nar/gkx1121>
- Kadioglu, O., Nass, J., Saeed, M. E. M., Schuler, B., & Efferth, T. (2015). Kaempferol is an anti-inflammatory compound with activity towards NF- $\kappa$ B pathway proteins. *Anticancer Research*, 35, 2645–2650.
- Kim, S. H., Park, J. G., Lee, J., Yang, W. S., Park, G. W., Kim, H. G., Yi, Y. S., Baek, K. S., Sung, N. Y., Hossen, M. J., & Lee, M. N. (2015). The dietary flavonoid kaempferol mediates anti-inflammatory responses via the Src, Syk, IRAK1, and IRAK4 molecular targets. *Mediators of Inflammation*, 2015, 1–15.
- Kirichok, Y., Krapivinsky, G., & Clapham, D. E. (2004). The mitochondrial calcium uniporter is a highly selective ion channel. *Nature*, 427, 360–364. <https://doi.org/10.1038/nature02246>
- Kon, N., Murakoshi, M., Isobe, A., Kagechika, K., Miyoshi, N., & Nagayama, T. (2017). DS16570511 is a small-molecule inhibitor of the mitochondrial calcium uniporter. *Cell Death Discovery*, 3, 17045. <https://doi.org/10.1038/cddiscovery.2017.45>
- Kosoglou, T., Statkevich, P., Johnson-Levonos, A. O., Paolini, J. F., Bergman, A. J., & Alton, K. B. (2005). Ezetimibe: A review of its metabolism, pharmacokinetics and drug interactions. *Clinical Pharmacokinetics*, 44, 467–494. <https://doi.org/10.2165/00003088-200544050-00002>
- Lambert, J. P., Luongo, T. S., Tomar, D., Jadiya, P., Gao, E., Zhang, X., Lucchese, A. M., Kolmetzky, D. W., Shah, N. S., & Elrod, J. W. (2019). MCUB regulates the molecular composition of the mitochondrial calcium uniporter channel to limit mitochondrial calcium overload during stress. *Circulation*, 140, 1720–1733. <https://doi.org/10.1161/CIRCULATIONAHA.118.037968>
- Langenbacher, A. D., Dong, Y., Shu, X., Choi, J., Nicoll, D. A., Goldhaber, J. I., Philipson, K. D., & Chen, J. N. (2005). Mutation in sodium-calcium exchanger 1 (NCX1) causes cardiac fibrillation in zebrafish. *Proceedings of the National Academy of Sciences of the United States of America*, 102, 17699–17704. <https://doi.org/10.1073/pnas.0502679102>
- Lee, C.-J., Moon, S.-J., Jeong, J.-H., Lee, S., Lee, M.-H., Yoo, S.-M., Lee, H. S., Kang, H. C., Lee, J. Y., Lee, W. S., Lee, H. J., Kim, E. K., Jhun, J. Y., Cho, M. L., Min, J. K., & Cho, Y. Y. (2018). Kaempferol targeting on the fibroblast growth factor receptor 3-ribosomal S6 kinase 2 signaling axis prevents the development of rheumatoid arthritis. *Cell Death & Disease*, 9, 401. <https://doi.org/10.1038/s41419-018-0433-0>
- Mammucari, C., Raffaello, A., Vecellio Reane, D., Gherardi, G., De Mario, A., & Rizzuto, R. (2018). Mitochondrial calcium uptake in organ

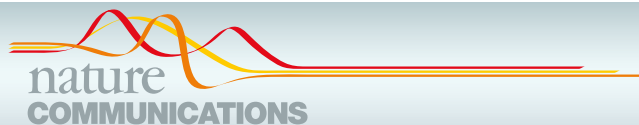
- physiology: From molecular mechanism to animal models. *Pflügers Archiv - European Journal of Physiology*, 470, 1165–1179. <https://doi.org/10.1007/s00424-018-2123-2>
- Min, C. K., Yeom, D. R., Lee, K.-E., Kwon, H.-K., Kang, M., Kim, Y.-S., Park, Z. Y., Jeon, H., & Kim, D. H. (2012). Coupling of ryanodine receptor 2 and voltage-dependent anion channel 2 is essential for  $\text{Ca}^{2+}$  transfer from the sarcoplasmic reticulum to the mitochondria in the heart. *The Biochemical Journal*, 447, 371–379. <https://doi.org/10.1042/BJ20120705>
- Montero, M., Lobatón, C. D., Hernández-Sanmiguel, E., Santodomingo, J., Vay, L., Moreno, A., & Alvarez, J. (2004). Direct activation of the mitochondrial calcium uniporter by natural plant flavonoids. *The Biochemical Journal*, 384, 19–24. <https://doi.org/10.1042/BJ20040990>
- Moretti, A., Bellin, M., Welling, A., Jung, C. B., Lam, J. T., Bott-Flügel, L., Dorn, T., Goedel, A., Höhnke, C., Hofmann, F., Seyfarth, M., Sinnecker, D., Schömig, A., & Laugwitz, K. L. (2010). Patient-specific induced pluripotent stem-cell models for long-QT syndrome. *The New England Journal of Medicine*, 363, 1397–1409. <https://doi.org/10.1056/NEJMoa0908679>
- Murugan, M., Santhakumar, V., & Kannurpatti, S. S. (2016). Facilitating mitochondrial calcium uptake improves activation-induced cerebral blood flow and behavior after mTBI. *Frontiers in Systems Neuroscience*, 10. <https://doi.org/10.3389/fnsys.2016.00019>
- Nathan, S. R., Pino, N. W., Arduino, D. M., Perocchi, F., MacMillan, S. N., & Wilson, J. J. (2017). Synthetic methods for the preparation of a functional analogue of Ru360, a potent inhibitor of mitochondrial calcium uptake. *Inorganic Chemistry*, 56, 3123–3126. <https://doi.org/10.1021/acs.inorgchem.6b03108>
- Némec, J., Kim, J. J., Gabris, B., & Salama, G. (2010). Calcium oscillations and T-wave lability precede ventricular arrhythmias in acquired long QT type 2. *Heart Rhythm*, 7, 1686–1694. <https://doi.org/10.1016/j.hrthm.2010.06.032>
- Némec, J., Kim, J. J., & Salama, G. (2016). The link between abnormal calcium handling and electrical instability in acquired long QT syndrome—Does calcium precipitate arrhythmic storms? *Progress in Biophysics and Molecular Biology*, 120, 210–221. <https://doi.org/10.1016/j.pbiomolbio.2015.11.003>
- O'Connell, T. D., Rodrigo, M. C., & Simpson, P. C. (2007). Isolation and culture of adult mouse cardiac myocytes. *Methods in Molecular Biology*, 357, 271–296. <https://doi.org/10.1385/1-59745-214-9:271>
- Pan, X., Liu, J., Nguyen, T. T., Liu, C., Sun, J., Teng, Y., Fergusson, M. M., Rovira, I. I., Allen, M., Springer, D. A., & Aponte, A. M. (2013). The physiological role of mitochondrial calcium revealed by mice lacking the mitochondrial calcium uniporter. *Nature Cell Biology*, 15, 1464–1472. <https://doi.org/10.1038/ncb2868>
- Patron, M., Granatiero, V., Espino, J., Rizzuto, R., & De Stefani, D. (2019). MICU3 is a tissue-specific enhancer of mitochondrial calcium uptake. *Cell Death and Differentiation*, 26, 179–195. <https://doi.org/10.1038/s41418-018-0113-8>
- Raffaello, A., De Stefani, D., Sabbadin, D., Teardo, E., Merli, G., Picard, A., Checchetto, V., Moro, S., Szabò, I., & Rizzuto, R. (2013). The mitochondrial calcium uniporter is a multimer that can include a dominant-negative pore-forming subunit. *The EMBO Journal*, 32, 2362–2376. <https://doi.org/10.1038/emboj.2013.157>
- Rebbeck, R. T., Essawy, M. M., Nitu, F. R., Grant, B. D., Gillispie, G. D., Thomas, D. D., Bers, D. M., & Cornea, R. L. (2017). High-throughput screens to discover small-molecule modulators of ryanodine receptor calcium release channels. *SLAS DISCOVERY: Advancing Life Sciences R&D*, 22, 176–186. <https://doi.org/10.1177/1087057116674312>
- Robert, V., Gurlini, P., Tosello, V., Nagai, T., Miyawaki, A., Di Lisa, F., & Pozzan, T. (2001). Beat-to-beat oscillations of mitochondrial  $[\text{Ca}^{2+}]$  in cardiac cells. *The EMBO Journal*, 20, 4998–5007. <https://doi.org/10.1093/emboj/20.17.4998>
- Rog-Zielinska, E. A., Johnston, C. M., O'Toole, E. T., Morpew, M., Hoenger, A., & Kohl, P. (2016). Electron tomography of rabbit cardiomyocyte three-dimensional ultrastructure. *Progress in Biophysics and Molecular Biology*, 121, 77–84. <https://doi.org/10.1016/j.pbiomolbio.2016.05.005>
- Sander, P., Gudermann, T., & Schredelseker, J. (2021). A calcium guard in the outer membrane: Is VDAC a regulated gatekeeper of mitochondrial calcium uptake? *International Journal of Molecular Sciences*, 22, 946. <https://doi.org/10.3390/ijms22020946>
- Schweitzer, M. K., Wilting, F., Sedej, S., Dreizehnter, L., Dupper, N. J., Tian, Q., Moretti, A., My, I., Kwon, O., Priori, S. G., Laugwitz, K. L., Storch, U., Lipp, P., Breit, A., Mederos y Schnitzler, M., Gudermann, T., & Schredelseker, J. (2017). Suppression of arrhythmia by enhancing mitochondrial  $\text{Ca}^{2+}$  uptake in catecholaminergic ventricular tachycardia models. *JACC: Basic to Translational Science*, 2, 737–746. <https://doi.org/10.1016/j.jacbts.2017.06.008>
- Sedej, S., Heinzel, F. R., Walther, S., Dybkova, N., Wakula, P., Groborz, J., Gronau, P., Maier, L. S., Vos, M. A., Lai, F. A., Napolitano, C., Priori, S. G., Kocksämper, J., & Pieske, B. (2010).  $\text{Na}^{+}$ -dependent SR  $\text{Ca}^{2+}$  overload induces arrhythmogenic events in mouse cardiomyocytes with a human CPVT mutation. *Cardiovascular Research*, 87, 50–59. <https://doi.org/10.1093/cvr/cvq007>
- Shimizu, H., Schredelseker, J., Huang, J., Lu, K., Naghdi, S., Lu, F., Franklin, S., Fiji, H. D. G., Wang, K., Zhu, H., Tian, C., Lin, B., Nakano, H., Ehrlich, A., Nakai, J., Stieg, A. Z., Gimzewski, J. K., Nakano, A., Goldhaber, J. I., ... Chen, J. N. (2015). Mitochondrial  $\text{Ca}^{2+}$  uptake by the voltage-dependent anion channel 2 regulates cardiac rhythmicity. *eLife*, 4, e04801. <https://doi.org/10.7554/eLife.04801>
- Waldeck-Weiermair, M., Deak, A. T., Groschner, L. N., Alam, M. R., Jean-Quartier, C., Malli, R., & Graier, W. F. (2013). Molecularly distinct routes of mitochondrial  $\text{Ca}^{2+}$  uptake are activated depending on the activity of the sarco/endoplasmic reticulum  $\text{Ca}^{2+}$  ATPase (SERCA). *The Journal of Biological Chemistry*, 288, 15367–15379. <https://doi.org/10.1074/jbc.M113.462259>
- Wilting, F., Kopp, R., Gurnev, P. A., Schedel, A., Dupper, N. J., Kwon, O., Nicke, A., Gudermann, T., & Schredelseker, J. (2020). The antiarrhythmic compound efsevin directly modulates voltage-dependent anion channel 2 by binding to its inner wall and enhancing mitochondrial  $\text{Ca}^{2+}$  uptake. *British Journal of Pharmacology*, 177, 2947–2958. <https://doi.org/10.1111/bph.15022>
- Woods, J. J., & Wilson, J. J. (2020). Inhibitors of the mitochondrial calcium uniporter for the treatment of disease. *Current Opinion in Chemical Biology*, 55, 9–18. <https://doi.org/10.1016/j.cbpa.2019.11.006>
- Wu, Y., Zhang, Q., & Zhang, R. (2017). Kaempferol targets estrogen-related receptor  $\alpha$  and suppresses the angiogenesis of human retinal endothelial cells under high glucose conditions. *Experimental and Therapeutic Medicine*, 14, 5576–5582. <https://doi.org/10.3892/etm.2017.5261>
- Yao, K., Chen, H., Liu, K., Langfald, A., Yang, G., Zhang, Y., Yu, D. H., Kim, M. O., Lee, M. H., Li, H., Bae, K. B., Kim, H. G., Ma, W. Y., Bode, A. M., Dong, Z., & Dong, Z. (2014). Kaempferol targets RSK2 and MSK1 to suppress UV radiation-induced skin cancer. *Cancer Prevention Research (Philadelphia, Pa.)*, 7, 958–967. <https://doi.org/10.1158/1940-6207.CAPR-14-0126>

## SUPPORTING INFORMATION

Additional supporting information may be found online in the Supporting Information section at the end of this article.

**How to cite this article:** Sander, P., Feng, M., Schweitzer, M. K., Wilting, F., Gutenthaler, S. M., Arduino, D. M., Fischbach, S., Dreizehnter, L., Moretti, A., Gudermann, T., Perocchi, F., & Schredelseker, J. (2021). Approved drugs ezetimibe and disulfiram enhance mitochondrial  $\text{Ca}^{2+}$  uptake and suppress cardiac arrhythmogenesis. *British Journal of Pharmacology*, 1–15. <https://doi.org/10.1111/bph.15630>

## 7 Publication II



### ARTICLE



<https://doi.org/10.1038/s41467-021-24869-0>

OPEN

# Cardiac-specific deletion of voltage dependent anion channel 2 leads to dilated cardiomyopathy by altering calcium homeostasis

Thirupura S. Shankar<sup>1,2</sup>, Dinesh K. A. Ramadurai<sup>1</sup>, Kira Steinhorst<sup>3</sup>, Salah Sommakia<sup>1</sup>, Rachit Badolia<sup>1</sup>, Aspasia Thodou Krokidi<sup>1</sup>, Dallen Calder<sup>1</sup>, Sutip Navankasattusas<sup>1</sup>, Paulina Sander<sup>1,3</sup>, Oh Sung Kwon<sup>4,5</sup>, Aishwarya Aravamudhan<sup>1</sup>, Jing Ling<sup>1</sup>, Andreas Dendorfer<sup>6,7</sup>, Changmin Xie<sup>8</sup>, Ohyun Kwon<sup>8</sup>, Emily H. Y. Cheng<sup>9</sup>, Kevin J. Whitehead<sup>10</sup>, Thomas Gudermann<sup>3,7</sup>, Russel S. Richardson<sup>5</sup>, Frank B. Sachse<sup>1,2</sup>, Johann Schredelseker<sup>3,7</sup>, Kenneth W. Spitzer<sup>1,10</sup>, Dipayan Chaudhuri<sup>1,10</sup> & Stavros G. Drakos<sup>1,2,10</sup>✉

Voltage dependent anion channel 2 (VDAC2) is an outer mitochondrial membrane porin known to play a significant role in apoptosis and calcium signaling. Abnormalities in calcium homeostasis often leads to electrical and contractile dysfunction and can cause dilated cardiomyopathy and heart failure. However, the specific role of VDAC2 in intracellular calcium dynamics and cardiac function is not well understood. To elucidate the role of VDAC2 in calcium homeostasis, we generated a cardiac ventricular myocyte-specific developmental deletion of *Vdac2* in mice. Our results indicate that loss of VDAC2 in the myocardium causes severe impairment in excitation-contraction coupling by altering both intracellular and mitochondrial calcium signaling. We also observed adverse cardiac remodeling which progressed to severe cardiomyopathy and death. Reintroduction of VDAC2 in 6-week-old knockout mice partially rescued the cardiomyopathy phenotype. Activation of VDAC2 by efsevin increased cardiac contractile force in a mouse model of pressure-overload induced heart failure. In conclusion, our findings demonstrate that VDAC2 plays a crucial role in cardiac function by influencing cellular calcium signaling. Through this unique role in cellular calcium dynamics and excitation-contraction coupling VDAC2 emerges as a plausible therapeutic target for heart failure.

<sup>1</sup>Nora Eccles Harrison Cardiovascular Research and Training Institute, University of Utah, Salt Lake City, UT, USA. <sup>2</sup>Department of Biomedical Engineering, University of Utah, Salt Lake City, UT, USA. <sup>3</sup>Walther Straub Institute of Pharmacology and Toxicology, Faculty of Medicine, LMU Munich, Munich, Germany. <sup>4</sup>Department of Kinesiology, University of Connecticut, Storrs, CT, USA. <sup>5</sup>Geriatric Research, Education, and Clinical Center, Salt Lake City VA Medical Center, Salt Lake City, UT, USA. <sup>6</sup>Walter-Brendel-Center of Experimental Medicine, Ludwig-Maximilians Universität Munich, Munich, Germany. <sup>7</sup>German Centre for Cardiovascular Research (DZHK), Partner Site Munich Heart Alliance, Munich, Germany. <sup>8</sup>Department of Chemistry and Biochemistry, University of California, Los Angeles, CA, USA. <sup>9</sup>Memorial Sloan Kettering Cancer Center, New York, NY, USA. <sup>10</sup>Division of Cardiovascular Medicine, University of Utah School of Medicine, Salt Lake City, UT, USA. ✉email: [Stavros.Drakos@hsc.utah.edu](mailto:Stavros.Drakos@hsc.utah.edu)

## ARTICLE

NATURE COMMUNICATIONS | <https://doi.org/10.1038/s41467-021-24869-0>

**N**on-ischemic dilated cardiomyopathy (DCM) is one of the most common causes that lead to the syndrome of chronic heart failure (HF) which is currently a growing global epidemic<sup>1,2</sup>. DCM is a condition in which the cardiac ventricular chambers enlarge and have impaired systolic and diastolic function. The impaired myocardial function has been partly attributed to alterations in the function of contractile proteins and excitation–contraction coupling (ECC)<sup>3</sup>. Calcium plays a crucial role in ECC and influences cardiac rhythmicity and cellular contraction. During systole, electrical excitation of the membrane causes L-type calcium channels (LTCC) to open and a small amount of calcium enters the cell which binds to ryanodine receptor 2 (RyR2) and triggers the sarcoplasmic reticulum (SR) to release some of its calcium reserve. This release results in an overall increase in the cytosolic calcium which binds to troponin thereby facilitating cellular contraction. The excess cytosolic calcium is pumped out of the cytoplasm through three main processes. Part of the calcium is pumped back into the SR through sarcoplasmic endoplasmic reticulum calcium ATPase 2a (SERCA2a) and the rest of the calcium is extruded out of the cell via the sodium–calcium exchanger (NCX1) and the sarcolemma calcium pump. The mitochondria also appear to play a role in calcium uptake during this process and its importance is under investigation<sup>4,5</sup>.

The voltage-dependent anion channel 2 (VDAC2) is a 32 kDa porin present on the mitochondrial outer membrane (MOM) and contributes to apoptosis, steroidogenesis, metabolite flux, and calcium homeostasis<sup>6</sup>. VDAC2 is known to interact with pro-apoptotic proteins such as Bcl2 family proteins. While VDAC2–BAK (Bcl2-antagonist/killer protein) interaction is reported to be highly important to control cellular apoptosis, it is still controversial if this interaction promotes or inhibits apoptosis. Studies show that VDAC2–BAK complex was absent during death stimulus and deletion of VDAC2 promotes apoptosis<sup>7</sup>. In contrast, other studies have shown that truncated-Bid (BH3-interacting domain death agonist) induced MOM permeabilization and cell death in wild-type (WT) but not in VDAC2 knock-out (KO) mouse embryonic fibroblasts<sup>8</sup>.

Calcium flux into the mitochondrial matrix takes place primarily through the mitochondrial calcium uniporter (MCU), present in the mitochondrial inner membrane (MIM). However, the initial calcium import into the inter-membrane space is through VDACS. The interaction between MOM and SR is crucial for this mitochondrial calcium signaling<sup>9</sup>. Evidence suggests that coupling of VDAC2 with sub-sarcolemmal RyR2 is essential for calcium transfer from SR to the mitochondria<sup>10</sup>. Mitochondrial calcium dynamics have mostly been associated with the MIM and primarily, the MCU. However, it has been reported that MCU-KO mice do not show any adverse cardiac phenotypes<sup>11,12</sup>. This suggests an important role of VDACS and MOM in mitochondrial calcium signaling.

Increasing evidence suggests the importance of VDAC2 in physiologic cardiac function and in this manuscript, we hypothesize that mitochondrial calcium dynamics have a significant influence in this process<sup>13,14</sup>. Increasing the calcium uptake through VDAC2 has been shown to reverse the arrhythmia phenotype observed in the tremblor zebrafish model (NCX1h mutant) and the tachycardia phenotype in mice with catecholaminergic polymorphic ventricular tachycardia (RYR2 mutant)<sup>13,14</sup>. Both these arrhythmic models have irregular cellular calcium signaling. Enhancing mitochondrial calcium uptake through VDAC2 using a small molecule called efsevin, pharmacologically helped restore the rhythmic phenotype in these models. VDAC2 knock-down in HL-1 cell line has shown to have specific effects on calcium homeostasis such as increased diastolic calcium and restricted calcium spark expansion<sup>15</sup>. However, after

a global knockdown of VDAC2 was shown to be embryonic lethal<sup>7</sup>, no further studies have investigated the effects of cardiac VDAC2-KO in animal models. Advancing our understanding of VDAC2's role in calcium signaling and ECC may have significant implications. In this study, in an effort to address this gap in knowledge we performed cardiac-specific *Vdac2* deletion and studied its effects on calcium cycling. Our results indicate a strong dependency on VDAC2 and cellular calcium dynamics to the ECC. VDAC2-KO mice showed significantly slower mitochondrial calcium uptake and altered cellular calcium signaling with smaller calcium transient, a slower rate of decay, and a slower rate of rising in cytosolic calcium. Adverse cardiac remodeling and severe cardiomyopathy led to the death of these KO mice. Reintroduction of VDAC2 in 6-week-old KO mice using an adeno-associated virus 9 (AAV9) vector seemed to partially rescue the cardiomyopathy phenotype suggesting a plausible role of VDAC2 as a therapeutic target in clinical HF. To evaluate this hypothesis, we took a gain-of-function approach and measured the effects of VDAC2 agonist efsevin in murine tissue from failing hearts: in line with the HF phenotype induced by VDAC2-KO, efsevin enhanced contractile force in failing myocardium from a murine pressure-overload model establishing VDAC2 as a promising target for HF.

## Results

**Cardiac-specific developmental deletion of VDAC2 causes DCM and leads to increased mortality.** Cardiac ventricle-specific developmental *Vdac2* KO and littermate WT were used for this study. Mice with either flox or Cre were used as WT and echocardiography data on flox or Cre only mice shows no significant differences (Supplementary Fig. 1a–g). Deletion of VDAC2 was confirmed using western blot (Fig. 1a). We observed no difference in VDAC1 and VDAC3 protein levels in VDAC2-KO mice (Supplementary Fig. 2a–c), suggesting a pure VDAC2-dependent phenotype. Increased mortality was observed in the KO between 5 and 20-weeks postpartum. Most of these events occurred during 20-weeks postpartum (Fig. 1b). Serial echocardiographic analysis, showed progressive deterioration of cardiac function in VDAC2-KO mice as reflected by significant reductions around 16 weeks in left ventricular (LV) ejection fraction (EF), fractional shortening (FS), and posterior wall thickness at systole (LVPW,s) and a significant increase in LV end-diastolic diameter (LVEDD), LV end-diastolic and end-systolic volumes (EDV and ESV, respectively). No difference in LV posterior wall thickness at diastole (LVPW,d) and LV mass (normalized to body weight) was observed (Fig. 1c–j). We are also providing Supplementary Table 1 which describes the cardiac phenotype during the entire development, including intra-uterine echocardiograms performed in pregnant mice<sup>16</sup>. We also found increased gene expression of NPPA in KO mice (Fig. 1m), all of which are hallmarks of DCM. Increased dilation was also evident from echocardiography and the KO hearts were significantly larger than WT hearts (Fig. 1k, l). VDAC2-KO mice also had significantly longer and thinner cardiomyocytes compared to WT mice at 16-weeks of age (Fig. 1n–p). Taken together, our results suggest that deletion of VDAC2 in the myocardium during development causes DCM and eventually leads to increased mortality.

**Altered gene and protein expression profiles indicate altered calcium signaling and regulation in VDAC2-KO.** Gene expression profile from ventricular RNA of 16-week-old KO mice showed a number of differentially expressed genes involved in calcium signaling and regulation. Calcium channel genes such as *Cacna1h*, a T-type calcium channel (Cav 3.2) was upregulated

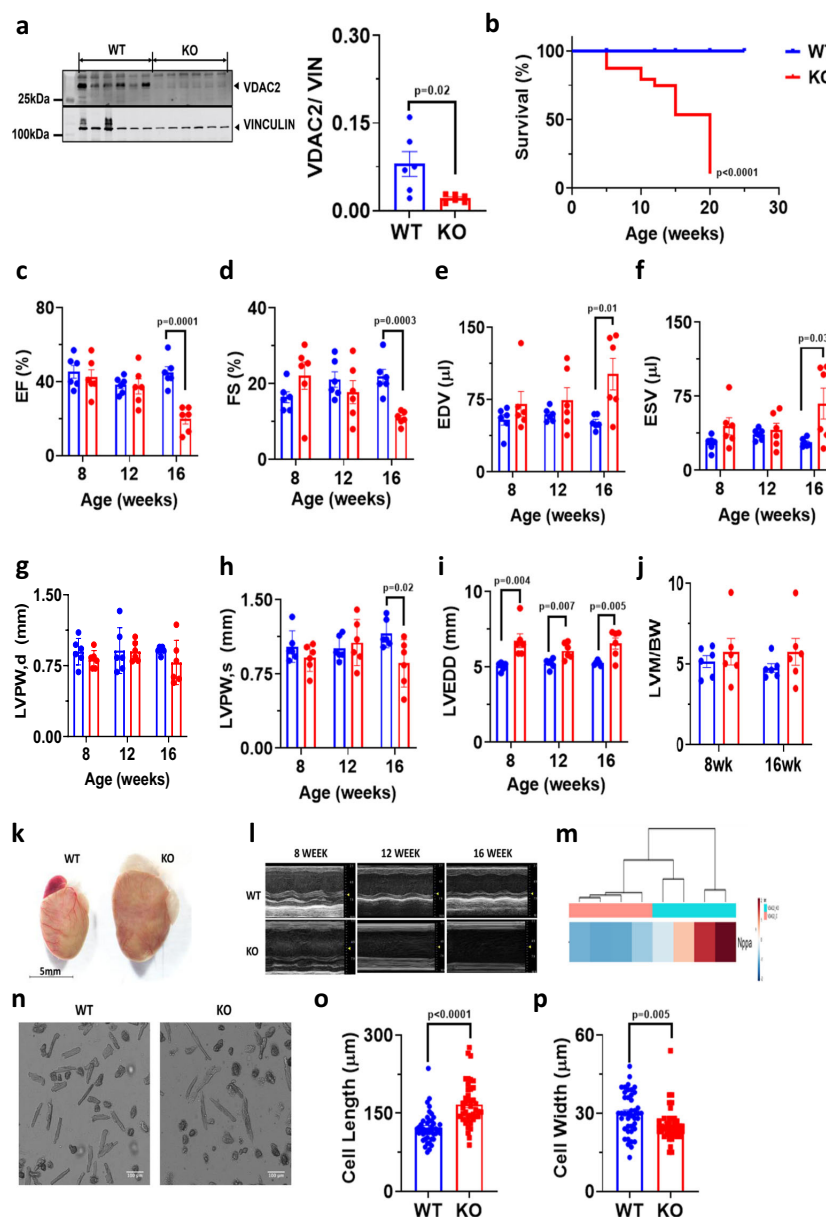
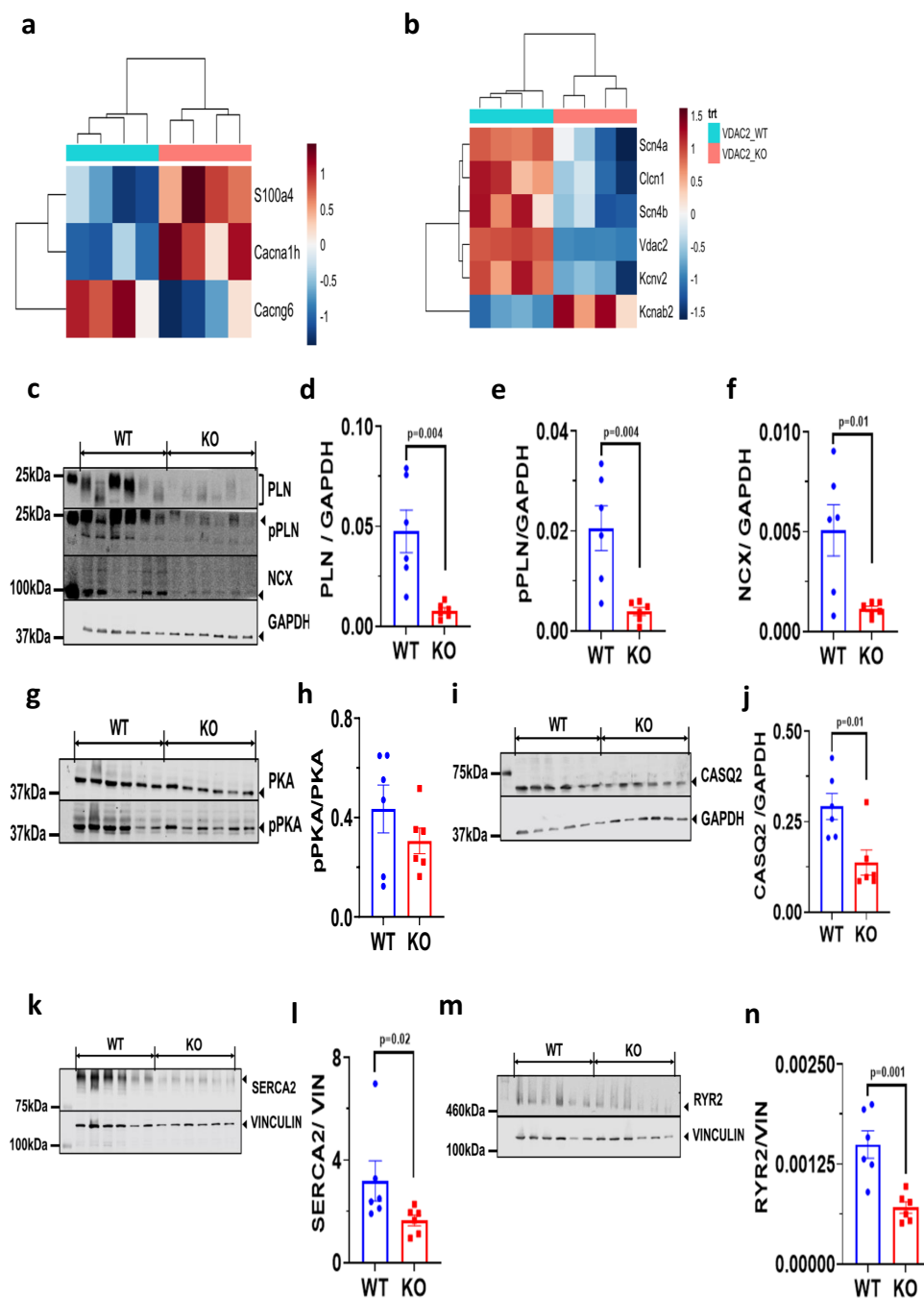


**Fig. 1** Cardiac-specific deletion of VDAC2 causes dilated cardiomyopathy and leads to increased mortality. **a** Western blot image of VDAC2 and lane-loading control VINCULIN and quantification in WT (Wild-type) and KO (Knock-out) using Image Studio Lite (version5.2.5) ( $p = 0.02$ ) ( $n = 6$ ); **b** Kaplan-Meier survival curve ( $n = 10$ ) ( $p < 0.0001$ ); **c-j** Echocardiography analysis of left ventricular ejection fraction (EF) ( $p = 0.000143$ ), fractional shortening (FS) ( $p = 0.000376$ ), left ventricular end-diastolic and end-systolic volumes (EDV and ESV) ( $p = 0.0132$  and  $p = 0.0311$ ), left-ventricular posterior wall thickness at diastole and systole (LVPW,d and LVPW,s) ( $p = \text{ns}$  and  $p = 0.0244$ ), left ventricular end-diastolic diameter (LVEDD) (8-week  $p = 0.004824$ ; 12-week  $p = 0.007670$  and 16-week  $p = 0.005986$ ) ( $n = 6$ ) and **j** left ventricular mass to body weight ratio (LVM/BW), respectively ( $n = 6$ ); **k** Representative heart image of 16-week-old mice (scale bar, 5 mm); **l** Representative m-mode image from echocardiography ( $n = 1$ ); **m** Differential expression of NPPA gene ( $n = 4$ ); **n** Representative ventricular cardiomyocyte image using confocal microscopy (scale bar, 100  $\mu\text{m}$ ); **o, p** Cardiomyocyte cell length ( $p < 0.0001$ ) and width ( $p = 0.0058$ ) measured using Zen5 imaging software, respectively ( $n = 42$ ,  $N = 3$ ).  $p$ -value: unpaired two-tailed  $t$ -test performed in panels **a**, **o**, and **p**, Mantel-Cox test performed in panel **b** and two-stage set-up multiple  $t$ -test (Benjamini, Krieger, and Yekutieli) performed for longitudinal echocardiographic data. Data are represented as differences between mean  $\pm$  SEM.



whereas *Cacng6*, a subunit of the LTCC was significantly down-regulated (Fig. 2a). Other ion channels were also differentially expressed between the two groups. Specifically, a significant downregulation of sodium and potassium ion channels was observed in VDAC2-KO mice, including *Scn4a*, *Scn4b*, and *Kcnv2*, all of which have been reported to play significant roles in

normal cardiac function (Fig. 2b). Proteins involved in ECC such as RYR2, SERCA2, NCX1, total and phosphorylated phospholamban (PLN), and calsequestrin (CASQ2, the SR calcium-binding protein) were significantly decreased in the KO (Fig. 2c–n). Collectively, these results suggest that loss of VDAC2 leads to abnormalities in cellular calcium signaling pathways.



**Fig. 2 Altered gene and protein expression profiles indicate altered calcium signaling and regulation in VDAC2-KO.** **a, b** Differential gene expression data derived from 16-week old cardiac ventricular tissue ( $n = 4$ ); **c–f** Western blot image of PLN ( $p = 0.0042$ ), pPLN ( $p = 0.0045$ ), and NCX ( $p = 0.0121$ ) along with lane-loading control GAPDH and respective quantification using Image Studio Lite (version 5.2.5) ( $n = 6$ ); **g, h** Western blot image of PKA and pPKA and quantification using Image Studio Lite (version 5.2.5) ( $p = \text{ns}$ ) ( $n = 6$ ); **i, j** Western blot image of CASQ2 and lane-loading control GAPDH and respective quantification using Image Studio Lite (version 5.2.5) ( $p = 0.0111$ ) ( $n = 6$ ); **k, l** Western blot image of SERCA2 and lane-loading control VINCULIN and quantification using Image Studio Lite (version 5.2.5) (Mann-Whitney:  $p = 0.0260$ ) ( $n = 6$ ); **m, n** Western blot image of RYR2 and lane-loading control VINCULIN and quantification using Image Studio Lite (version 5.2.5) ( $p = 0.0018$ ) ( $n = 6$ ).  $p$ -value: unpaired two-tailed  $t$ -test and two-tailed Mann-Whitney test performed. Data are represented as mean  $\pm$  SEM.

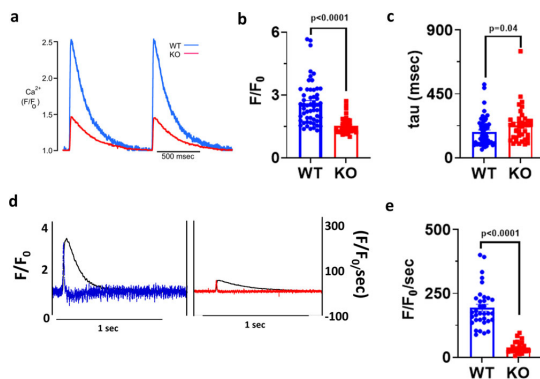


**Fig. 3 Impaired calcium cycling in VDAC2-KO cardiomyocytes.** **a** Representative calcium transient image of 16-week-old mice (Time frame, 500 ms); **b** Amplitude ( $F/F_0$ ) data ( $p < 0.0001$ ) (WT  $n = 54$ , KO  $n = 38$ ,  $N = 3$ ); **c** Rate of calcium uptake ( $\tau$ ) (ms) ( $p = 0.0492$ ) (WT  $n = 54$ , KO  $n = 38$ ,  $N = 3$ ); **d** Representative image of rate of calcium release of 16-week-old mice (Time frame, 1 s); **e** Rate of calcium release ( $F/F_0/s$ ) ( $p < 0.0001$ ) (WT  $n = 34$ , KO  $n = 23$ ,  $N = 3$ ).  $p$ -value: unpaired two-tailed  $t$ -test performed in all comparisons. Data are represented as mean  $\pm$  SEM.

**Impaired calcium cycling in VDAC2-KO cardiac myocytes.** To further assess calcium handling in these mice, we recorded calcium transients in 16-week-old cardiac myocytes. Compared to WT, VDAC2-KO myocytes had smaller calcium transients ( $F/F_0$ ) with a slower rate of decay ( $\tau$ ) and slower maximum rate of rising ( $F/F_0/s$ ) (Fig. 3a–e). To investigate if the decreased calcium transients are directly attributable to the lack of VDAC2 we tested the effects of VDAC2 agonist efsavin<sup>14</sup> on calcium transients in WT cardiomyocytes and found the opposite effect, namely an increase in calcium transient amplitude and an acceleration of the decay phase (Supplementary Fig. 3a–c). SERCA2a and NCX1 are the two main channels involved in cytosolic calcium clearance during diastole and we showed that these protein levels are significantly reduced in VDAC2-KO (Fig. 2f and l). Co-immunoprecipitation (Co-IP) studies using whole-heart lysate and pull-down using VDAC2 antibody revealed VDAC2–SERCA2 interaction and VDAC2–NCX1 interaction, respectively. VDAC2-KO heart was used as a negative control for co-IP (Fig. 4a). This interaction was also confirmed by immunofluorescence and proximity ligation assays (PLA) (Fig. 4b, c). We hypothesize that these interactions, similar to the previously discovered VDAC2–RyR2 interaction<sup>10</sup>, are crucial for calcium uptake by the mitochondria and indirectly by the SR. As a result, a disruption of this interaction caused drastic changes in the calcium signaling in the cardiac myocytes. This altered calcium signaling may explain bradyarrhythmia observed in VDAC2-KO (Fig. 5a, b)<sup>17</sup>. Additionally, in agreement with the altered gene expression of the above-mentioned ion channels, the action

potential (AP) of the KO was different from that of WT with a significantly longer AP duration at 50% repolarization ( $APD_{50}$ ) and a normal 90% repolarization ( $APD_{90}$ ) (Fig. 5c–e). Collectively, we found significant differences in most aspects of calcium cycling in the VDAC2-KO, which presumably contributes to the progressive decline in myocardial function.

#### Altered mitochondrial structure and function in VDAC2-KO.

Transmission electron microscopy (TEM) performed on 16-week-old KO and WT hearts showed substantial alterations in mitochondrial distribution and structure (Fig. 6a–c). KO mitochondria were significantly smaller, disoriented, and less dense compared to WT mitochondria. We did not observe any significant difference in dynamin-related protein 1 (DRP1) levels (a marker for mitochondrial fission) although it showed a trend towards an increase in KO mice (Fig. 6d, e). We also observed a significant reduction in the rate of calcium uptake in KO mitochondria suggesting VDAC2 plays an important role in mitochondrial calcium transport (Fig. 6f–h). A significant decline in MCU and NCLX protein levels was also observed in the KO (Fig. 6i–k). These proteins are known to play an important role in mitochondrial calcium transport and signaling and the decreased protein level in the KO is consistent with the slower rate of calcium uptake.

#### Increased cardiac fibrosis observed in VDAC2-KO.

Gene expression profile showed a significant upregulation of extracellular matrix (ECM) proteins and collagen encoding genes including *Col3a1*, *Col5a2*, and *Mmp12* in the KO that suggests increased collagen deposition and fibrosis (Fig. 7a). Kyoto Encyclopedia of Genes and Genomes (KEGG) pathway analysis in KO mice indicated that the ECM production pathway changes reached the highest statistical significance (Fig. 7b). Masson's trichrome stain and TEM on 16-week-old mice hearts showed significantly higher collagen content in the KO (Fig. 7c–f). The observed increased myocardial fibrosis is consistent with adverse structural and functional myocardial remodeling and cardiomyopathy in the KO mice.

#### Metabolic alterations observed in VDAC2-KO.

Since VDAC2 is known to interact with a number of key enzymes like phosphofructokinase (PFK) and hexokinase (HK) that are involved in glycolysis and is known to transport a number of metabolites and ATP, we also measured the RNA and protein levels of specific enzymes in key metabolic pathways. The volcano plot from RNA sequencing data showed significant differences in enzymes involved in metabolism and we observed an overall down-regulation of enzyme levels involved in glycolysis, tricarboxylic acid (TCA) cycle, and glycolytic accessory pathways. Specifically, enzymes including transketolase (TKT), succinyl-CoA ligase (SUCLA2), pyruvate dehydrogenase (PDH), and pyruvate carboxylase (PC). However, no significant difference was observed in fatty acid oxidation (FAO) pathways (Supplementary Fig. 4a–o). VINCULIN and GAPDH were used as lane-loading controls and

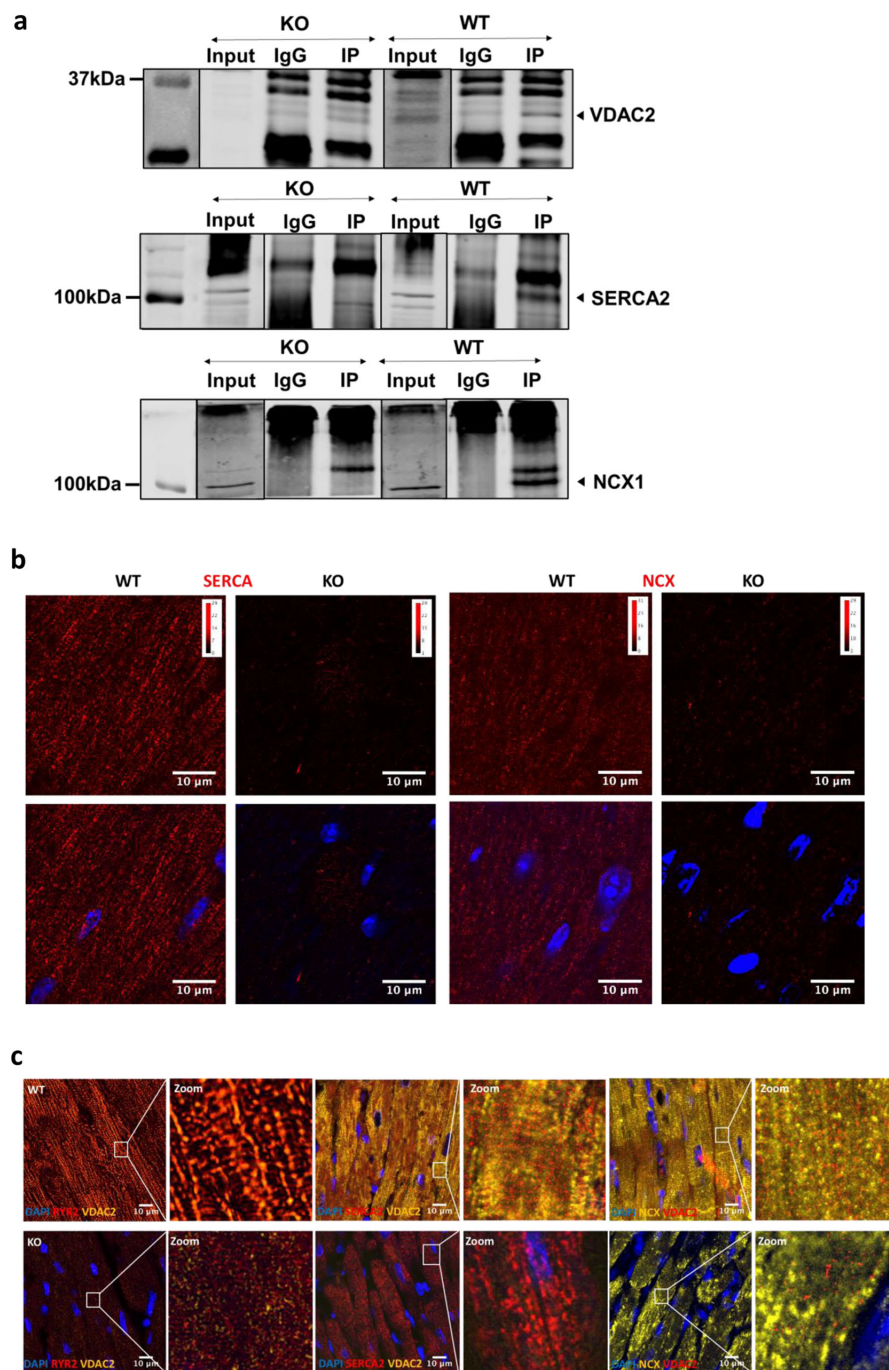


**Fig. 4** Cross-talk between mitochondria and ER/SR facilitates mitochondrial calcium cycling. **a** Representative co-immunoprecipitation image from a cardiac ventricular sample of 8-week-old mice ( $n = 3$ ) in WT and KO (Input—non-IP sample; IgG—control antibody; IP—VDAC2 protein pull-down); **b** Representative proximity ligation assay image for VDAC2-SERCA2 and VDAC2-NCX1 interaction in 8-week-old mice (scale bar, 10 μm) ( $n = 3$ ); **c** Representative immunofluorescence image from 16-week-old mice heart (scale bar, 10 μm) ( $n = 3$ ).

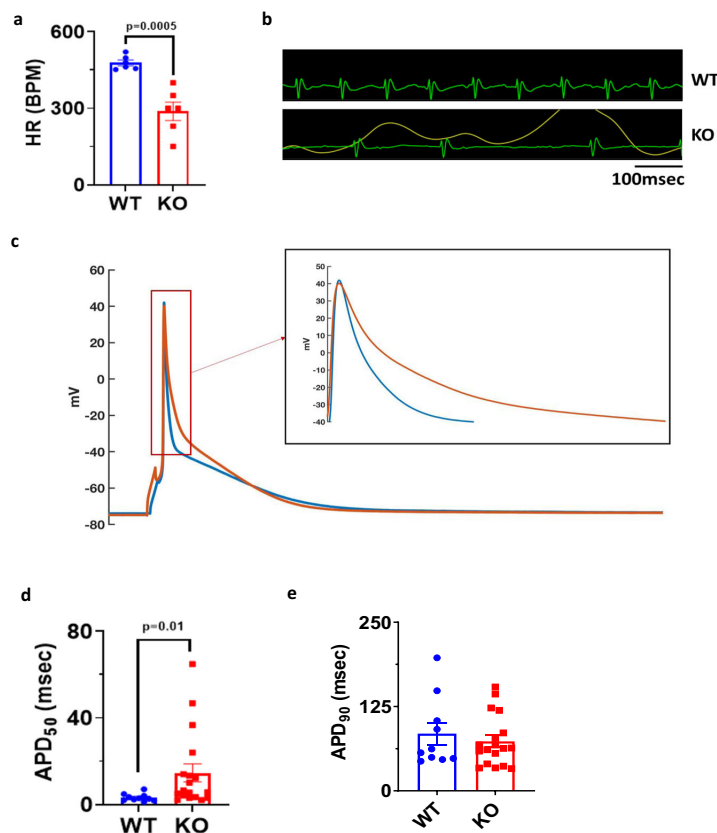


**Fig. 5** Altered action potential in VDAC2-KO cardiomyocytes. **a** Heart rate (HR), beats per minute (BPM) ( $p = 0.0005$ ) ( $n = 6$ ); **b** Representative ECG of 16-week-old mice (time frame, 100 ms); **c** Representative action potential image of 16-week-old mice cardiomyocyte (time frame, 100 ms); **d, e** Action potential repolarization duration at 50% and 90%, respectively (two-tailed Welch test:  $APD_{90} p = ns$ ,  $APD_{50} p = 0.0148$ ) (WT  $n = 10$ , KO  $n = 18$ ,  $N = 3$ ).  $p$ -value: unpaired two-tailed  $t$ -test and two-tailed Welch test performed. Data are represented as mean  $\pm$  SEM.

we observed no difference in these protein levels between WT and KO (Supplementary Fig. 4p).

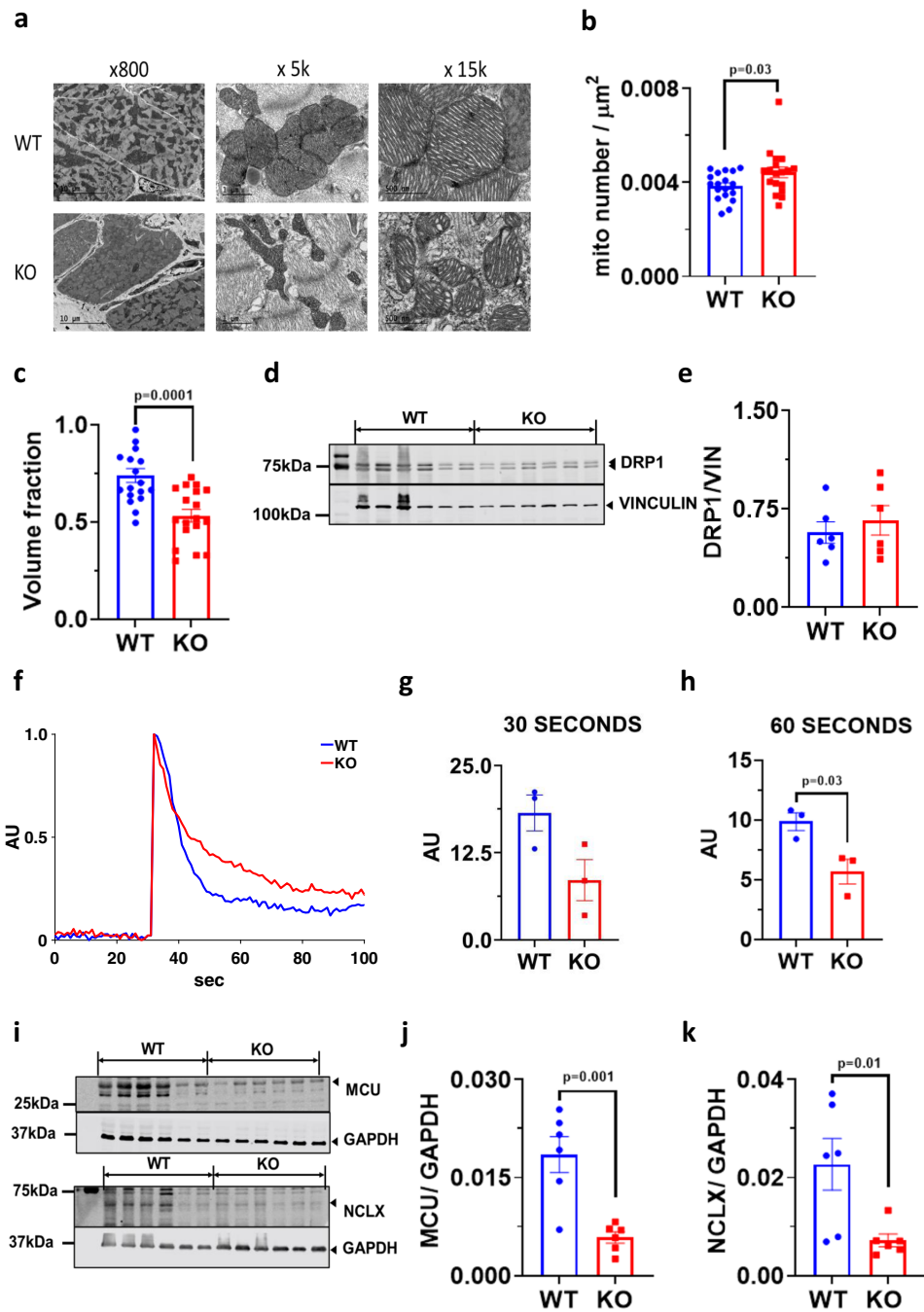
**No significant difference in mitochondrial ROS production.** VDAC2-KO did not show a significant difference (compared to WT) in reactive oxygen species (ROS) production upon inhibition of complex I and complex III using rotenone and antimycin, respectively (Supplementary Fig. 5a–d). However, we found a trend ( $p = 0.08$ ) towards a decrease in complex II in the KO (Supplementary Fig. 5e–i).

**Unaltered mitochondrial respiration.** Oxidative phosphorylation (OXPHOS) measurements with LV myocardial tissue showed no difference in mitochondrial oxygen consumption between the WT and KO under normal conditions (Supplementary Fig. 6a–i). This suggests that VDAC2 is not essential for normal mitochondrial respiration despite its role in calcium signaling. These results are similar to those observed in previous publications with MCU-KO<sup>11,18</sup>.

**Partial rescue of HF phenotype upon VDAC2 re-introduction.** Cardiac ventricular myocyte-specific reintroduction of VDAC2 in KO and WT mice was assessed using western blot and qRT-PCR

(Fig. 8a, b). Serial echocardiography was performed on these mice up to 10 weeks post-injection (16-week-old mice) to get comparable results. Cardiac structural and functional improvement was observed in KO mice injected with AAV9- $\alpha$ MHC-VDAC2-GFP vector evident from relative improvement in EF, FS, and LV volumes and from a decrease in LV diameter compared to KO mice injected with control AAV9- $\alpha$ MHC-GFP vector (Fig. 8c–g). Complete rescue of the phenotype was not observed, however, the re-introduction of VDAC2 aided in better cardiac functioning.

**VDAC2 as a pharmacological target for HF.** We show that VDAC2 regulates cardiac calcium signaling without having major effects on bioenergetics and VDAC2 deletion causes DCM, making it a candidate structure for HF therapy. We therefore, addressed the question of increasing VDAC2s calcium uptake activity could enhance cardiac contractile force in HF. Therefore, we used the established model of pressure overload-induced HF by transverse aortic constriction (TAC). Since the administration of efsevin to mice is difficult for more than a few days due to its short plasma half-life time and efsevin is not orally bioavailable, we took advantage of organotypic heart slices and investigated the effect of efsevin on myocardial contractile strength. Strikingly, efsevin enhanced contractile strength and accelerated relaxation in both control and failing hearts (Fig. 9a, b).

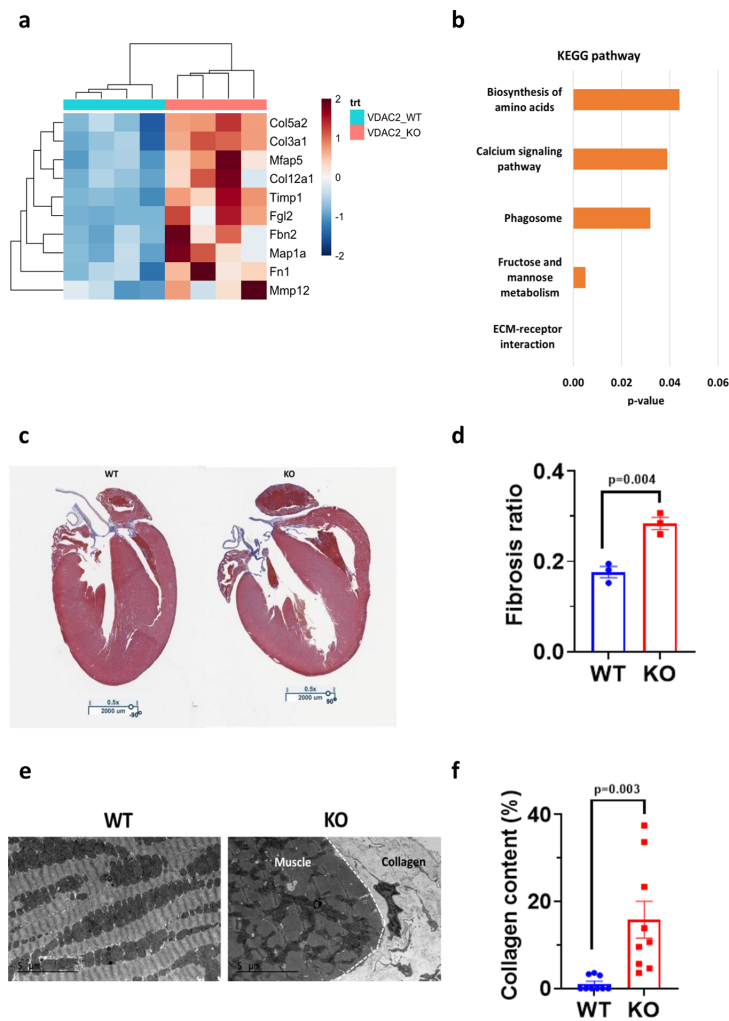


**Discussion**

In this study, we investigated the role of VDAC2 in the heart by creating a cardiac ventricular myocyte-specific deletion of VDAC2 using  $\alpha$ -Myosin heavy chain ( $\alpha$ MHC) promoter. We observed increased postnatal mortality along with severe impairment in cardiac structure and function consistent with

DCM. Our gene and protein studies suggested altered calcium signaling in the KO mice. In agreement with these data, the KO showed smaller calcium transients, a slower decay time, and a slower rate of calcium release. Substantial adverse cardiac remodeling and mitochondrial disorganization along with slower mitochondrial calcium uptake were also observed in the KO

**Fig. 6 Altered mitochondrial structure and function in VDAC2-KO.** **a** Representative transmission electron microscopy image at  $\times 800$ ,  $\times 5000$  and  $\times 15,000$  magnifications (scale bar, 10  $\mu\text{m}$ , 1  $\mu\text{m}$ , and 500 nm, respectively) ( $n = 3$ ); **b** Number of mitochondria per unit area measured using Adobe Photoshop CC 2019 ( $p = 0.0365$ ) ( $n = 18$  images,  $N = 3$ ); **c** Mitochondrial volume fraction measured using Adobe Photoshop CC 2019 using  $22 \times 14$  grid ( $p = 0.0001$ ) ( $n = 18$  images,  $N = 3$ ); **d, e** Western blot image of DRP1 and lane-loading control VINCULIN and quantification using Image Studio Lite (version 5.2.5) ( $p = \text{ns}$ ) ( $n = 6$ ); **f** Representative mitochondrial calcium uptake image produced using MATLAB ( $n = 3$ ); **g, h** Mitochondrial calcium uptake in the first 30 s ( $p = \text{ns}$ ) and 60 s of calcium pulse ( $p = 0.0300$ ) ( $n = 3$ ), respectively; **i-k** Western blot image of MCU ( $p = 0.0014$ ) and NCLX ( $p = 0.0169$ ) along with respective lane-loading control GAPDH and quantification using Image Studio Lite (version 5.2.5) ( $n = 6$ ).  $p$ -value: unpaired two-tailed  $t$ -test performed in all comparisons. Data are represented as  $\pm$ SEM.

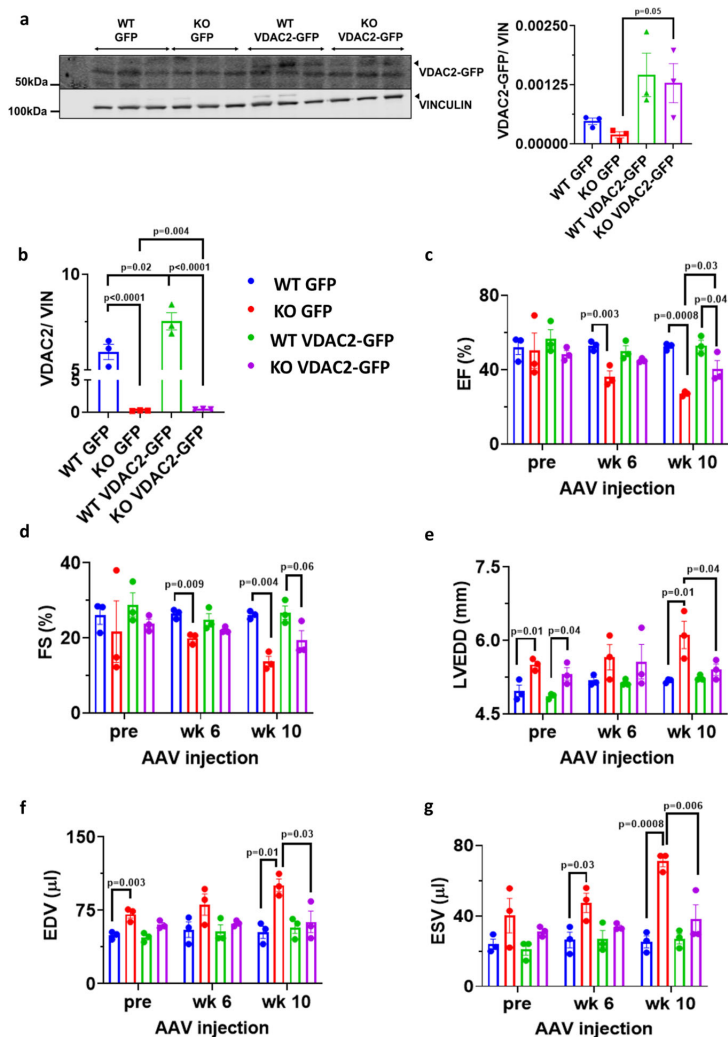


**Fig. 7 Increased cardiac fibrosis observed in VDAC2-KO.** **a** Differential gene expression data from 16-week-old mice ventricular sample ( $n = 4$ ); **b** KEGG pathway analysis of differentially expressed genes in KO indicates ECM production pathway as highest statistical significance ( $n = 4$ ); **c** Representative Masson's trichrome stain image ( $\times 0.5$  magnification; scale bar, 2000  $\mu\text{m}$ ) ( $n = 3$ ); **d** Fibrosis quantification using Aperio software and colocalization v9 algorithm ( $p = 0.0043$ ) ( $n = 3$ ); **e** Representative transmission electron microscopy image (scale bar, 5  $\mu\text{m}$ ) ( $n = 3$ ); **f** Collagen quantification using ImageJ software ( $p = 0.0033$ ) ( $n = 9$  images,  $N = 3$ ).  $p$ -value: unpaired two-tailed  $t$ -test performed in all comparisons. One-tail Fisher Exact test performed for KEGG pathway analysis. Data are represented as  $\pm$ SEM.

indicating that VDAC2 plays a crucial role in cardiac functioning by maintaining mitochondrial and cellular calcium homeostasis. Additionally, reintroduction of VDAC2 in young-KO mice showed a partial rescue of the cardiomyopathy phenotype suggesting the importance of VDAC2 in normal cardiac functioning.

Mitochondria-ER/SR interactions have long been studied and it is commonly believed that this interaction is crucial for mitochondrial calcium dynamics<sup>9,19,20</sup>. Mitochondria are known to recognize calcium-rich niches near SERCA2, RYR2, and NCX1 where major calcium transport happens<sup>21</sup>. We show in this study

## ARTICLE

NATURE COMMUNICATIONS | <https://doi.org/10.1038/s41467-021-24869-0>

**Fig. 8 Partial rescue of HF phenotype upon VDAC2 reintroduction.** **a** Western blot image of VDAC2-GFP and lane-loading control VINCULIN and quantification using Image Studio Lite (version 5.2.5) (KO GFP vs. KO VDAC2-GFP  $p=0.0568$ ) ( $n=3$ ); **b** qRT-PCR of *Vdac2* normalized to *Vcl* (Vinculin) (KO GFP vs. KO VDAC2-GFP  $p=0.0044$ ) ( $n=3$ ); **c-g** Serial echocardiography parameter including ejection fraction (EF) (week 6: WT GFP vs. KO GFP  $p=0.0036$ , week 10: WT GFP vs. KO GFP  $p=0.0008$ , WT VDAC2-GFP vs. KO VDAC2-GFP  $p=0.0456$ , KO GFP vs. KO VDAC2-GFP  $p=0.0359$ ), fractional shortening (FS) (week 6: WT GFP vs. KO GFP  $p=0.0091$ ; week 10: WT GFP vs. KO GFP  $p=0.0043$ , WT VDAC2-GFP vs. KO VDAC2-GFP  $p=0.0652$ ), left ventricular end diastolic diameter (LVEDD) (pre: WT GFP vs. KO GFP  $p=0.0169$ , WT VDAC2-GFP vs. KO VDAC2-GFP  $p=0.0407$ ; week 10: WT GFP vs. KO GFP  $p=0.0107$ , KO GFP vs. KO VDAC2-GFP  $p=0.0444$ ), end diastolic and end systolic volumes (EDV (pre: WT GFP vs. KO GFP  $p=0.0032$ ; week 10: WT GFP vs. KO GFP  $p=0.0104$ , KO GFP vs. KO VDAC2-GFP  $p=0.0378$ ) and ESV (week 6: WT GFP vs. KO GFP  $p=0.03$ , week 10: WT GFP vs. KO GFP  $p=0.0008$ , KO GFP vs. KO VDAC2-GFP  $p=0.0066$ ) respectively ( $n=3$ ).  $p$ -value: unpaired  $t$ -test performed in all comparisons between KO GFP and KO VDAC2-GFP in panels **a** and **b**. Ordinary one-way ANOVA was performed for echocardiographic data and panel **b**. Data are represented as  $\pm$ SEM.

that the crosstalk of VDAC2 with both calcium release through—RYR2 and diastolic calcium removal by SERCA2 and NCX1 plays an important role in determining cellular calcium homeostasis and when this crosstalk is lost, there is a significant impairment in both mitochondrial and cytosolic calcium signaling. We also observed a significant reduction in most calcium handling proteins like RYR2, SERCA2, NCX1, and CASQ2 in VDAC2-KO mice. While these results are unexpected, they might be explained

by different hypotheses: It is feasible that the lack of mitochondrial calcium uptake specifically through the loss of RYR2–VDAC2 connection results in a lack of energy demand which was shown to depend on mitochondrial calcium uptake<sup>22</sup>. In this scenario the basic metabolism of VDAC2-KO cells would be comparable to WT (as demonstrated in our results), while they are unable to adapt to higher workload under stress situations and might consecutively down-regulate calcium handling

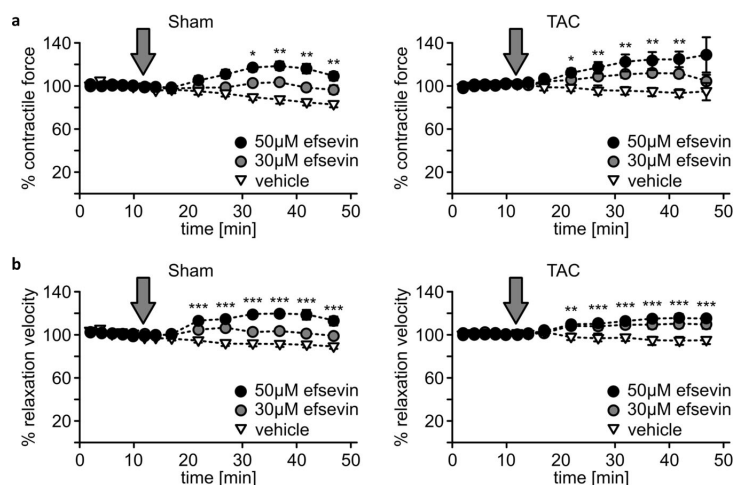


**Fig. 9** Enhanced contractile force and accelerated relaxation speed in myocardial tissue upon VDAC2 activation. **a** Measurement of relative contractile force in organotypic myocardial slices from both Sham- (left panel) and TAC-operated mice (right panel) after superfusion with either 30 or 50  $\mu$ M of the VDAC2 agonist efsevin. Each dot represents the quantification of twitch amplitudes over 20 s at indicated time points. The gray arrow indicates the start of efsevin superfusion (left panel: DMSO vs. 30  $\mu$ M Efsevin: 10 min  $p = 0.016$ , 32 min  $p = 0.010$ , 37 min  $p = 0.0004$ , 42 min  $p = 0.0012$  and 47 min  $p = 0.0062$ ; DMSO vs. 50  $\mu$ M Efsevin: 22 min  $p = 0.0007$ , 27–47 min  $p < 0.0001$ , respectively) (right panel: DMSO vs. 30  $\mu$ M Efsevin: 17 min  $p = 0.0038$ , 22 min  $p = 0.0009$ , 27 min  $p = 0.00031$ , 32 min  $p = 0.00029$ , 37 min  $p = 0.00015$ , 42 min  $p = 0.00073$ ; DMSO vs. 50  $\mu$ M Efsevin: 22 min  $p = 0.0218$ , 27 min  $p = 0.0044$ , 32 min  $p = 0.0037$ , 37 min  $p = 0.0031$ , 42 min  $p = 0.0034$ ). **b** Relaxation speed of twitches of myocardial slices shown in **a** ( $N = 8$ ,  $n = 22$  slices for TAC,  $N = 6$ ,  $n = 14$  slices for Sham) (left panel: DMSO vs. 30  $\mu$ M Efsevin: 22 min  $p = 0.0072$ , 27 min  $p = 0.00019$ , 32 min  $p = 0.044$ , 37 min  $p = 0.0125$ , 42 min  $p = 0.0145$ , 47 min  $p = 0.0308$ ; DMSO vs. 50  $\mu$ M Efsevin: 22–47 min  $p < 0.0001$  respectively) (right panel: DMSO vs. 30  $\mu$ M Efsevin: 22 min  $p < 0.0001$ , 27 min  $p = 0.0001$ , 32 min  $p < 0.0001$ , 37 min  $p < 0.0001$ , 42 min  $p = 0.0001$ , 47 min  $p = 0.0002$ ; DMSO vs. 50  $\mu$ M Efsevin: 22 min  $p = 0.002$ , 27 min  $p = 0.0001$ , 32–42 min  $p < 0.0001$ , respectively, 47 min  $p = 0.0001$ ).  $p$ -value: unpaired  $t$ -test performed in all comparisons. \* $<0.05$ , \*\* $<0.01$  and \*\*\* $<0.001$ . Data are represented as  $\pm$ SEM.

proteins. Alternatively, the down-regulation might be a result of compensatory mechanism to the slower rate of calcium uptake observed in the KO. Additionally, a down-regulation due to loss of structural integrity of the myocardium as observed in our experiment is feasible. Also, our data stands in contrast to previous observations that knock-down of VDAC2 in HL-1 cells did not alter expression levels of calcium handling proteins<sup>10</sup>. However, major differences between the model systems might explain these discrepancies: Partial inhibition of VDAC2 (~75%) was achieved using viral transduction and cells were cultured in vitro for limited time. It is thus feasible that the down-regulation of these proteins is masked either by the remaining VDAC2 expression, the lack of triggers present in vivo-like pressure or adrenergic stimulation, or that these translational changes only manifest after a longer time.

The significant impairment in SR-mediated calcium release and uptake in VDAC2-KO mice can be associated with reduced RYR2 and SERCA2 activities, respectively. We also observed a significant downregulation of total and phosphorylated PLN in VDAC2-KO which may account for the reduced SERCA2 activity and slower rate of decline in calcium transient. Additionally, the varying molecular weights seen in total PLN protein is likely due to post-translational modification of PLN by phosphorylation at different sites or different combination of sites including Ser10, Ser16, and/or Thr17. Therefore, an average intensity of the bands was taken and normalized with GAPDH<sup>23–25</sup>. Our co-IP studies suggest an interaction of VDAC2 with SERCA2. We propose that this interaction might be important for facilitating mitochondrial calcium uptake and also indirectly influencing cytosolic calcium signaling. Another pathway for calcium extrusion from the cytoplasm is through NCX1 and we observed that VDAC2

interacts with NCX1. This interaction, similar to that with SERCA2 and RyR2, is also likely to influence cellular calcium signaling. Sub-cellular regions near RyR2, SERCA2, and NCX1 act as calcium compartments with markedly different calcium concentration than the bulk cytosol and both the interaction of VDAC2 with calcium handling proteins and the localization of mitochondria near these regions indicates a substantial role of mitochondrial calcium uptake for cellular calcium handling. We propose that upon disruption of this interaction, there is less overall mitochondrial calcium uptake and reduced cytosolic calcium clearance which leads to impaired intracellular calcium signaling (Supplementary Fig. 7).

In agreement with other studies, we showed that VDAC2 is crucial for cellular calcium cycling and normal cardiac functioning, thereby making it a promising therapeutic target for DCM and chronic HF<sup>6,15</sup>. To test this hypothesis, we investigated the potency of efsevin as a therapeutic agent for the treatment of HF. Indeed, efsevin enhanced contractile force in organotypic tissue slices of failing murine myocardium, establishing VDAC2 as a promising target for HF.

HF is associated with an increased risk for arrhythmia and efsevin was previously suggested to suppress arrhythmogenesis in cardiomyocytes<sup>13,14</sup> suggesting a role for VDAC2 also as a protective pathway against arrhythmia. This data is backed up by our findings, that VDAC2-KO mice also experienced arrhythmias. We hypothesize that the altered calcium signaling (reduced CASQ2, RYR2, and SERCA2 activities) has the potential to cause these arrhythmias<sup>26,27</sup>. The reduced CASQ2 activity suggests reduced RyR2 sensitivity to cytosolic calcium which in turn explains the reduced gene expression of L-type calcium channel<sup>28</sup>. Additionally, the expression of T-type calcium channels in the

## ARTICLE

NATURE COMMUNICATIONS | <https://doi.org/10.1038/s41467-021-24869-0>

adult KO myocardium is indicative of disease states such as cardiomyopathies and HF where increased expression of T-type channels in adult ventricular myocytes leads to increased susceptibility to arrhythmias<sup>29,30</sup>. The cellular patch-clamp experiments in the VDAC2-KO showed a tendency towards increased early after depolarizations perhaps due to reactivation of these calcium channels<sup>31</sup>. We also observed a significantly longer APD<sub>50</sub> in the KO which can be explained by the genetic down-regulation of the transient outward channel thereby making VDAC2 influence on the cardiomyocyte even more prominent.

VDAC2-tubulin interaction and VDAC2-PFKP interaction have been studied in cancer metabolism research where specifically targeting VDAC2 has shown to down-regulate glycolysis thereby preventing cancer cell growth and proliferation<sup>32,33</sup>. In agreement with this work, we also observed significant alterations in a number of enzymes involved in glucose metabolism, its accessory pathways, and the TCA cycle but no difference was observed in FAO or electron transport chain (ETC). This unaltered FAO and ETC may help explain the relatively unaltered mitochondrial respiration since these metabolic pathways provide the necessary ATP.

VDAC2 plays an important role in apoptosis by interacting with BAK, a proapoptotic protein, and keeping it inactive<sup>34</sup>. Essentially, VDAC2-BAK interaction prevents cellular apoptosis, and *Vdac2* deletion results in free (or active) BAK thus causing excessive apoptosis<sup>35</sup>. We hypothesize that this increased apoptosis during late cardiac development might contribute to the increased fibrosis observed in our VDAC2-KO mice.

Calcium release into the cytoplasm is mainly mediated by the RyR2 and previous publications have established the importance of physical interaction between VDAC2 and RyR2 for normal calcium transport into the mitochondria<sup>10</sup>. Mitochondrial calcium uptake was significantly impaired in our VDAC2-KO mice indicating the importance of VDAC2 in mitochondrial calcium transport. A similar reduction in mitochondrial calcium uptake was observed in MCU-KO mice, however, no other phenotypical difference was observed between the MCU-WT and MCU-KO<sup>36</sup>, indicating differences in the role of these two transporters in cellular calcium handling. One explanation derived from this work is that VDAC might act as a scaffolding protein to link the MCU to other calcium handling proteins and thus creating cellular calcium microdomains, while MCU might serve as the controller of mitochondrial calcium uptake. This is in line with observations that VDAC2 was described to be a vividly interacting channel<sup>20</sup>.

Overall, our findings highlight the importance of VDAC2 in influencing ECC and cardiac disease progression. Previous research has shown that increased calcium uptake through VDAC2 (using efsevin) reverses arrhythmic phenotypes. Here, we demonstrate the crucial role of VDAC2 in ECC and the pathogenesis of DCM and provide reasonable evidence for VDAC2 to serve as a therapeutic target for HF. Thus, drugs targeting VDAC2 might fulfill a double role by suppressing cardiac arrhythmia and enhancing cardiac function.

## Methods

**Animals and animal care.** All animal studies were performed in accordance with the University of Iowa Animal Care and Use Committee (IACUC). All procedures involving animals were approved by the Animal Care and Use Committee of the University of Utah and complied with the American Physiological Society's *Guiding Principles in the Care and Use of Animals* and the UK Animals (Scientific Procedures) Act 1986 guidelines. The mice were housed in 12 h dark/light cycle at 70 °F and 40% humidity.

**Generation of cardiac-specific knockout.** C57BL6J mice were used for all experiments. Both male and female mice were used for all experiments. *Vdac2* flox/flox mice were obtained from Ren et al.<sup>35</sup>. The founder mice were cross-bred with

transgenic  $\alpha$ MHC-Cre (Jackson Laboratory#009074)<sup>37</sup> and the resulting heterozygous (*Vdac2* flox/+;  $\alpha$ MHC-Cre) mice were crossed to obtain a cardiac ventricular myocyte-specific deletion of VDAC2.

**Echocardiographic analysis.** Mice were anesthetized with 1.5% Isoflurane (Vet One, NDC13985-046-60) during echocardiography. Echocardiographic images were taken on the Vivo system. Echoes were performed serially from embryonic age 17 to 16 weeks post-natal. 2D long-axis and short-axis views were obtained and used for analysis using Vivo strain software (version 3.1.1). Two consecutive cardiac cycles were used for all the measurements. Limb leads were used to record an electrocardiogram (ECG).

**Collagen content evaluation/Masson's trichrome stain.** Mice were euthanized using sodium pentobarbital (NDC76478-501-50). Hearts were harvested and formalin-fixed for 48 h followed by paraffin embedding. 5  $\mu$ m thick sections were cut and stained with Trichrome for fibrosis analysis using the Dako automated special stainer. The slides for fibrosis analysis were scanned under  $\times 20$  and analyzed using Aperio Image Scope software (version 12.3.2.8013) (using the colocalization v9 algorithm)<sup>38</sup>. A ratio of the total stained area to the collagen-stained area was reported.

**Cardiomyocyte isolation.** Adult mice were anesthetized with sodium pentobarbital (50 mg kg<sup>-1</sup>) and the excised heart was attached to an aortic cannula and perfused with solutions gassed with 100% O<sub>2</sub> and held at 37 °C, pH 7.3. Perfusion with a 0 mM Ca<sup>2+</sup> solution for 5 min was followed by 15 min of perfusion with the same solution containing 1 mg ml<sup>-1</sup> collagenase (type II, Worthington Biochemical, Freehold, NJ, USA) and 0.1 mg/ml protease (type XIV, Sigma Chemical, catalog #P5147). The heart was then perfused for 1 min with a stopping solution (the same solution containing 20% serum and 0.2 mM CaCl<sub>2</sub>). All perfusions were performed at a flow rate of 2 ml min<sup>-1</sup>. The atria were removed and the ventricles were minced and shaken for 10 min, and then filtered through a nylon mesh. Cells were stored at 37 °C in a normal HEPES buffered solution. All myocytes used in this study were rod-shaped, had well-defined striations, and did not spontaneously contract. Experiments were performed within 7 h of isolation.

**Cell super-fusion chamber.** The Plexiglas cell bath had a clear glass bottom and was mounted on the stage of an inverted microscope (Diaphot, Nikon, Japan). The temperature of the solutions in the super-fusion chamber was 36  $\pm$  0.3 °C. Bathing solutions flowed continuously through the bath at 4 ml min<sup>-1</sup>, and solution depth was held at  $\sim$ 2–3 mm. Exchange of the bath solution required  $\sim$ 5 s. The bottom of the bath was coated with laminin (Collaborative Research, Bedford, MA, USA) to improve cell adhesion.

**Cell bathing solutions and pipette filling solutions.** The normal control bathing solution contained (mM): 126.0 NaCl, 11.0 dextrose, 4.4 KCl, 1.0 MgCl<sub>2</sub>, 1.08 CaCl<sub>2</sub>, and 24.0 HEPES titrated to pH 7.4 with 1 M NaOH. The pipette solution used for recording APs contained (mM): 110.0 KCl, 5.0 NaCl, 5.0 MgATP, 5.0 phosphocreatine, 1.0 NaGTP, 10.0 HEPES titrated to pH 7.2 with 1 M KOH.

**AP measurement.** Transmembrane potential ( $V_m$ ) was measured with borosilicate glass suction pipettes (resistance 1–2 M $\Omega$  when filled) connected to an Axoclamp 2B amplifier system (Axon Instruments/Molecular Devices) in bridge mode<sup>39</sup>. The  $V_m$  signal was filtered at 5 kHz, digitized at 50 kHz with a 16-bit A/D converter (Digidata 1322A), and analyzed using PCLAMP 8 software (Molecular Devices). APs were triggered with brief (2–3 ms) square pulses of depolarizing intracellular current ( $\sim$ 2 nA). APD<sub>50</sub> and APD<sub>90</sub> were measured.

**Intracellular calcium concentration measurement.** Calcium transients were detected in single myocytes with an epifluorescence system using the fluorescent indicator, Fluo-4. Cells were incubated in the normal control solution containing 12.5  $\mu$ M Fluo4-AM (Invitrogen, catalog#F14201) and 0.3 mM probenecid (Sigma, catalog #P8761) at 30 °C for 20 min. The cells were then continuously bathed in the same solution containing no indicator. Probenecid (0.3 mM) was included in the bathing solutions to help retard fluo-4 loss from the cells. Fluorescence emission (535 nm, bandpass filter) was collected with a photomultiplier tube via a  $\times 40$  objective during continuous excitation at 485 nm. Calcium transients were elicited with field stimulation at a cycle length of 1 s.

**TEM and analysis.** LV transmural samples from 16-week-old mice were used for this study. Tissue samples were fixed overnight at 4 °C in 0.1 M sodium cacodylate buffer containing 1% paraformaldehyde and 2.5% glutaraldehyde. Samples were washed with the same buffer and post-fixed for 2 h in 2% osmium tetroxide buffered with cacodylate buffer. Samples were then rinsed in nano-pure water and stained with en-bloc stain for 1 h at room temperature in uranyl acetate. Tissues were then dehydrated through a graded series of ethanol: 10 min in 50%, 3  $\times$  10 min in 70%, 2  $\times$  10 min in 95%, 4  $\times$  10 min in absolute ethanol, and 3  $\times$  10 min with absolute acetone. Samples were incubated at room temperature in a gradually



**Table 1 List of antibodies used.**

Resource	Concentration	Identifier	Source
<i>Western blot-antibodies</i>			
Voltage-dependent anion-selective channel protein 2 (VDAC2)	1:1000	9412S	Cell Signaling Technology
Voltage-dependent anion-selective channel protein 1 (VDAC1)	1:1000	ab14734	Abcam
Voltage-dependent anion-selective channel protein 3 (VDAC3)	1:1000	ab130561	Abcam
Vinculin	1:1000	13901S	Cell Signaling Technology
Glyceraldehyde 3-phosphate dehydrogenase (GAPDH)	1:1000	5174S	Cell Signaling Technology
Transketolase (TKT)	1:500	8616S	Cell Signaling Technology
Methylenetetrahydrofolate dehydrogenase 1 (MTHFD1)	1:500	sc-271412	Santa Cruz Biotech
Aldolase B (ALDOB)	1:200	sc-365449	Santa Cruz Biotech
Serine hydroxymethyltransferase 1 (SHMT1)	1:500	8071S	Cell Signaling Technology
Isocitrate dehydrogenase (IDH1/2)	1:500	sc-373816	Santa Cruz Biotech
Phosphofructokinase 1 (PFK1)	1:500	sc-166722	Santa Cruz Biotech
Pyruvate carboxylase (PC)	1:1000	NBP1-49536	Novus Bio
Pyruvate dehydrogenase (PDH)	1:500	3205S	Cell Signaling Technology
Lactate dehydrogenase (LDH)	1:1000	3582S	Cell Signaling Technology
Hexokinase 1 (HK1)	1:500	2024S	Cell Signaling Technology
Calsequestrin 2 (CASQ2)	1:500	ab3516	Abcam
Citrate synthase (CS)	1:1000	14309S	Cell Signaling Technology
Succinyl Co-A synthetase (SUCLG2)	1:1000	8071S	Cell Signaling Technology
Succinate dehydrogenase A (SDHA)	1:1000	5839S	Cell Signaling Technology
Sodium-calcium exchanger 1 (NCX1)	1:500	ab151608	Abcam
Sarcoplasmic endoplasmic reticular calcium ATPase 2 (SERCA2)	1:500	4388S	Cell Signaling Technology
Ryanodine receptor 2 (RYR2)	1:500	MA3-916	ThermoFisher Scientific
Phospholamban (PLN)	1:1000	14562S	Cell Signaling Technology
Phospho-phospholamban (pPLN)	1:1000	8496S	Cell Signaling Technology
Protein kinase A (PKA)	1:500	SAB4502337	Sigma Aldrich
Phospho-protein kinase A (pPKA)	1:500	SAB4503969	Sigma Aldrich
Mitochondrial calcium uniporter (MCU)	1:500	14997S	Cell Signaling Technology
Mitochondrial sodium calcium exchanger (NCLX)	1:500	SAB2102181	Sigma Aldrich
Dynamin-related protein 1 (DRP1)	1:500	14647S	Cell Signaling Technology
Oxidative phosphorylation (OXPHOS)	1:1000	ab110413	Abcam
IRDye 680RD Donkey anti-Mouse Secondary	1:10,000	926-68072	LI-COR Biosciences
IRDye 800CW Donkey anti-Rabbit Secondary	1:10,000	926-32212	LI-COR Biosciences
<i>Co-immunoprecipitation-antibodies</i>			
Voltage-dependent anion-selective channel protein 2 (VDAC2)	5 µg	PA5-28106	ThermoFisher Scientific
Immunoglobulin G (IgG)	5 µg	AC005	AbClonal
<i>Immunofluorescence/proximity ligation assay—antibodies/stain</i>			
4',6-diamidino-2-phenylindole (DAPI)	1:1000	D3571	ThermoFisher Scientific
Voltage-dependent anion-selective channel protein 2 (VDAC2)	1:1000	66388-1-IG	ThermoFisher Scientific
Sodium-calcium exchanger 1 (NCX1)	1:500	ab151608	Abcam
Sarcoplasmic endoplasmic reticular calcium ATPase 2 (SERCA2)	1:500	4388S	Cell Signaling Technology
Ryanodine receptor 2 (RYR2)	1:500	MA3-916	ThermoFisher Scientific
<i>Quantitative reverse transcription-PCR-primers</i>			
Voltage-dependent anion-selective channel protein 2 (VDAC2)		Mm00834279_m1	ThermoFisher Scientific
Vinculin		Mm00447745_m1	ThermoFisher Scientific

increasing concentration of epoxy resin (Electron Microscopy Science, Hatfield, PA) to facilitate infiltration. Samples were then transferred to 50% resin in acetone for 1 h and overnight in 75% resin in acetone. Samples were then transferred to 100% resin for 8 h with three fresh resin changes. Samples were then embedded and polymerized at 60 °C for 48 h. Ultrathin sections (70 nm) were obtained with a diamond knife (Diatome) using Leica UC6 (Leica Microsystems, Vienna, Austria). Sections were post-stained with saturated uranyl acetate for 10 min followed by Reinold stain for 5 min. Sections were imaged at 120 kV with JEOL 1400 Plus<sup>40</sup>. Mitochondrial density and number analysis were performed using Adobe Photoshop tool using ×1500 images. A 22 × 14 grid was used for density measurements. The same images were used for collagen quantification using Fiji software. The ratio of collagen area to total area was reported.

**Mitochondria isolation and calcium uptake.** Mice were euthanized using carbon dioxide for 3 min and the heart was excised. The atria were removed and the ventricles were used for mitochondria isolation using differential centrifugation<sup>41</sup>. Protein estimation was performed using Pierce Assay. 100 µg of protein was used per trial, resuspended in 100 µL of a solution containing (in mM): 125.0 KCl, 20.0 HEPES, 10.0 K<sub>2</sub>HPO<sub>4</sub>, 5.0 Glutamate, 5.0 Malate, and 1 µM Oregon Green BAPTA/6F (pH 7.2 with 1 M KOH). Imaging was performed on a Biotek Cytation 5 instrument in 96-well flat-bottomed plates. Baseline measurements were taken for 30 s and 12 µM calcium chloride was injected and the fluorescence (excitation

490 nm, emission 517 nm) was measured for 3 min to obtain the calcium uptake slope.

**Retro-orbital injections.** 6-week-old WT and KO mice were randomly chosen to receive either AAV9-αMHC-VDAC2-GFP vector or control AAV9-αMHC-GFP vector. *N* = 3 mice were used in each group and a total of four groups were used (WT-AAV and KO-AAV received the vector with VDAC2 and WT-GFP and KO-GFP received control vector). A concentration of 3.1 × 10<sup>12</sup> VG kg<sup>-1</sup> was used for each injection and the mice were serially echoed for 10 weeks post-injection.

**RNA extraction, sequencing, and qRT-PCR.** miRNeasy Mini kit (Qiagen) was used for RNA extraction from the LV transmural sample. The extracted RNA was used for total RNA sequencing (RNA Seq). Agilent RNA Screen Tape Assay was used for QC experiments. Illumina TruSeq Stranded RNA kit was used for library preparation and Ribo-Zero Gold was used to remove rRNA and the sequencing was performed on an Illumina HiSeq 2500 with 50 bp single-end reads. The same RNA was used for cDNA synthesis (NEB #E3010S) and qRT-PCR was performed using *Vdac2* and *Vcl* (VINCULIN) primers (Table 1).

**RNA Seq analysis.** RNA Seq analysis was performed with the High-Throughput Genomics and Bioinformatics Analysis Shared Resource at Huntsman Cancer

## ARTICLE

NATURE COMMUNICATIONS | <https://doi.org/10.1038/s41467-021-24869-0>

Institute at the University of Utah. mm10, M\_musculus\_Dec\_2011, GRCh38 genome build was used for sequence alignment. Sample outliers were checked by summarizing the output files from cutadapt, FastQC, Picard CollectRnaSeqMetrics, STAR, and feature counts by using the previously described method<sup>42</sup>. 5% false discovery rate (FDR) with DeSeq2 (version 1.24.0) was used to identify differentially expressed genes<sup>43</sup>. Genes were filtered using the following criteria: adjusted  $p$ -value < 0.05, absolute log<sub>2</sub> fold change > 0.585 and normalized base mean > 30<sup>43</sup>. Heat maps were produced using the R library pheatmap. KEGG<sup>44</sup> and Ingenuity pathway analysis (IPA) software was used for gene ontology analysis.

**Protein extraction and Western blotting.** WT and KO mice hearts ( $n = 6$  each) were excised. 30  $\mu$ g of transmural LV sample was homogenized using metal beads for 3 min in RIPA buffer with 2 $\times$  protease and phosphatase inhibitor (Thermo-Scientific #1861281). The homogenate was transferred to a new tube containing 10  $\mu$ l of 1 $\times$  PMSF and allowed to rotate for 30 min at 4 °C and centrifuged at 11,000  $\times$  g for 10 min at 4 °C. The supernatant was used for protein estimation using the Pierce BCA Protein Assay kit (Thermo-Scientific #23225). An equal volume of 2 $\times$  Laemmli buffer (with 10% DTT) was added to the sample and boiled for 10 min at 98 °C.

30  $\mu$ g protein was used for SDS-PAGE. The gel was run at constant volts (50 V) and proteins were transferred to nitrocellulose membrane at constant current (350 mA). For RYR2, proteins were transferred at constant volt (40 V) overnight. The membranes were blocked for 1 h with 5% non-fat milk and probed with primary antibodies overnight in the cold room. Antibodies and the concentration used are listed in Table 1. Blots were washed with 1 $\times$  PBST thrice and probed with a secondary antibody for 1 h. Blots were washed with 1 $\times$  PBST thrice prior to scanning using LI-COR. Image Studio Lite software was used to analyze the protein blots. Each blot had its own lane loading control and the values were normalized accordingly.

**Co-immunoprecipitation.** 30  $\mu$ g of LV transmural sample from 8-week-old WT and KO mice were used for protein extraction and quantification was done using a BCA assay kit. Protein A magnetic beads (Bio-Rad, catalog#161-4011) were washed thrice with 1 $\times$  PBST. 4 mg ml<sup>-1</sup> of lysate was precleared by rotating with beads for 30 min at 4 °C and 10% of the precleared lysate was saved as input. 5  $\mu$ g of antibody (Table 1) was used for conjugation with the beads by rotating at room temperature for 10 min, followed by washing twice with 1 $\times$  PBST and once with the lysis buffer (Cell Signaling, catalog #9806). The precleared lysate and antibody were kept for rotation at room temperature for 1 h. The magnet was then washed thrice with 1 $\times$  PBST, magnetized and the elute was boiled at 70 °C for 10 min with 40  $\mu$ l of 1 $\times$  Laemmli buffer (10%  $\beta$ -mercaptoethanol) and used for western blot.

**Immunofluorescence.** 16-week-old mice hearts were fixed in 10% paraformaldehyde for 4–6 h followed by paraffin embedding. Samples were cut at 5  $\mu$ m thickness and deparaffinized and antigen retrieval was performed. The antibodies used are listed in Table 1. Secondary anti-mouse, anti-rabbit, or anti-goat were used appropriately. All images for each protein were acquired using the same laser setting and processed using Fiji software.

**Proximity ligation assay.** 16-week-old mice heart samples embedded in paraffin were used for this assay. Duolink In Situ PLA probe anti-mouse, anti-rabbit, and anti-goat were used (DUO92001, DUO92005, and DUO92015). The antibodies used are listed in Table 1. Samples were processed using the manufacturer's protocol. All images for each combination were acquired using the same laser settings and processed using Fiji software.

**Force measurements in murine organotypic slices.** Hearts from adult mice were excised after cervical dislocation and flushed in ice-cold preparation buffer (in mM): 136.0 NaCl, 5.4 KCl, 1.0 MgHPO<sub>4</sub>, 0.9 CaCl<sub>2</sub>, 30.0 2,3-Butanedioneminoxime, 5.0 HEPES, pH 7.4. For sectioning, hearts were embedded in low melting agarose and cut into 300  $\mu$ m-thick coronary plane slices using a LeicaVT1200S vibratome and glued (Histoacryl, B. Brain Melsungen AG, Germany) onto small plastic triangles cut from 0.1 mm-thick polyester copier clear before being mounted in an organ bath chamber (Mayflower, Hugo Sachs Elektronik; HSE, Germany). Contractility was measured under a constant flow-through (4 ml min<sup>-1</sup>) in pre-warmed measuring buffer (in mM): 136.0 NaCl, 5.4 KCl, 1.0 MgCl<sub>2</sub>, 0.33 NaH<sub>2</sub>PO<sub>4</sub>, 10.0 Glucose, 1.8 CaCl<sub>2</sub>, 23.0 NaHCO<sub>3</sub>, pH 7.4, 37 °C under electrical pacing at 3 Hz and force was recorded by a force transducer connected to an amplifier (Hugo Sachs, Germany) using WinEDR (University of Strathclyde, UK). Kinetics of single twitches was analyzed using LabChart Reader (ADInstruments).

**TAC surgery.** TAC<sup>45</sup> was performed on RyR2<sup>R4496C+/-</sup> knock-in mice<sup>46</sup>, which were previously described to develop a severe form of HF<sup>47</sup>. In brief, 8–14-week-old mice were anesthetized by medetomidine/midazolam/fentanyl (0.5, 5.0, and 0.05 mg kg<sup>-1</sup> body weight intraperitoneally, respectively) and the aorta was constricted around a 27-gauge needle. Sham mice underwent the same procedure without aortic constriction. 6 weeks after surgery, mice were sacrificed by cervical dislocation, hearts were isolated and flushed (in mM): 136.0 NaCl, 5.4 KCl, 1.0

MgCl<sub>2</sub>, 0.33 NaH<sub>2</sub>PO<sub>4</sub>, 10.0 Glucose, 0.9 CaCl<sub>2</sub>, 30.0 2,3-butanedioneminoxime, 5.0 HEPES, pH 7.4, 4 °C and success of TAC surgery was confirmed by measuring the heart weight to tibia length ratio.

**Statistics and reproducibility.** All data were summarized as  $\pm$ SEM. GraphPad Prism (version 8.2.1) was used for all statistical analyses. A two-tailed test was performed in all comparisons. Unpaired Student's  $t$ -test was used for all analyses with WT and KO. Multiple  $t$ -test and one-way ANOVA were used for longitudinal echocardiographic data and while comparing multiple groups, respectively.  $p$ -value < 0.05 was considered statistically significant. All experiments were repeated independently (at least three biological replicates, and three technical replicates wherever applicable) with reproducible results. Samples used for western blot quantification were from the same gel and when unavoidable, were processed in parallel.

**Reporting summary.** Further information on research design is available in the Nature Research Reporting Summary linked to this article.

**Data availability**

Source data are provided within this manuscript as a source data file. RNA sequencing is uploaded to NCBI's GEO database under accession code GSE168487. Source data are provided with this paper.

Received: 28 May 2020; Accepted: 6 July 2021;

Published online: 28 July 2021

**References**

- Luscher, T. F. Heart failure: the cardiovascular epidemic of the 21st century. *Eur. Heart J.* **36**, 395–397 (2015).
- van der Meer, P., Gaggin, H. K. & Dec, G. W. ACC/AHA versus ESC guidelines on heart failure: JACC guideline comparison. *J. Am. Coll. Cardiol.* **73**, 2756–2768 (2019).
- Hasenfuss, G. et al. Alteration of contractile function and excitation-contraction coupling in dilated cardiomyopathy. *Circ. Res.* **70**, 1225–1232 (1992).
- Bers, D. M. Cardiac excitation-contraction coupling. *Nature* **415**, 198–205 (2002).
- Eisner, D. A., Caldwell, J. L., Kistamas, K. & Trafford, A. W. Calcium and excitation-contraction coupling in the heart. *Circ. Res.* **121**, 181–195 (2017).
- Naghdi, S. & Hajnoczky, G. VDACC2-specific cellular functions and the underlying structure. *Biochim. Biophys. Acta* **1863**, 2503–2514 (2016).
- Cheng, E. H., Sheiko, T. V., Fisher, J. K., Craigen, W. J. & Korsmeyer, S. J. VDACC2 inhibits BAK activation and mitochondrial apoptosis. *Science* **301**, 513–517 (2003).
- Roy, S. S., Ehrlich, A. M., Craigen, W. J. & Hajnoczky, G. VDACC2 is required for truncated BID-induced mitochondrial apoptosis by recruiting BAK to the mitochondria. *EMBO Rep.* **10**, 1341–1347 (2009).
- Eisner, V., Csordas, G. & Hajnoczky, G. Interactions between sarcoplasmic reticulum and mitochondria in cardiac and skeletal muscle—pivotal roles in Ca(2+)- and reactive oxygen species signaling. *J. Cell Sci.* **126**, 2965–2978 (2013).
- Min, C. K. et al. Coupling of ryanodine receptor 2 and voltage-dependent anion channel 2 is essential for Ca(2+)-transfer from the sarcoplasmic reticulum to the mitochondria in the heart. *Biochem. J.* **447**, 371–379 (2012).
- Pan, X. et al. The physiological role of mitochondrial calcium revealed by mice lacking the mitochondrial calcium uniporter. *Nat. Cell Biol.* **15**, 1464–1472 (2013).
- Murphy, E. et al. Unresolved questions from the analysis of mice lacking MCU expression. *Biochem. Biophys. Res. Commun.* **449**, 384–385 (2014).
- Shimizu, H. et al. Mitochondrial Ca(2+)-uptake by the voltage-dependent anion channel 2 regulates cardiac rhythmicity. *Elife* **4**, 04801 (2015).
- Schweitzer, M. K. et al. Suppression of arrhythmia by enhancing mitochondrial Ca(2+)-uptake in catecholaminergic ventricular tachycardia models. *JACC Basic Transl. Sci.* **2**, 737–747 (2017).
- Subedi, K. P. et al. Voltage-dependent anion channel 2 modulates resting Ca(2+)-sparks, but not action potential-induced Ca(2+)-signaling in cardiac myocytes. *Cell Calcium* **49**, 136–143 (2011).
- Navankasattusas, S. et al. The netrin receptor UNC5B promotes angiogenesis in specific vascular beds. *Development* **135**, 659–667 (2008).
- Landstrom, A. P., Dobrev, D. & Wehrens, X. H. T. Calcium signaling and cardiac arrhythmias. *Circ. Res.* **120**, 1969–1993 (2017).
- Kwong, J. Q. et al. The mitochondrial calcium uniporter selectively matches metabolic output to acute contractile stress in the heart. *Cell Rep.* **12**, 15–22 (2015).

19. Sharma, V. K., Ramesh, V., Franzini-Armstrong, C. & Sheu, S. S. Transport of Ca<sup>2+</sup> from sarcoplasmic reticulum to mitochondria in rat ventricular myocytes. *J. Bioenerg. Biomembr.* **32**, 97–104 (2000).
20. Sander, P., Gudermann, T. & Schredelseker, J. A Calcium guard in the outer membrane: is VDAC a regulated gatekeeper of mitochondrial calcium uptake? *Int. J. Mol. Sci.* **22**, 22020946 (2021).
21. Dewenter, M., von der Lieth, A., Katus, H. A. & Backs, J. Calcium signaling and transcriptional regulation in cardiomyocytes. *Circ. Res.* **121**, 1000–1020 (2017).
22. Morkin, E. Control of cardiac myosin heavy chain gene expression. *Microsc. Res. Tech.* **50**, 522–531 (2000).
23. Imagawa, T., Watanabe, T. & Nakamura, T. Subunit structure and multiple phosphorylation sites of phospholamban. *J. Biochem.* **99**, 41–53 (1986).
24. Wegener, A. D. & Jones, L. R. Phosphorylation-induced mobility shift in phospholamban in sodium dodecyl sulfate–polyacrylamide gels. Evidence for a protein structure consisting of multiple identical phosphorylatable subunits. *J. Biol. Chem.* **259**, 1834–1841 (1984).
25. Colyer, J. Phosphorylation states of phospholamban. *Ann. N. Y. Acad. Sci.* **853**, 79–91 (1998).
26. Anderson, M. E. Multiple downstream proarrhythmic targets for calmodulin kinase II: moving beyond an ion channel-centric focus. *Cardiovasc. Res.* **73**, 657–666 (2007).
27. Federico, M., Valverde, C. A., Mattiazzi, A. & Palomeque, J. Unbalance between sarcoplasmic reticulum Ca<sup>2+</sup> uptake and release: a first step toward Ca<sup>2+</sup> triggered arrhythmias and cardiac damage. *Front. Physiol.* **10**, 2019.01630 (2020).
28. Chen, X. et al. Sorcin ablation plus beta-adrenergic stimulation generate an arrhythmogenic substrate in mouse ventricular myocytes. *J. Mol. Cell. Cardiol.* **114**, 199–210 (2018).
29. Xu, M., Welling, A., Paparisto, S., Hofmann, F. & Klugbauer, N. Enhanced expression of L-type Cav1.3 calcium channels in murine embryonic hearts from Cav1.2-deficient mice. *J. Biol. Chem.* **278**, 40837–40841 (2003).
30. Cribbs, L. T-type calcium channel expression and function in the diseased heart. *Channels* **4**, 447–452 (2010).
31. Kistamas, K. et al. Calcium handling defects and cardiac arrhythmia syndromes. *Front. Pharm.* **11**, 72 (2020).
32. Maldonado, E. N. VDAC-tubulin, an anti-Warburg pro-oxidant switch. *Front. Oncol.* **7**, 4 (2017).
33. Zhou, K. et al. VDAC2 interacts with PFKF to regulate glucose metabolism and phenotypic reprogramming of glioma stem cells. *Cell Death Dis.* **9**, 988 (2018).
34. Chin, H. S. et al. VDAC2 enables BAX to mediate apoptosis and limit tumor development. *Nat. Commun.* **9**, 4976 (2018).
35. Ren, D. et al. The VDAC2-BAK rheostat controls thymocyte survival. *Sci. Signal.* **2**, ra48 (2009).
36. Harrington, J. L. & Murphy, E. The mitochondrial calcium uniporter: mice can live and die without it. *J. Mol. Cell. Cardiol.* **78**, 46–53 (2015).
37. Oka, T. et al. Cardiac-specific deletion of Gata4 reveals its requirement for hypertrophy, compensation, and myocyte viability. *Circ. Res.* **98**, 837–845 (2006).
38. Drakos, S. G. et al. Impact of mechanical unloading on microvasculature and associated central remodeling features of the failing human heart. *J. Am. Coll. Cardiol.* **56**, 382–391 (2010).
39. Warren, M. et al. Blockade of CaMKII depresses conduction preferentially in the right ventricular outflow tract and promotes ischemic ventricular fibrillation in the rabbit heart. *Am. J. Physiol. Heart Circ. Physiol.* **312**, H752–H767 (2017).
40. Cluntun, A. A. et al. The pyruvate-lactate axis modulates cardiac hypertrophy and heart failure. *Cell Metab.* <https://doi.org/10.1016/j.cmet.2020.12.003> (2020).
41. Sommakia, S. et al. Mitochondrial cardiomyopathies feature increased uptake and diminished efflux of mitochondrial calcium. *J. Mol. Cell. Cardiol.* **113**, 22–32 (2017).
42. Ewels, P., Magnusson, M., Lundin, S. & Kaller, M. MultiQC: summarize analysis results for multiple tools and samples in a single report. *Bioinformatics* **32**, 3047–3048 (2016).
43. Love, M. I., Huber, W. & Anders, S. Moderated estimation of fold change and dispersion for RNA-seq data with DESeq2. *Genome Biol.* **15**, 550 (2014).
44. Kanehisa, M. & Goto, S. KEGG: Kyoto Encyclopedia of Genes and Genomes. *Nucleic Acids Res.* **28**, 27–30 (2000).
45. Muhlfield, C. et al. Hypoinnervation is an early event in experimental myocardial remodelling induced by pressure overload. *J. Anat.* **222**, 634–644 (2013).
46. Cerrone, M. et al. Bidirectional ventricular tachycardia and fibrillation elicited in a knock-in mouse model carrier of a mutation in the cardiac ryanodine receptor. *Circ. Res.* **96**, e77–e82 (2005).
47. Sedej, S. et al. Subclinical abnormalities in sarcoplasmic reticulum Ca(2+) release promote eccentric myocardial remodeling and pump failure death in response to pressure overload. *J. Am. Coll. Cardiol.* **63**, 1569–1579 (2014).

#### Acknowledgements

This work was supported by American Heart Association-Heart Failure Strategically Focused Research Network, Grant 16SFRN2902000 (Dr. Drakos); National Heart, Lung, and Blood Institute (NHLBI) RO1 Grant HL135121-01 (Dr. Drakos); NHLBI RO1 Grant HL132067-01A1 (Dr. Drakos). National Heart, Lung, and Blood Institute (NHLBI) RO1 Grant GM071779 (Dr. Kwon). Additional support was provided by the Nora Eccles Treadwell Foundation to Dr. Drakos.

#### Author contributions

T.S.S. designed and performed experiments, analyzed data, and drafted the manuscript. D.K.A.R., K.S., S.S., R.B., A.T.K. and D. Ca performed experiments and helped to analyze the data. S.N. helped to analyze the data, edited the manuscript, and revised it critically for intellectual content. P.S., O.S.K., A.A., A.D. performed experiments, edited the manuscript, and revised it critically for intellectual content. J.L. and C.X. edited the manuscript and revised it critically for intellectual content. O.K. and C.X. synthesized efsavin and provided the required quantities to perform the requested experiments. K.S., P.S., A.D. and J.S. performed all experiments on efsavin, analyzed data, and edited the manuscript. O.K., E.H.Y.C., K.J.W., T.G., R.S.R., F.B.S., K.W.S., J.S. and D.Ch. helped with the data analysis, edited the manuscript, and revised it critically for intellectual content. S.G.D. provided overall guidance, conceived the research concept, supervised the study and data analysis, and critically revised the manuscript for intellectual content.

#### Competing interests

The authors declare no competing interests.

#### Additional information


**Supplementary information** The online version contains supplementary material available at <https://doi.org/10.1038/s41467-021-24869-0>.

**Correspondence** and requests for materials should be addressed to S.G.D.

**Peer review information** *Nature Communications* thanks Walter Koch and the other, anonymous, reviewer(s) for their contribution to the peer review of this work. Peer reviewer reports are available.

**Reprints and permission information** is available at <http://www.nature.com/reprints>

**Publisher's note** Springer Nature remains neutral with regard to jurisdictional claims in published maps and institutional affiliations.

 **Open Access** This article is licensed under a Creative Commons Attribution 4.0 International License, which permits use, sharing, adaptation, distribution and reproduction in any medium or format, as long as you give appropriate credit to the original author(s) and the source, provide a link to the Creative Commons license, and indicate if changes were made. The images or other third party material in this article are included in the article's Creative Commons license, unless indicated otherwise in a credit line to the material. If material is not included in the article's Creative Commons license and your intended use is not permitted by statutory regulation or exceeds the permitted use, you will need to obtain permission directly from the copyright holder. To view a copy of this license, visit <http://creativecommons.org/licenses/by/4.0/>.

© The Author(s) 2021

## 8 Supplementary: Publication III



International Journal of  
Molecular Sciences



Review

# A Calcium Guard in the Outer Membrane: Is VDAC a Regulated Gatekeeper of Mitochondrial Calcium Uptake?

Paulina Sander <sup>1</sup>, Thomas Gudermann <sup>1,2</sup> and Johann Schredelseker <sup>1,2,\*</sup>

<sup>1</sup> Walther Straub Institute of Pharmacology and Toxicology, Faculty of Medicine, LMU Munich, 80336 Munich, Germany; paulina.sander@campus.lmu.de (P.S.); thomas.gudermann@lrz.uni-muenchen.de (T.G.)

<sup>2</sup> Deutsches Zentrum für Herz-Kreislauf-Forschung, Partner Site Munich Heart Alliance, Munich, Germany

\* Correspondence: johann.schredelseker@lmu.de; Tel.: +49-(0)89-2180-73831

**Abstract:** Already in the early 1960s, researchers noted the potential of mitochondria to take up large amounts of  $\text{Ca}^{2+}$ . However, the physiological role and the molecular identity of the mitochondrial  $\text{Ca}^{2+}$  uptake mechanisms remained elusive for a long time. The identification of the individual components of the mitochondrial calcium uniporter complex (MCUC) in the inner mitochondrial membrane in 2011 started a new era of research on mitochondrial  $\text{Ca}^{2+}$  uptake. Today, many studies investigate mitochondrial  $\text{Ca}^{2+}$  uptake with a strong focus on function, regulation, and localization of the MCUC. However, on its way into mitochondria  $\text{Ca}^{2+}$  has to pass two membranes, and the first barrier before even reaching the MCUC is the outer mitochondrial membrane (OMM). The common opinion is that the OMM is freely permeable to  $\text{Ca}^{2+}$ . This idea is supported by the presence of a high density of voltage-dependent anion channels (VDACs) in the OMM, forming large  $\text{Ca}^{2+}$  permeable pores. However, several reports challenge this idea and describe VDAC as a regulated  $\text{Ca}^{2+}$  channel. In line with this idea is the notion that its  $\text{Ca}^{2+}$  selectivity depends on the open state of the channel, and its gating behavior can be modified by interaction with partner proteins, metabolites, or small synthetic molecules. Furthermore, mitochondrial  $\text{Ca}^{2+}$  uptake is controlled by the localization of VDAC through scaffolding proteins, which anchor VDAC to ER/SR calcium release channels. This review will discuss the possibility that VDAC serves as a physiological regulator of mitochondrial  $\text{Ca}^{2+}$  uptake in the OMM.

**Keywords:** mitochondrial calcium uptake; VDAC; MCU



**Citation:** Sander, P.; Gudermann, T.; Schredelseker, J. A Calcium Guard in the Outer Membrane: Is VDAC a Regulated Gatekeeper of Mitochondrial Calcium Uptake? *Int. J. Mol. Sci.* **2021**, *22*, 946. <https://doi.org/10.3390/ijms22020946>

Received: 23 December 2020

Accepted: 14 January 2021

Published: 19 January 2021

**Publisher's Note:** MDPI stays neutral with regard to jurisdictional claims in published maps and institutional affiliations.



**Copyright:** © 2021 by the authors. Licensee MDPI, Basel, Switzerland. This article is an open access article distributed under the terms and conditions of the Creative Commons Attribution (CC BY) license (<https://creativecommons.org/licenses/by/4.0/>).

### 1. Introduction

Mitochondria are known as the cell's powerhouses as they produce ATP by oxidative phosphorylation. However, already in the 1950s and 1960s, researchers noted the potential of mitochondria to sequester vast amounts of  $\text{Ca}^{2+}$  [1,2], while the role of this mitochondrial  $\text{Ca}^{2+}$  uptake and the involved molecular players remained elusive. Many proteins including RyR, LetM1, or UCP2/3 had been suggested to mediate mitochondrial  $\text{Ca}^{2+}$  uptake, before the molecular identity of the MCU complex (MCUC) in the inner mitochondrial membrane was identified as the main route of  $\text{Ca}^{2+}$  uptake in the early 2010s. Subsequently, research on mitochondrial  $\text{Ca}^{2+}$  uptake experienced a revival when molecular structures and knock-out models of the individual MCUC components became available. However, on its way into mitochondria  $\text{Ca}^{2+}$  has to pass two membranes, and the first barrier before  $\text{Ca}^{2+}$  even reaches the MCUC is the outer mitochondrial membrane (OMM), a fact that is still often neglected in current literature, where the OMM is described as freely permeable to ions. Indeed, the term mitochondrial  $\text{Ca}^{2+}$  uniport is often used synonymously for mitochondrial  $\text{Ca}^{2+}$  uptake, and some textbook representations do not even show the OMM but depict the MCUC such that it is directly facing the cytosol.

The OMM is widely occupied by large pore-forming structures, the voltage-dependent anion channels (VDACs), which mediate the flux of ions and metabolites over the OMM.

While bacteria express only one form of VDAC, higher eukaryotes express multiple isoforms. In yeast, two isoforms are described, while plants and animals express three isoforms (VDAC1-3).

In a ground-setting publication in 2001, Shoshan-Barmatz and colleagues provided several lines of evidence that the voltage-dependent anion channel (VDAC) is the main carrier for  $\text{Ca}^{2+}$  over the OMM [3]: when inserted into planar lipid bilayers, VDAC1 was permeable to  $\text{Ca}^{2+}$ , and VDAC1 reconstituted into liposomes mediated  $\text{Ca}^{2+}$  efflux from these vesicles. These *in situ* results are supported by the observations that VDAC1 overexpression enhanced  $\text{Ca}^{2+}$  uptake into mitochondria [4], and knock-down of VDAC1 reduced mitochondrial  $\text{Ca}^{2+}$  uptake [5] *in vitro* in cultured cells. Already in these early publications, it was noted that the  $\text{Ca}^{2+}$  flux through VDAC could be blocked by ruthenium red (RuR) and  $\text{La}^{3+}$  and that VDAC possesses a  $\text{Ca}^{2+}$  binding site, raising the intriguing hypothesis that VDAC is not freely permeable to  $\text{Ca}^{2+}$  but might present a regulated barrier for  $\text{Ca}^{2+}$  flux over the OMM.

However, considering that VDAC forms a pore large enough to allow the passage of metabolites such as ATP, two questions arise: how can such a big pore be regulated at the molecular level and is the regulation of mitochondrial  $\text{Ca}^{2+}$  uptake at the outer mitochondrial membrane physiologically relevant?

Several recent reports have argued in favor of a regulation of mitochondrial  $\text{Ca}^{2+}$  uptake at the OMM: (i) the tight connection between VDAC1 and the IP3 receptor (IP3R) was reported to be a key regulatory mechanism to either promote enhanced cellular metabolism or to induce apoptosis by modulating mitochondrial  $\text{Ca}^{2+}$  signaling [5,6], (ii) regulation of VDAC-mediated  $\text{Ca}^{2+}$  uptake through channel monoubiquitylation [7] was demonstrated to be critically involved in the pathophysiology of Parkinson's disease and to mediate programmed cell death after DNA damage [8], and (iii) our lab has recently demonstrated that the small compound efsevin modulates VDAC2 and, thereby, amplifies mitochondrial  $\text{Ca}^{2+}$  uptake approx. 3-fold in cardiomyocytes [9,10]. This amplification induces a protective effect against cardiac arrhythmia, both *in vitro* and *in vivo*.

In this review, we will first discuss possible regulatory mechanisms of mitochondrial  $\text{Ca}^{2+}$  uptake through VDAC and then review their putative roles in cell physiology and pathophysiology.

## 2. Mechanisms to Control the $\text{Ca}^{2+}$ Conductance of VDAC

### 2.1. Structure and Electrophysiological Properties of VDACS

The common perception that VDAC creates pores in the OMM that are freely permeable to ions is closely related to its structure. VDACS are 30–35 kD transmembrane proteins consisting of approximately 280–300 amino acids, depending on isoform and species. They form barrel-like pores consisting of 19  $\beta$ -sheets aligned in an antiparallel orientation. On the N-terminal end, an  $\alpha$ -helix lines the channel pore inside the barrel [11,12]. The odd-numbered 19  $\beta$ -sheet geometry is unique for pores within the OMM and was postulated to possess superior properties regarding voltage sensitivity, mitochondrial targeting, and lipid-modulated stability over barrels with a higher or lower number of sheets [13]. The pore has a diameter of approx. 18–20 Å [14]. Nevertheless, despite this large diameter, the channel can undergo conformational changes of a still unknown structural nature, which induce a significant change in the channel's conductance and ion selectivity. When purified VDAC is inserted into artificial lipid bilayers the channel is in a high-conductance state at neutral potential that is classically also referred to as the open state. Upon gradual polarization of the membrane, the channel starts gating at around  $\pm 20$ –30 mV between this high-conductance state and several gated states, which are also referred to as closed states (Figures 1 and 2). In these states, the conductance of the channel is reduced to approximately 50% [15–18]. By using  $\text{CaCl}_2$  as the charge carrier, the channel was shown to be permeable for  $\text{Ca}^{2+}$ . Interestingly, the ion selectivity of the channel changes upon gating from a higher anion selectivity in the high-conductance state to a lower selectivity and, thus, higher proportional conductance for  $\text{Ca}^{2+}$  in the gated states [3,19–21]. Though

this observation is consistent, the degree of ion selectivity varies between distinct reports and experimental conditions depending on, e.g., the concentration of  $\text{CaCl}_2$  used or the composition of the bilayer making an estimation of VDACs ion selectivity in the native environment in the cell difficult. Nevertheless, the relative permeability of cations over anions in VDAC1 was identified experimentally and by molecular simulations to be in the range of 0.05 to 0.4 for the high-conductance state, while the relative permeability for cations over anions was almost 1 for the gated states [3,19–21] for VDAC1 and VDAC2 [10]. Ambiguity exists concerning the electrophysiological properties of VDAC3. While initially reported to form channels with low conductance and weak voltage-dependent gating [22], this isoform was later reported to have similar electrophysiological properties as VDAC1 and VDAC2 [23]. However, to our knowledge, no reports are available for the ion selectivity and  $\text{Ca}^{2+}$  conductance of VDAC3.

The transition between high-conductance and gated states induces drastic changes in the permeability and selectivity. Although, lipid bilayer experiments are performed in an artificial and rather unphysiological system and care must be taken when transferring them directly to the *in vivo* situation, it is conceivable that gating of the channel presents a mechanism to regulate not only ATP, but also  $\text{Ca}^{2+}$  flux over the OMM. However, gating of the channel was experimentally induced by voltage, and although several mechanisms to create and regulate a membrane potential over the OMM were postulated [24–26], it remains controversial whether this is a physiologically relevant trigger of gating. Several other factors including  $\text{Ca}^{2+}$  [27], metabolites [28], the lipidic environment [29–32], temperature [33], small molecules [10,34,35], interacting proteins [6,36,37], and biochemical modifications of the channel itself [38,39] were reported to either modify voltage-induced gating or to induce channel closure on their own. Among those is also the intriguing hypothesis of an entirely different mode of channel gating, namely a closure by occlusion of the large VDAC pore by a “molecular plug” mechanism (Figure 1). In the following, we will discuss the different modes of gating in respect to the  $\text{Ca}^{2+}$  conductance of the channel.

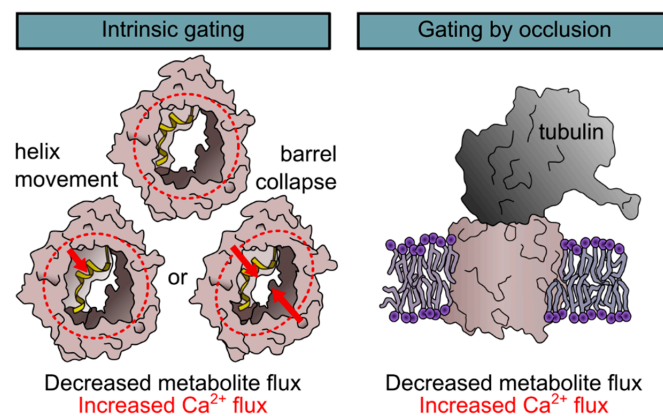


**Figure 1.** Mechanisms of voltage-dependent anion channels (VDAC) gating. Two mechanisms for the gating of VDACs were described, namely gating by an intrinsic conformational change (left) and gating by occlusion (right). The first is experimentally induced by voltage but is modulated by extrinsic parameters such as protein interactions, the lipidic environment or posttranslational modifications. Intrinsic gating results in a conformational change of a yet unknown nature. Several models ranging from a movement of the N-terminal  $\alpha$ -helix to a collapse of the barrel were suggested. The second mechanism that was observed for VDAC gating is gating by occlusion by, e.g., free tubulin through a molecular plug model. Both mechanisms were shown to block metabolite flux and to induce a lower anion selectivity and, thus, an increased  $\text{Ca}^{2+}$  flux.

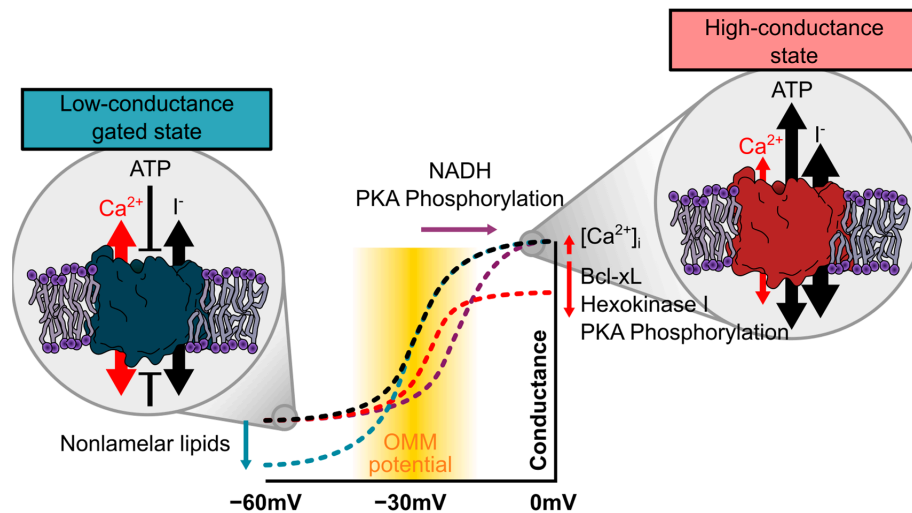


**Figure 2.** Regulation of voltage-dependent gating of VDAC. While VDAC almost exclusively resides in its anion-selective and metabolite-permeable high-conductance state at neutral potentials, it starts gating within the range of  $-20$  to  $-30$  mV (black line), which is well within the predicted range of an OMM potential (yellow zone). Note that the conductance–voltage relation of VDAC is symmetrical, and only the negative side is depicted. At potentials below  $-40$  mV, it almost exclusively resides in the low-conductance state that is impermeable to ATP but shows a higher permeability of  $\text{Ca}^{2+}$ . Several factors were reported to modulate this voltage–conductance relationship. The phosphorylation status or binding of protein partners such as Bcl-xL or hexokinase I were suggested to facilitate channel gating and, thus, induce both a right-shift of the voltage dependence and a reduction in the maximum conductance at potentials close to neutral (red line), while  $\text{Ca}^{2+}$  is suggested to facilitate channel opening and, thus, has an opposite effect. Nonlamellar lipids were demonstrated to promote channel closure at very negative potentials (blue).

### 2.1.1. Regulation of $\text{Ca}^{2+}$ Conductance by Gating

Evidence for the ability of the channel to undergo intrinsic conformational changes for gating was provided by lipid bilayer experiments on purified channels [15,16]. VDAC heterologously expressed in *E. coli* and, subsequently, purified and refolded from inclusion bodies forms functional channels in lipid bilayers, which are completely devoid of any regulatory partners that might be associated with the channel in its native environment [10,11]. These channels are able to reversibly gate between the high-conductance and gated states indicating that gating is an intrinsic property of the channel protein. Various models were proposed to explain the molecular movements underlying gating of VDACS (Figure 1). Many of these models involve participation of the N-terminal  $\alpha$ -helix and include mechanisms with relatively small movements of the helix inside the barrel [17,40] and models in which the helix moves outside of the barrel and induces its collapse leading to channel closure [20,41]. However, while deletion of the helix abrogated voltage-gating of the channel, cross-linking of the helix against the channel wall did not [42]. This favors a model in which the helix stabilizes the barrel, while gating is induced by a yet uncharacterized deformation of the barrel.

As described earlier, gating of the channel was demonstrated to directly affect its  $\text{Ca}^{2+}$  conductance, hence gating would be an intriguing possibility to regulate VDAC  $\text{Ca}^{2+}$  flow. However, the existence of voltage-dependent gating in the native environment remains controversial. Several extrinsic factors were described to influence and modulate voltage-gating of the channel and are discussed later.

### 2.1.2. Regulation of $\text{Ca}^{2+}$ Conductance by Occlusion

In addition to the intrinsic gating of the channel, another intriguing hypothesis that was more recently developed is a regulation of the channel by occlusion. Given the large

pore size of the channel, which is wide enough for the passage of metabolites, it appears conceivable that metabolites or domains of interacting proteins enter the channel to serve as “channel plugs”. Among those suggested to serve as molecular plugs is NADH: while it was known for long that NADH closes VDAC [28,43], it was only recently found in a combination of high-resolution NMR with molecular dynamics simulations that NADH reduces conduction sterically by binding into the open pore at the hinge of the pore lining helix without a structural change of the channel [44]. Other partners suggested to mediate channel occlusion are free tubulin, which was demonstrated to interact with VDAC through its C-terminus [45–47] (Figure 1), and  $\alpha$ -synuclein, which blocks the channel by occlusion but also translocates through the channel [48]. Although to our knowledge, no reports have selectively evaluated the influence of channel occlusion on  $\text{Ca}^{2+}$  specifically, the occluded state was also demonstrated to make the channel more cation selective [49], thus suggesting a higher  $\text{Ca}^{2+}$  permeability.

Interestingly, a recent study using NADH measurements combined with mathematical modeling has proposed that in cardiac cells 98% of all VDACS reside in a state that is impermeable for ATP, but it remains speculative whether this is the gated or occluded state [50]. It raises, however, the interesting possibility that 98% of VDACS are in a  $\text{Ca}^{2+}$  conducting state.

## 2.2. Modification of the Gating Profile of VDAC

In the following, we will summarize factors that were discussed as possible physiological triggers that control gating or occlusion of the channel.

### 2.2.1. An OMM Potential as a Trigger for VDAC Gating

The most straight-forward idea when bearing the lipid bilayer experiments in mind is a regulation of the channel by voltage. Since VDAC resides in its high-conductance state at 0 mV and only starts gating at potentials above 20 to 30 or below  $-20$  to  $-30$  mV, a physiologically relevant voltage-dependent gating of the apo-form of the channel would depend on a membrane potential across the OMM. Although the generation of a membrane potential has often been considered impossible due to the high abundance and high conductance of VDACS in the OMM, a series of modeling studies by Victor and Sergy Lemeshko provides reasonable evidence for a membrane potential over the OMM. This potential was suggested to be created by a spatial separation of VDAC from the electron transport chain and to be regulated through the local concentration of ADP within the contact sites and the Gibbs free energy of the hexokinase reaction bound to VDAC [51]. Most strikingly, it was calculated to be well within the range of VDAC gating [24,52,53]. Experimental studies using pH indicators selectively targeted into the intermembrane space (IMS) have found a pH in the IMS, which is approximately 0.5 to 0.7 lower than in the cytosol, suggesting an even more negative potential of approx.  $-40$  mV and acidification of the IMS as a modulator of the membrane potential [26].

Another hypothesis suggests that at points where the IMM is in close contact to the OMM [54], possibly at sites of VDAC and MCUC interaction [55], the strong negative potential of the IMM induces a local OMM potential by capacitive coupling between the two membranes, which allows voltage-gating of VDAC [25]. This is particularly interesting, since these contact sites are believed to be the sites of mitochondrial  $\text{Ca}^{2+}$  uptake (see Section 2.4) and closure of the channel by a local negative potential could induce a higher  $\text{Ca}^{2+}$  conductance specifically in these areas.

Taken together, such a potential difference in the OMM could very likely be at least one factor contributing to the regulation of the channel. It is feasible that voltage induces gating of the channel, while interaction partners and channel modifications shift the channels open probability towards a preferentially high-conductance or gated state (Figure 2).



### 2.2.2. Effects of $\text{Ca}^{2+}$ on VDAC Gating

Besides conducting  $\text{Ca}^{2+}$ , several lines of evidence suggest that the channel is also regulated by  $\text{Ca}^{2+}$  and that  $\text{Ca}^{2+}$  can regulate its  $\text{Ca}^{2+}$  conductance. In their 2001 report, Shoshan-Barmatz and colleagues were among the first to suggest that VDAC1 has a  $\text{Ca}^{2+}$  binding site. This was based on several lines of evidence: (i) a  $\text{Ca}^{2+}$  induced shift in electrophoretic mobility of VDAC1, (ii) a blockade of the channel by  $\text{La}^{3+}$ , which could be reversed by the addition of EGTA, and (iii) an inhibition of the channel by ruthenium derivatives such as RuR, Ru360 [3], or AzRu [56] that was reversed by the addition of  $\text{Ca}^{2+}$ . More recently, a combination of NMR and single-molecule force spectroscopy revealed that VDAC barrels are highly flexible, but a significant reduction in conformational variability is induced when  $\text{Ca}^{2+}$  is bound to the channel [57]. In a very detailed work, the lab of György Hajnóczky showed that the channel resides in a non-conducting state, with openings to the low-conductance states in the absence of  $\text{Ca}^{2+}$ , but starts gating and mainly resides in the high-conductance state as the concentration of  $\text{Ca}^{2+}$  increases [27], indicating a regulation of the channel through  $\text{Ca}^{2+}$ . Indeed, the relationship between the external  $\text{Ca}^{2+}$  concentration and the uptake rate of  $\text{Ca}^{2+}$  into VDAC liposomes follows a non-linear relation, indicating the presence of a  $\text{Ca}^{2+}$ -regulated  $\text{Ca}^{2+}$  flux through VDAC [27].

In an effort to localize the  $\text{Ca}^{2+}$  binding site, it was observed that the addition of an excess amount of  $\text{Ca}^{2+}$  prevented the blocking effect of RuR, which was reinstalled after the addition of EGTA. This suggests that ruthenium derivatives compete with  $\text{Ca}^{2+}$  for the same binding site [56]. Mutation of a glutamate residue at position 73 (E73) eliminated the blocking effect of RuR, establishing this residue as a primary candidate for the  $\text{Ca}^{2+}$ -mediated control. However, E73 is located on the outside of the barrel facing the lipidic environment [11,12], and although molecular simulations predict a thinning of the nearby membrane due to the charged nature of E73 [58], it remains controversial whether  $\text{Ca}^{2+}$  can enter the lipidic environment of the membrane. Alternatively, the mere presence of E73 could stabilize the channel in a conformation that is required for  $\text{Ca}^{2+}$ -mediated channel regulation.

Nevertheless, a regulation of the channels  $\text{Ca}^{2+}$  transport activity by E73 was recently confirmed in physiological experiments, where  $\text{Ca}^{2+}$  transfer from lysosomes into mitochondria after lysosomal  $\text{Ca}^{2+}$  release through TRPML1 was shown to depend on E73 [59]. In agreement with this,  $\text{Ca}^{2+}$  transfer from the SR into mitochondria in cardiomyocytes is also regulated through E73 [60]. These findings again highlight the presence of a  $\text{Ca}^{2+}$  regulated uptake of  $\text{Ca}^{2+}$  through VDAC.

### 2.2.3. Modulation of VDAC Gating by Posttranslational Modification

A common way to regulate ion channels are posttranslational modifications. Phosphorylation of all three VDAC isoforms was repeatedly reported, and several studies showed that PKA phosphorylation results in altered gating properties of VDAC. Interestingly, PKA phosphorylation affected channel gating asymmetrically with no influence at positive potentials but a reduction in both single channel conductance and open probability at negative potentials [61,62]. This is in line with the idea that, if a potential is established at all across the outer membrane, this would be a negative potential. Similar results were obtained for phosphorylation of VDAC by c-Jun N-terminal Kinase-3 (JNK3), which also led to a lower single-channel conductance and a reduction in open probability [63]. Although the authors of these studies only delineate a role of VDAC phosphorylation for the regulation of apoptosis, the modulatory effect of VDAC on apoptosis was critically linked to its  $\text{Ca}^{2+}$  conductance [5]. In later studies, both PKA-phosphorylation mediated by the 18 kDa translocator protein TSPO [64] and phosphorylation by PKC $\epsilon$  reduced mitochondrial  $\text{Ca}^{2+}$  accumulation [65].

These experiments are difficult to interpret. Bilayer experiments indicate that phosphorylation of VDAC-induced voltage-dependent closure of the channel and in vitro phosphorylation of VDAC by either glycogen synthase kinase-3 $\beta$  (GSK3 $\beta$ ) or cAMP-dependent protein kinase A (PKA) increased tubulin binding and, thereby, channel occlusion [66]. Both

the voltage-closed state and the tubulin-bound occluded state were reported to induce  $\text{Ca}^{2+}$  flux, and the bilayer experiments are, thus, not in line with the physiological observations of a limited  $\text{Ca}^{2+}$  uptake after PKA phosphorylation [65]. This might indicate that results from lipid bilayers are too simplistic, and an additional degree of regulation exists *in vivo*.

A critical link between posttranslational modifications and  $\text{Ca}^{2+}$  conductance *in vivo* was established in a recent study where PINK1-dependent monoubiquitinylation of VDAC1 was directly shown to limit mitochondrial  $\text{Ca}^{2+}$  uptake. Abolishing VDAC1 monoubiquitinylation by introducing a K247R mutation in VDAC1 induced a Parkinson disease phenotype in fruitflies was associated with excessive apoptosis and could be relieved by MCU knock-out [7]. Although mechanistical data on how monoubiquitinylation decreases  $\text{Ca}^{2+}$  flux are missing in this report, these data directly indicate that reducing mitochondrial  $\text{Ca}^{2+}$  uptake through VDAC1 monoubiquitinylation is a critical mechanism to suppress apoptosis.

#### 2.2.4. Modulation of VDAC Gating through the Lipidic Environment

Finally, the lipidic environment was shown to influence ion channels properties, and corresponding observations were also made for VDAC. When inserted into lipid bilayers, the addition of nonlamellar lipids such as phosphatidylethanolamine (PE) or cardiolipin induced asymmetry in voltage gating, evident by increased channel closure at negative potentials [29]. A similar effect was recently also reported for the neuroprotective cholesterol-like synthetic compound olesoxime, which also induced channel gating at more negative potentials [67]. This effect might again be relevant when VDAC is exposed to a negative potential in the OMM to facilitate or prevent gating of the channel. Additionally, the lipidic environment might also modulate the channels' interaction with its molecular plugs. The neuroprotective cholesterol-like lipid olesoxime prevented the interaction of VDAC with  $\alpha$ -synuclein and, thereby, affected not only VDAC voltage gating but also binding of  $\alpha$ -synuclein to the channel [67]. As a third way to regulate VDAC through the lipidic environment, molecular dynamics simulations suggested that interactions of lipids with acidic residues of VDAC might modulate the anion selectivity of the channel [30].

Although lipid bilayer experiments and molecular dynamics simulations might not directly recapitulate channel function *in vivo* due to the simplicity of the system and the lack of additional regulatory factors present in its native environment, a regulation of the channel by membrane lipids might fine-tune channel activity in response to cellular stimuli also there. Indeed, a change in the membrane composition was reported, for example for the induction of apoptosis [68].

#### 2.3. Regulation of VDAC $\text{Ca}^{2+}$ Flux by Protein Partners

Many of the aforementioned mechanisms might be regulated by partner proteins. VDAC was shown to interact with many cellular proteins ranging from small signaling molecules to large enzymes and other ion channels, and these interactions are often associated with  $\text{Ca}^{2+}$  homeostasis or regulated by  $\text{Ca}^{2+}$ .

In particular, members of the Bcl-2 family were described to influence mitochondrial  $\text{Ca}^{2+}$  uptake by binding to VDAC, presumably at a structure formed by the N-terminal helix and the loop connecting beta sheets 14 and 15 [36,69]. Bcl-xL was demonstrated to selectively interact with VDAC1 and VDAC3 but not VDAC2. Huang et al. report enhanced mitochondrial  $\text{Ca}^{2+}$  uptake, when Bcl-xL is associated with the channel [36] in permeabilized cells. Similarly, also the Bcl-2 member Mcl-1 interacts with VDAC1 and VDAC3 but only weakly with VDAC2 to promote the uptake of  $\text{Ca}^{2+}$  into mitochondria [70]. However, other reports in intact cells found that Bcl-xL limits  $\text{Ca}^{2+}$  uptake into mitochondria [71,72], differences that were explained by experimental disparities between whole cell experiments in which mitochondrial  $\text{Ca}^{2+}$  uptake is triggered by local IP3Rs in  $\text{Ca}^{2+}$  microdomains within contact sites of mitochondria and the SR and permeabilized cells in which mitochondrial  $\text{Ca}^{2+}$  uptake is triggered by a global rise in  $\text{Ca}^{2+}$  (see also Section 2.4). Interestingly, in lipid bilayers Bcl-xL induced a reduction in channel conductance, while

preserving voltage gating [73], indicating that the Bxl-xL induced channel closure is distinct from voltage-gated closure but might also affect its  $\text{Ca}^{2+}$  conductance.

Furthermore, several enzymes have been found to interact with VDAC to regulate its  $\text{Ca}^{2+}$  flux. Among those are reports about GAPDH, which was recently shown to interact with VDAC1 to enhance the uptake of  $\text{Ca}^{2+}$  into VDAC1-containing protoliposomes [37] and the 18 kDa translocator protein TSPO, also referred to as the peripheral benzothiazepine receptor (PBR), a mitochondrial protein that forms a complex with VDAC, which, when inserted into lipid bilayers, was sensitive to its ligand hemin [74]. The addition of hemin closed VDAC and by this limited  $\text{Ca}^{2+}$  uptake into mitochondria. Although these interactions do not go into mechanistical detail, in particular, the question of why closure of the channel would decrease  $\text{Ca}^{2+}$  conductance, which is opposing to other results, they highlight the importance of direct or indirect protein–protein interactions for the regulation of VDAC.

Apart from interactions that were shown to directly alter VDAC electrophysiology or mitochondrial  $\text{Ca}^{2+}$  fluxes VDAC was repeatedly shown to interact with  $\text{Ca}^{2+}$  handling proteins, such as the SR  $\text{Ca}^{2+}/\text{K}^{+}$  channel mitsugumin-23 [75], the L-type  $\text{Ca}^{2+}$  channel [76], the RyR [77], MCU [55], and the IP3R in a complex that is highly regulated through different proteins such as DJ-1 [78], grp75, or transglutaminase 2 [79]. Although these interactions were not directly shown to modulate VDAC, they still highlight its important role in  $\text{Ca}^{2+}$  handling.

Taken together, several proteins modulate VDAC directly or through higher protein complexes. However, only a small number of these reports specifically investigated  $\text{Ca}^{2+}$  conductance. Thus, ambiguity still exists about the  $\text{Ca}^{2+}$  conductivity of the gated and occluded states in vivo. Several reports indicate reduced  $\text{Ca}^{2+}$  uptake upon VDAC closure [74], while other reports do not observe changes on  $\text{Ca}^{2+}$  flux despite closure of the channel [80]. This might in part be explained by distinct modes of VDAC closure, whereof some affect  $\text{Ca}^{2+}$  conductivity and some do not, but it needs further research to selectively discriminate between them.

#### 2.4. Regulation by Subcellular Localization in $\text{Ca}^{2+}$ Microdomains

Finally, another powerful regulatory mechanism for cellular  $\text{Ca}^{2+}$  fluxes and  $\text{Ca}^{2+}$  signaling pathways is subcellular localization. In line with the idea that VDAC regulates the  $\text{Ca}^{2+}$  flux over the OMM, a distinct subcellular localization within sites of  $\text{Ca}^{2+}$  mobilization was also observed for VDAC.

Most eminently, mitochondria intimately and dynamically interact with the internal  $\text{Ca}^{2+}$  stores of the ER/SR in regions where the two organelles are densely tethered. Those sites of ER/SR-mitochondrial coupling, called mitochondrial-associated membranes (MAMs), are a key player in  $\text{Ca}^{2+}$  shuttling. MAMs cover approximately 5–20 percent of the mitochondrial surface in mammalian cells [81]. Interestingly, VDAC is not homogeneously distributed across the OMM and certain VDAC isoforms occur more frequently in MAMs and in close vicinity to ER/SR  $\text{Ca}^{2+}$  release sites, where local cytosolic  $\text{Ca}^{2+}$  can reach particularly high levels [54,77,82–84]. The IP3R, the  $\text{Ca}^{2+}$  release channel in the ER membrane of non-excitable cells is tethered to VDAC1 but not VDAC2 or VDAC3 [5,85], through the anchoring protein grp75 [85,86]. More recent studies have shown that in cardiomyocytes VDAC2 is analogously coupled to RyR2 [10,77]. For the subsequent transport of  $\text{Ca}^{2+}$  into mitochondria, the SR-OMM contact points align with contact points of OMM and IMM [54], and VDAC1 physically and functionally interacts with the MCUC [55].

These couplons of  $\text{Ca}^{2+}$  release (IP3R/RyR2),  $\text{Ca}^{2+}$  shuttling (VDACs), and  $\text{Ca}^{2+}$  uptake sites (MCUC) provide an efficient route for direct  $\text{Ca}^{2+}$  shuttling from high  $\text{Ca}^{2+}$  microdomains of the SR into mitochondria. They were shown to be dynamic, as they can change in response to cytosolic or extracellular triggers to regulate mitochondrial  $\text{Ca}^{2+}$  uptake [8,86] and are intensively regulated at different levels under physiological and pathophysiological conditions [8,78,87] (see Sections 3 and 4).

However, intracellular  $\text{Ca}^{2+}$  transfer between organelles regulated through VDAC localization is not an exclusive mechanism limited to the contact sites with the ER/SR. The lysosomal  $\text{Ca}^{2+}$  release channel TRPML1 was shown to selectively interact with VDAC1 but not VDAC2 or VDAC3 to mediate  $\text{Ca}^{2+}$  transfer from lysosomes to mitochondria. Interestingly, this VDAC1-mediated lysosome–mitochondria  $\text{Ca}^{2+}$  transfer was shown to be regulated by  $\text{Ca}^{2+}$  through residue E73 [59].

It is tempting to speculate that the subcellular localization not only positions VDAC in an ideal environment for  $\text{Ca}^{2+}$  transfer from the ER into mitochondria but also enables a higher degree of regulation. As such, it is feasible that the high  $\text{Ca}^{2+}$  concentration within this microdomain, local changes in OMM membrane potential, or a different set of partner proteins in this micro-environment allow for distinct regulation of channels inside the MAM compared to channels outside of the MAM (Figure 3).

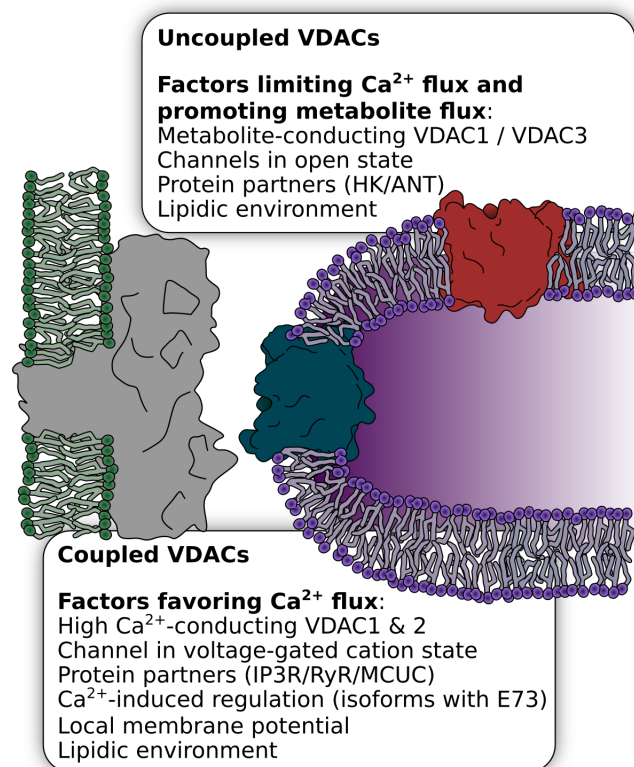


**Figure 3.** Regulation of VDAC by subcellular localization. A fraction of VDAC channels was shown to be present in couplons with  $\text{Ca}^{2+}$  release channels of the ER/SR, in particular VDAC1 with the IP3R or VDAC2 with the RyR. These couplons represent hotspots of  $\text{Ca}^{2+}$ -mediated regulation of mitochondrial activity. In addition to the strategic positioning of VDAC in close vicinity to the mouth of the release channels, other factors might regulate VDAC within and outside the couplons for the specialized tasks within these environments. These include isoform selectivity, protein partners, the lipidic environment, and the voltage-gated state of the channel. Depending on the VDAC localization, these factors might determine whether VDAC serves as a  $\text{Ca}^{2+}$  or metabolite channel.

#### 2.4.1. Regulation of the OMM $\text{Ca}^{2+}$ Flux by Different VDAC Isoforms

An alternative but also associated form of regulation might be achieved by isoform specificity. While the three VDAC isoforms are certainly able to fulfill to some degree redundant and compensatory functions between each other, they also have different channel

properties, different expression levels, and specific protein interaction partners, indicating that the isoforms serve different physiological tasks [88]. Furthermore, the same VDAC isoform might perform distinct roles in different tissues or cell types depending on its microenvironment. The specific knock-out of individual VDAC isoforms provided first insights into their function: VDAC1 KO mice are viable and studies with VDAC1<sup>-/-</sup> mice confirmed that it is mainly involved in metabolite exchange and pro-apoptotic processes [89], whereof the latter is believed to be mediated by mitochondrial Ca<sup>2+</sup> uptake. Indeed, in VDAC1<sup>-/-</sup> HeLa cells, the transfer of local, low-amplitude Ca<sup>2+</sup> signals was selectively abolished. However, mitochondrial Ca<sup>2+</sup> uptake after maximum agonist response was still measurable, indicating that other VDAC isoforms, presumably outside of the IP3R couplons, are able to take up Ca<sup>2+</sup> from high-amplitude signals [5].

In contrast to VDAC1, a global VDAC2 KO, was demonstrated to be lethal at around E10.5 to E11.5 of embryonic development. Furthermore, a heart-specific VDAC2 knockout showed postnatal onset of progressive fibrosis and cardiomyopathy, resulting in early mortality indicating a, presumably cardiac, role of VDAC2, which cannot be fulfilled by the two other isoforms [90]. One intriguing possibility is that the other VDAC isoforms cannot form the specific interaction of VDAC2 with RyR2 in the highly specialized heart muscle cells [77]. This would result in decreased mitochondrial Ca<sup>2+</sup> uptake via RyR2 and VDAC2 and associated downstream effects such as, for example, cytosolic Ca<sup>2+</sup> overload, a lack of mitochondrial energy–demand matching, or an impairment in mitochondrial function.

It is, thus, conceivable that the IP3R-VDAC1 coupling is required for the control of apoptosis through local low-amplitude Ca<sup>2+</sup> signals. In cardiomyocytes, however, where local RyR-mediated Ca<sup>2+</sup> signals of the SR are of a higher magnitude and more frequent, the presence of VDAC1 within these couplons would induce immediate apoptosis due its interaction with pro-apoptotic protein partners and/or other regulatory mechanisms that are specific for VDAC1. Therefore, in the heart, VDAC2 mediates a more effective flux of Ca<sup>2+</sup> into mitochondria in the MAM, where it shapes cytosolic Ca<sup>2+</sup> signals and rapidly accommodates energy–demand matching, while VDAC1 is located outside of the couplons and mediates metabolite flux. Indeed, VDAC2 was shown to have a different distribution of charges within the pore, which mediates a lower anion selectivity [91]. Enhanced apoptosis that might be induced by this process could be suppressed by the anti-apoptotic inhibition of BAK activation by VDAC2 [92]. The existence of IP3R-VDAC1 couplons in cardiomyocytes is under debate but would not contradict this picture.

In contrast to VDAC1 and VDAC2, the role of VDAC3 in Ca<sup>2+</sup> signaling is questionable. Indeed, VDAC3 lacks residue E73 that was reported to be important for Ca<sup>2+</sup>-dependent regulation of the channel and is conserved in both VDAC1 and VDAC2.

#### 2.4.2. Regulation of OMM Ca<sup>2+</sup> Flux by VDAC Expression Levels

A very direct way to regulate ion channel activity is the variation of the mere number of channels by adapting expression levels. Indeed, several reports have identified a variation in expression levels as a way to regulate VDAC activity. A first hint that expression levels of VDAC1 can control life and death of the cell was that downregulation of VDAC1 inhibited cell growth and overexpression lead to cell death [93]. This process seems to be physiologically relevant, since in podocytes, induction of apoptosis was shown to cause an increased expression of both VDAC1 and the IP3R, presumably to enhance mitochondrial Ca<sup>2+</sup> uptake. Likewise, in diabetes, coronary endothelia cells display higher rates of apoptosis due to mitochondrial Ca<sup>2+</sup> overload, which was linked to enhanced VDAC1 protein levels [94]. Vice-versa, a selective downregulation of VDAC1 but not VDAC2 was suggested to serve as a cardioprotective pathway during ischemia reperfusion [95].

Several pathways have been described to control VDAC expression. VDAC1 downregulation during ischemia reperfusion was shown to depend on liproxstatin-1 [95], and the transcription factors GATA1 and MYBL2 were reported to bind to and activate the VDAC2 promoter, to suppresses autophagy [96]. Another expression regulator could be Ca<sup>2+</sup> itself. Interestingly, in a recent report, elevation of intracellular Ca<sup>2+</sup> levels by Ca<sup>2+</sup>

mobilizing agents induced overexpression of VDAC1, while chelation of intracellular  $\text{Ca}^{2+}$  reduced VDAC1 expression [97].

### 3. Physiological Relevance of a $\text{Ca}^{2+}$ Flux Regulation at the OMM

Mitochondria play a pivotal role in sensing, regulating, and decoding cellular  $\text{Ca}^{2+}$  signals. Mitochondrial  $\text{Ca}^{2+}$  can induce apoptotic signals and decode a “survival or death decision”, increase mitochondrial metabolism to adjust to a higher energy demand, or modulate cytosolic  $\text{Ca}^{2+}$  signals. While the main  $\text{Ca}^{2+}$  uptake route is supposed to be via MCUC in the IMM, a substantial part of the decoding could also be controlled by the permeability of the outer membrane for  $\text{Ca}^{2+}$  via VDACs and is regulated at different levels like isoform specificity, localization, and regulation of the individual channels.

One hypothesis of how VDAC mediates distinct  $\text{Ca}^{2+}$ -induced signals is maybe best explained by taking highly specialized cells such as cardiomyocytes as an example. Cardiomyocytes are characterized by precisely regulated  $\text{Ca}^{2+}$  oscillations and critically depend on constant energy supply. Here, VDAC2 interacts with RyR2 in subsarcolemmal regions and at SR–mitochondria contact sites (see Section 2.4) and transfers beat-to-beat  $\text{Ca}^{2+}$  signals into mitochondria to respond to an increased workload with increased ATP synthesis. While VDAC2 is “occupied” with  $\text{Ca}^{2+}$  shuttling, VDAC1 could fulfill the function of a metabolite transporter across the outer membrane to ensure the supply of metabolites to the cytosol.

Although this is still only a hypothetical model, several experimental observations are in agreement with this split of specialized tasks between the isoforms and between coupled and uncoupled VDACs, respectively: VDAC2 was suggested to be less anion selective and, thus, more permeable to  $\text{Ca}^{2+}$ . Furthermore, it was proposed that the close proximity of the IMM and OMM in the contact sites favors voltage-induced VDAC closure, which additionally favors  $\text{Ca}^{2+}$  flux, whereas VDACs that are distributed outside of these contact sites might be in an open state [25], thus favoring the flux of metabolites (Figure 3). A specific interaction of VDAC1 with ANT [98] and hexokinase (HK) might additionally favor the high-conductance state of VDAC1 and, thus, provide an effective metabolite exchange across the OMM. In this scenario, the lack of coupling of the proapoptotic VDAC1 with the high-efficiency  $\text{Ca}^{2+}$  release sites around RyR clusters and the anti-apoptotic features of VDAC2 prevent apoptosis induction. However, in addition to these highly efficient RyR2-VDAC2 clusters, the canonical VDAC1-IP3R clusters were also observed in cardiomyocytes [87], which might be located in areas distinct from the RyR2-VDAC2 clusters away from the SR  $\text{Ca}^{2+}$  release sites within the Z-bands and be important for mediating apoptosis.

Indeed, the VDAC1-mediated mitochondrial  $\text{Ca}^{2+}$  flux at IP3R clusters was shown to regulate apoptosis: here, VDAC1 significantly contributes to the determination of cell fate towards survival or death [99–101]. Mitochondrial  $\text{Ca}^{2+}$  signals can either boost mitochondrial respiration or induce apoptosis. Therefore, they need to be meticulously regulated, and it is assumed that numerous factors, in particular the interaction of VDAC1 with the IP3R, HK, and Bcl-2 family members, regulate this process. Apoptosis induction was shown to increase expression and interaction of VDAC1 with the IP3R, presumably to enhance mitochondrial  $\text{Ca}^{2+}$  uptake [5,94]. However, blocking  $\text{Ca}^{2+}$  release via IP3R or mitochondrial  $\text{Ca}^{2+}$  uptake leads to necrosis of cancer cells but not normal cells [102]. These results highlight once more the importance of  $\text{Ca}^{2+}$  signal fine tuning within nanodomains to control cellular metabolism and apoptosis but also show that more work is necessary to elucidate the exact mechanisms of VDAC-controlled mitochondrial  $\text{Ca}^{2+}$  uptake.

### 4. Regulation of VDAC-Mediated $\text{Ca}^{2+}$ Flux under Pathophysiological Conditions

Considering the prominent role of VDAC-mediated  $\text{Ca}^{2+}$  signaling, it is only consistent that altered  $\text{Ca}^{2+}$  handling via VDAC is also associated with pathophysiology of many diseases, including cancer, cardiovascular diseases, and neurodegenerative diseases.

Cancer cell growth relies on adaptations in cell metabolism and bioenergetics, and VDACs significantly contribute to these alterations by regulating metabolite and ion flux into and out of mitochondria [103–105]. A central role in oncogenic behavior was ascribed to mitochondrial  $\text{Ca}^{2+}$  remodeling [106], and specifically, the VDAC1-mediated association between the ER and mitochondria was suggested to be essential for cancer cell viability. Indeed, both blocking of the IP3R  $\text{Ca}^{2+}$  release and blocking of mitochondrial  $\text{Ca}^{2+}$  uptake, respectively, lead to necrosis of cancer cells but not normal cells [102]. Strikingly, down-regulation of VDAC1 via RNA interference was shown to limit cancer cell growth in vitro and tumor development in vivo without otherwise affecting the mice [107,108]. Several mechanisms were suggested to regulate VDACs  $\text{Ca}^{2+}$  conductance in cancer: hexokinase specifically interacts with VDAC1 in cancer cells to promote metabolism and to reduce apoptosis [6]. In non-small cell lung cancer cells Mcl-1, an anti-apoptotic member of the Bcl-2 family, interacts with VDAC to enhance mitochondrial  $\text{Ca}^{2+}$  uptake and ROS production resulting in an increased cancer cell migration [70].

Abnormal mitochondrial  $\text{Ca}^{2+}$  handling, resulting in energy failure, is a key factor of heart failure. Several reports describe the involvement of VDAC in this process. In ventricular cardiomyocytes isolated from failing rat hearts, the expression of the Bcl-2 family member BNIP3 was found to be significantly increased. An interaction of BNIP3 with VDAC and a consecutive shift of  $\text{Ca}^{2+}$  from the SR into mitochondria results in decreased SR  $\text{Ca}^{2+}$  content and mitochondrial damage [109]. Likewise, during remodeling after myocardial infarction, reactive aldehydes such as 4-hydroxynonenal are produced by mitochondria and by a yet not understood mechanism bind to VDAC1 and MCU to promote formation of ER–mitochondria contact sites and ultimately mitochondrial  $\text{Ca}^{2+}$  accumulation [87]. Another study showed that in diabetes, heart failure develops due to coronary microvascular rarefaction induced by apoptosis in coronary endothelia through increased VDAC1 expression [94]. Strikingly, overexpression of hexokinase 2 reduced mitochondrial overload and apoptosis [110]. Similarly, excessive VDAC-mediated  $\text{Ca}^{2+}$  transfer was also suggested in ischemia reperfusion (I/R), and a block of mitochondrial  $\text{Ca}^{2+}$  uptake was shown to be beneficial for the survival of cardiac tissue [111,112]. The close proximity between VDAC1 and SR  $\text{Ca}^{2+}$  handling proteins has been shown to be significant during I/R. Resveratrol, a polyphenolic compound in red wine, prevents VDAC1 upregulation in I/R, leading to a reduced infarct size in vivo [113]. Liprostatin-1 was shown to be protective against I/R injury by decreasing VDAC1 expression and, thus, reducing low-amplitude apoptotic  $\text{Ca}^{2+}$  shuttling by the IP3R-Grp75-VDAC1 complex [95]. In adult mouse cardiomyocytes, the inhibition of GSK3 $\beta$ , which promotes an increased  $\text{Ca}^{2+}$  shuttling between IP3R and VDAC1, limits the  $\text{Ca}^{2+}$  transfer from SR/ER to mitochondria and prevents mitochondrial  $\text{Ca}^{2+}$  overload [114].

All these data indicate that mitochondrial dysfunction through  $\text{Ca}^{2+}$  overload is a key player in heart failure and I/R. However, contrarily to these results, other studies propose heart failure to be associated with a reduced ER–mitochondria coupling: in diabetes type 2, where a reduced  $\text{Ca}^{2+}$  shuttling in MAM regions was repeatedly demonstrated for many tissues [115–117], a reduction in IP3R-VDAC1 interaction and, thus, a decrease in IP3 stimulated  $\text{Ca}^{2+}$  transfer to mitochondria was observed for cardiomyocytes. The impaired SR–mitochondrial  $\text{Ca}^{2+}$  coupling resulted in an impairment of mitochondrial energy supply, reduced cell contraction, and thus, cardiomyopathy [118].

These data are in line with the idea that an enhanced mitochondrial  $\text{Ca}^{2+}$  uptake can be protective in pressure overload induced heart failure: TSPO closely interacts with VDAC1, acts as a negative regulator, and decreases mitochondrial  $\text{Ca}^{2+}$  uptake by inhibiting VDAC1 expression and mediating PKA phosphorylation [74,119]. Mice that underwent transverse aortic banding surgery showed significantly higher expression levels of TSPO, and cardiac TSPO-ko substantially limited the progression of pressure-induced HF and maintained cardiac function in vivo [120]. Taken together, myocardial remodeling during heart failure was repeatedly shown to affect SR–mitochondria coupling and in particular

VDAC-mediated  $\text{Ca}^{2+}$  transfer; however, further research is needed to clarify opposing results of a diminished or increased ER/SR–mitochondria coupling.

Considering the important role of VDAC in physiological and especially pathophysiological modulation of mitochondrial  $\text{Ca}^{2+}$  uptake in the heart, it is, however, tempting to investigate the potential of drugs that interfere with this process. Indeed, our lab has recently described a very prominent role of the small molecular VDAC2 modulator efsevin. In lipid bilayer experiments, efsevin induced gating of VDAC2 and promoted the closed state of the channel [10]. In cardiomyocytes, this specifically increased  $\text{Ca}^{2+}$  transfer from the SR into mitochondria and, thereby, spatially and temporally restricted diastolic  $\text{Ca}^{2+}$  sparks and prevented the formation of arrhythmogenic  $\text{Ca}^{2+}$  waves [9]. Most importantly, efsevin significantly reduced ventricular tachycardia in mice.

Additionally, for neurodegenerative diseases disruption of functional ER–mitochondrial  $\text{Ca}^{2+}$  homeostasis was shown to be associated with diseases such as Parkinson’s disease (PD), Alzheimer’s disease (AD), and amyotrophic lateral sclerosis (ALS) [121]. One protein that has been associated with the early-onset of PD is DJ-1, which was recently shown to interact with the IP3R-Grp75-VDAC1 complex [78,122]. DJ-1 reduction functionally correlates with decreased mitochondrial  $\text{Ca}^{2+}$  uptake and cells expressing PD-associated DJ-1 mutants showed impaired mitochondrial function [78,123]. A recent study has further demonstrated that functional ER–mitochondria interactions are of great importance for axon regeneration after injury. The results suggest that increased Grp75 expression enhances ER–mitochondria tethering, which leads to an increase in mitochondrial  $\text{Ca}^{2+}$  uptake that seems to be beneficial for axon regeneration [124].

## 5. Conclusions

Taken together, the compiled data indicate that VDAC-mediated mitochondrial  $\text{Ca}^{2+}$  uptake, in particular, though its close interaction with the ER/SR calcium release sites, is an important modulator of physiology and pathophysiology of the cell. However, discrepancies exist between results obtained from lipid bilayer experiments and experiments performed in cells, in particular concerning the flux of  $\text{Ca}^{2+}$  upon channel closure, indicating that in the native environment other or additional levels of VDAC regulation exist and lipid bilayer experiments should not be overinterpreted. VDAC-mediated mitochondrial  $\text{Ca}^{2+}$  uptake represents a critical component to decipher cellular  $\text{Ca}^{2+}$  signals and to mediate either enhanced energy production or induction of apoptosis but also to fine-tune intracellular  $\text{Ca}^{2+}$  signals. Additionally, at least in cardiomyocytes, it further shapes cytosolic  $\text{Ca}^{2+}$  signals and acts as a buffer to blunt cytosolic  $\text{Ca}^{2+}$  spikes. VDAC-mediated  $\text{Ca}^{2+}$  uptake is regulated at different levels, ranging from expression to protein partners as well as intrinsic properties of VDAC, which can adapt multiple states of conductance. However, the specific molecular mechanisms leading to these different conductance states have not been fully resolved and care should be taken when using the term “channel closure”, since voltage-induced closure, as well as occlusion, prevents the flux of metabolites but increases  $\text{Ca}^{2+}$  flux. Future studies are needed to resolve open questions such as the role of voltage gating in vivo the relevance of VDAC gating cellular physiology and the selective contribution of the regulation of mitochondrial  $\text{Ca}^{2+}$  uptake at the OMM and IMM, respectively.

**Author Contributions:** P.S. and J.S. performed literature review and wrote the manuscript. T.G. and J.S. provided resources and funding. All authors revised and edited the manuscript. All authors have read and agreed to the published version of the manuscript.

**Funding:** This research was in part funded by the German Research Foundation (DFG), grant number SCHR 1471/1-1 to J.S.

**Acknowledgments:** The authors thank Annette Nicke and Simon Huber for critical comments on the manuscripts.

**Conflicts of Interest:** The authors declare no conflict of interest.



## References

1. Slater, E.C.; Cleland, K.W. The calcium content of isolated heart-muscle sarcosomes. *Biochem. J.* **1953**, *54*, xxii. [[PubMed](#)]
2. DeLuca, H.F.; Engstrom, G.W. Calcium uptake by rat kidney mitochondria. *Proc. Natl. Acad. Sci. USA* **1961**, *47*, 1744–1750. [[CrossRef](#)] [[PubMed](#)]
3. Gincel, D.; Zaid, H.; Shoshan-Barmatz, V. Calcium binding and translocation by the voltage-dependent anion channel: A possible regulatory mechanism in mitochondrial function. *Biochem. J.* **2001**, *358*, 147–155. [[CrossRef](#)] [[PubMed](#)]
4. Rapizzi, E.; Pinton, P.; Szabadkai, G.; Wieckowski, M.R.; Vandecasteele, G.; Baird, G.; Tuft, R.A.; Fogarty, K.E.; Rizzuto, R. Recombinant expression of the voltage-dependent anion channel enhances the transfer of  $Ca^{2+}$  microdomains to mitochondria. *J. Cell Biol.* **2002**, *159*, 613–624. [[CrossRef](#)] [[PubMed](#)]
5. De Stefani, D.; Bononi, A.; Romagnoli, A.; Messina, A.; De Pinto, V.; Pinton, P.; Rizzuto, R. VDAC1 selectively transfers apoptotic  $Ca^{2+}$  signals to mitochondria. *Cell Death Differ.* **2012**, *19*, 267–273. [[CrossRef](#)] [[PubMed](#)]
6. Azoulay-Zohar, H.; Israelson, A.; Abu-Hamad, S.; Shoshan-Barmatz, V. In self-defence: Hexokinase promotes voltage-dependent anion channel closure and prevents mitochondria-mediated apoptotic cell death. *Biochem. J.* **2004**, *377*, 347–355. [[CrossRef](#)]
7. Ham, S.J.; Lee, D.; Yoo, H.; Jun, K.; Shin, H.; Chung, J. Decision between mitophagy and apoptosis by Parkin via VDAC1 ubiquitination. *Proc. Natl. Acad. Sci. USA* **2020**, *117*, 4281–4291. [[CrossRef](#)]
8. Zheng, P.; Chen, Q.; Tian, X.; Qian, N.; Chai, P.; Liu, B.; Hu, J.; Blackstone, C.; Zhu, D.; Teng, J.; et al. DNA damage triggers tubular endoplasmic reticulum extension to promote apoptosis by facilitating ER-mitochondria signaling. *Cell Res.* **2018**, *28*, 833–854. [[CrossRef](#)]
9. Schweitzer, M.K.; Wilting, F.; Sedej, S.; Dreizehnter, L.; Dupper, N.J.; Tian, Q.; Moretti, A.; My, I.; Kwon, O.; Priori, S.G.; et al. Suppression of Arrhythmia by Enhancing Mitochondrial  $Ca^{2+}$  Uptake in Catecholaminergic Ventricular Tachycardia Models. *JACC Basic Transl. Sci.* **2017**, *2*, 737–746. [[CrossRef](#)]
10. Wilting, F.; Kopp, R.; Gurnev, P.A.; Schedel, A.; Dupper, N.J.; Kwon, O.; Nicke, A.; Gudermann, T.; Schredelseker, J. The antiarrhythmic compound efsevin directly modulates voltage-dependent anion channel 2 by binding to its inner wall and enhancing mitochondrial  $Ca^{2+}$  uptake. *Br. J. Pharmacol.* **2020**, *177*, 2947–2958. [[CrossRef](#)]
11. Ujwal, R.; Cascio, D.; Colletier, J.-P.; Faham, S.; Zhang, J.; Toro, L.; Ping, P.; Abramson, J. The crystal structure of mouse VDAC1 at 2.3 Å resolution reveals mechanistic insights into metabolite gating. *Proc. Natl. Acad. Sci. USA* **2008**, *105*, 17742–17747. [[CrossRef](#)] [[PubMed](#)]
12. Schredelseker, J.; Paz, A.; López, C.J.; Altenbach, C.; Leung, C.S.; Drexler, M.K.; Chen, J.-N.; Hubbell, W.L.; Abramson, J. High-Resolution Structure and Double Electron-Electron Resonance of the Zebrafish Voltage Dependent Anion Channel 2 Reveal an Oligomeric Population. *J. Biol. Chem.* **2014**, *289*, 12566–12577. [[CrossRef](#)] [[PubMed](#)]
13. Srivastava, S.R.; Mahalakshmi, R. Evolutionary selection of a 19-stranded mitochondrial  $\beta$ -barrel scaffold bears structural and functional significance. *J. Biol. Chem.* **2020**, *295*, 14653–14665. [[CrossRef](#)] [[PubMed](#)]
14. Choudhary, O.P.; Paz, A.; Adelman, J.; Colletier, J.-P.; Abramson, J.; Grabe, M. Characterizing ATP Permeation through the Voltage-Dependent Anion Channel VDAC. *Biophys. J.* **2014**, *106*, 147a–148a. [[CrossRef](#)]
15. Colombini, M. Voltage gating in the mitochondrial channel, VDAC. *J. Membr. Biol.* **1989**, *111*, 103–111. [[CrossRef](#)]
16. Menzel, V.A.; Cassarà, M.C.; Benz, R.; De Pinto, V.; Messina, A.; Cunsolo, V.; Saletti, R.; Hinsch, K.; Hinsch, E. Molecular and functional characterization of VDAC2 purified from mammal spermatozoa. *Biosci. Rep.* **2009**, *29*, 351–362. [[CrossRef](#)]
17. Mertins, B.; Psakias, G.; Grosse, W.; Back, K.C.; Salisowski, A.; Reiss, P.; Koert, U.; Essen, L.-O. Flexibility of the N-Terminal mVDAC1 Segment Controls the Channel's Gating Behavior. *PLoS ONE* **2012**, *7*, e47938. [[CrossRef](#)]
18. Guardiani, C.; Magri, A.; Karachitos, A.; Di Rosa, M.C.; Reina, S.; Bodrenko, I.; Messina, A.; Kmita, H.; Ceccarelli, M.; De Pinto, V.  $\gamma$ VDAC2, the second mitochondrial porin isoform of *Saccharomyces cerevisiae*. *Biochim. Biophys. Acta Bioenerg.* **2018**, *1859*, 270–279. [[CrossRef](#)]
19. Tan, W.; Colombini, M. VDAC closure increases calcium ion flux. *Biochim. Biophys. Acta* **2007**, *1768*, 2510–2515. [[CrossRef](#)]
20. Zachariae, U.; Schneider, R.; Briones, R.; Gattin, Z.; Demers, J.-P.; Giller, K.; Maier, E.; Zweckstetter, M.; Griesinger, C.; Becker, S.; et al.  $\beta$ -Barrel Mobility Underlies Closure of the Voltage-Dependent Anion Channel. *Structure* **2012**, *20*, 1540–1549. [[CrossRef](#)]
21. Pavlov, E.; Grigoriev, S.M.; Dejean, L.M.; Zweihorn, C.L.; Mannella, C.A.; Kinnally, K.W. The mitochondrial channel VDAC has a cation-selective open state. *Biochim. Biophys. Acta Bioenerg.* **2005**, *1710*, 96–102. [[CrossRef](#)] [[PubMed](#)]
22. Checchetto, V.; Reina, S.; Magri, A.; Szabo, I.; De Pinto, V. Recombinant human voltage dependent anion selective channel isoform 3 (hVDAC3) forms pores with a very small conductance. *Cell. Physiol. Biochem.* **2014**, *34*, 842–853. [[CrossRef](#)] [[PubMed](#)]
23. Queral-Martín, M.; Bergdoll, L.; Teijido, O.; Munshi, N.; Jacobs, D.; Kuszak, A.J.; Protchenko, O.; Reina, S.; Magri, A.; De Pinto, V.; et al. A lower affinity to cytosolic proteins reveals VDAC3 isoform-specific role in mitochondrial biology. *J. Gen. Physiol.* **2020**, *152*. [[CrossRef](#)]
24. Lemeshko, V.V. Model of the Outer Membrane Potential Generation by the Inner Membrane of Mitochondria. *Biophys. J.* **2002**, *82*, 684–692. [[CrossRef](#)]
25. Adams, V.; Bosch, W.; Schlegel, J.; Wallimann, T.; Bridczka, D. Further characterization of contact sites from mitochondria of different tissues: Topology of peripheral kinases. *Biochim. Biophys. Acta Biomembr.* **1989**, *981*, 213–225. [[CrossRef](#)]
26. Porcelli, A.M.; Ghelli, A.; Zanna, C.; Pinton, P.; Rizzuto, R.; Rugolo, M. pH difference across the outer mitochondrial membrane measured with a green fluorescent protein mutant. *Biochem. Biophys. Res. Commun.* **2005**, *326*, 799–804. [[CrossRef](#)]

27. Báthori, G.; Csordás, G.; Garcia-Perez, C.; Davies, E.; Hajnóczky, G.  $\text{Ca}^{2+}$ -dependent control of the permeability properties of the mitochondrial outer membrane and voltage-dependent anion-selective channel (VDAC). *J. Biol. Chem.* **2006**, *281*, 17347–17358. [[CrossRef](#)]
28. Lee, A.C.; Xu, X.; Colombini, M. The role of pyridine dinucleotides in regulating the permeability of the mitochondrial outer membrane. *J. Biol. Chem.* **1996**, *271*, 26724–26731. [[CrossRef](#)]
29. Rostovtseva, T.K.; Kazemi, N.; Weinrich, M.; Bezrukov, S.M. Voltage gating of VDAC is regulated by nonlamellar lipids of mitochondrial membranes. *J. Biol. Chem.* **2006**, *281*. [[CrossRef](#)]
30. Van Liefferinge, F.; Krammer, E.-M.; Sengupta, D.; Prévost, M. Lipid composition and salt concentration as regulatory factors of the anion selectivity of VDAC studied by coarse-grained molecular dynamics simulations. *Chem. Phys. Lipids* **2019**, *220*, 66–76. [[CrossRef](#)]
31. Budelier, M.M.; Cheng, W.W.L.; Bergdoll, L.; Chen, Z.-W.; Janetka, J.W.; Abramson, J.; Krishnan, K.; Mydock-McGrane, L.; Covey, D.F.; Whitelegge, J.P.; et al. Photoaffinity labeling with cholesterol analogues precisely maps a cholesterol-binding site in voltage-dependent anion channel-1. *J. Biol. Chem.* **2017**, *292*, 9294–9304. [[CrossRef](#)] [[PubMed](#)]
32. Briones, R.; Weichbrodt, C.; Paltrinieri, L.; Mey, I.; Villinger, S.; Giller, K.; Lange, A.; Zweckstetter, M.; Griesinger, C.; Becker, S.; et al. Voltage Dependence of Conformational Dynamics and Subconducting States of VDAC-1. *Biophys. J.* **2016**, *111*, 1223–1234. [[CrossRef](#)] [[PubMed](#)]
33. Queralto-Martín, M.; Hoogerheide, D.P.; Noskov, S.Y.; Berezhkovskii, A.M.; Rostovtseva, T.K.; Bezrukov, S.M. VDAC gating thermodynamics, but not gating kinetics, are virtually temperature-independent. *Biophys. J.* **2020**, *119*, 2584–2592. [[CrossRef](#)] [[PubMed](#)]
34. Tewari, D.; Ahmed, T.; Chirasani, V.R.; Singh, P.K.; Maji, S.K.; Senapati, S.; Bera, A.K. Modulation of the mitochondrial voltage dependent anion channel (VDAC) by curcumin. *Biochim. Biophys. Acta* **2015**, *1848*, 151–158. [[CrossRef](#)] [[PubMed](#)]
35. Tewari, D.; Majumdar, D.; Vallabhaneni, S.; Bera, A.K. Aspirin induces cell death by directly modulating mitochondrial voltage-dependent anion channel (VDAC). *Sci. Rep.* **2017**, *7*, 45184. [[CrossRef](#)]
36. Huang, H.; Hu, X.; Eno, C.O.; Zhao, G.; Li, C.; White, C. An interaction between Bcl-xL and the voltage-dependent anion channel (VDAC) promotes mitochondrial  $\text{Ca}^{2+}$  uptake. *J. Biol. Chem.* **2013**, *288*, 19870–19881. [[CrossRef](#)]
37. Tarze, A.; Deniaud, A.; Le Bras, M.; Maillier, E.; Molle, D.; Laroche, N.; Zamzami, N.; Jan, G.; Kroemer, G.; Brenner, C. GAPDH, a novel regulator of the pro-apoptotic mitochondrial membrane permeabilization. *Oncogene* **2007**, *26*, 2606–2620. [[CrossRef](#)]
38. Okazaki, M.; Kurabayashi, K.; Asanuma, M.; Saito, Y.; Dodo, K.; Sodeoka, M. VDAC3 gating is activated by suppression of disulfide-bond formation between the N-terminal region and the bottom of the pore. *Biochim. Biophys. Acta Biomembr.* **2015**, *1848*, 3188–3196. [[CrossRef](#)]
39. Maurya, S.R.; Mahalakshmi, R. N-helix and Cysteines Inter-regulate Human Mitochondrial VDAC-2 Function and Biochemistry. *J. Biol. Chem.* **2015**, *290*, 30240–30250. [[CrossRef](#)]
40. Shuvo, S.R.; Ferens, F.G.; Court, D.A. The N-terminus of VDAC: Structure, mutational analysis, and a potential role in regulating barrel shape. *Biochim. Biophys. Acta Biomembr.* **2016**, *1858*, 1350–1361. [[CrossRef](#)]
41. Choudhary, O.P.; Ujwal, R.; Kowallis, W.; Coalson, R.; Abramson, J.; Grabe, M. The Electrostatics of VDAC: Implications for Selectivity and Gating. *J. Mol. Biol.* **2010**, *396*, 580–592. [[CrossRef](#)] [[PubMed](#)]
42. Tejjido, O.; Ujwal, R.; Hillerdal, C.-O.; Kullman, L.; Rostovtseva, T.K.; Abramson, J. Affixing N-terminal  $\alpha$ -helix to the wall of the voltage-dependent anion channel does not prevent its voltage gating. *J. Biol. Chem.* **2012**, *287*, 11437–11445. [[CrossRef](#)] [[PubMed](#)]
43. Zizi, M.; Forte, M.; Blachly-Dyson, E.; Colombini, M. NADH regulates the gating of VDAC, the mitochondrial outer membrane channel. *J. Biol. Chem.* **1994**, *269*, 1614–1616. [[CrossRef](#)]
44. Böhm, R.; Amodeo, G.F.; Murlidaran, S.; Chavali, S.; Wagner, G.; Winterhalter, M.; Brannigan, G.; Hiller, S. The Structural Basis for Low Conductance in the Membrane Protein VDAC upon  $\beta$ -NADH Binding and Voltage Gating. *Structure* **2020**, *28*, 206–214.e4. [[CrossRef](#)]
45. Rostovtseva, T.K.; Gurnev, P.A.; Hoogerheide, D.P.; Rovini, A.; Sirajuddin, M.; Bezrukov, S.M. Sequence diversity of tubulin isoforms in regulation of the mitochondrial voltage-dependent anion channel. *J. Biol. Chem.* **2018**, *293*, 10949–10962. [[CrossRef](#)]
46. Puurand, M.; Tepp, K.; Timohhina, N.; Aid, J.; Shevchuk, I.; Chekulayev, V.; Kaambre, T. Tubulin  $\beta$ II and  $\beta$ III Isoforms as the Regulators of VDAC Channel Permeability in Health and Disease. *Cells* **2019**, *8*, 239. [[CrossRef](#)]
47. Rostovtseva, T.K.; Sheldon, K.L.; Hassanzadeh, E.; Monge, C.; Saks, V.; Bezrukov, S.M.; Sackett, D.L. Tubulin binding blocks mitochondrial voltage-dependent anion channel and regulates respiration. *Proc. Natl. Acad. Sci. USA* **2008**, *105*, 18746–18751. [[CrossRef](#)]
48. Hoogerheide, D.P.; Gurnev, P.A.; Rostovtseva, T.K.; Bezrukov, S.M. Mechanism of  $\alpha$ -synuclein translocation through a VDAC nanopore revealed by energy landscape modeling of escape time distributions. *Nanoscale* **2017**, *9*, 183–192. [[CrossRef](#)]
49. Gurnev, P.A.; Rostovtseva, T.K.; Bezrukov, S.M. Tubulin-blocked state of VDAC studied by polymer and ATP partitioning. *FEBS Lett.* **2011**, *585*, 2363–2366. [[CrossRef](#)]
50. Simson, P.; Jepihina, N.; Laasmaa, M.; Peterson, P.; Birkedal, R.; Vendelin, M. Restricted ADP movement in cardiomyocytes: Cytosolic diffusion obstacles are complemented with a small number of open mitochondrial voltage-dependent anion channels. *J. Mol. Cell. Cardiol.* **2016**, *97*, 197–203. [[CrossRef](#)]
51. Lemeshko, V.V. VDAC electronics: 1. VDAC-hexo(glucokinase) generator of the mitochondrial outer membrane potential. *Biochim. Biophys. Acta Biomembr.* **2014**, *1838*, 1362–1371. [[CrossRef](#)] [[PubMed](#)]

52. Lemeshko, V.V. VDAC electronics: 5. Mechanism and computational model of hexokinase-dependent generation of the outer membrane potential in brain mitochondria. *Biochim. Biophys. Acta Biomembr.* **2018**, *1860*, 2599–2607. [[CrossRef](#)]
53. Lemeshko, V.V. Electrical control of the cell energy metabolism at the level of mitochondrial outer membrane. *Biochim. Biophys. Acta Biomembr.* **2021**, *1863*, 183493. [[CrossRef](#)] [[PubMed](#)]
54. García-Pérez, C.; Schneider, T.G.; Hajnóczky, G.; Csordás, G. Alignment of sarcoplasmic reticulum-mitochondrial junctions with mitochondrial contact points. *Am. J. Physiol. Heart Circ. Physiol.* **2011**, *301*, H1907-15. [[CrossRef](#)] [[PubMed](#)]
55. Liao, Y.; Hao, Y.; Chen, H.; He, Q.; Yuan, Z.; Cheng, J. Mitochondrial calcium uniporter protein MCU is involved in oxidative stress-induced cell death. *Protein Cell* **2015**, *6*, 434–442. [[CrossRef](#)] [[PubMed](#)]
56. Israelson, A.; Abu-Hamad, S.; Zaid, H.; Nahon, E.; Shoshan-Barmatz, V. Localization of the voltage-dependent anion channel-1 Ca<sup>2+</sup>-binding sites. *Cell Calcium* **2007**, *41*, 235–244. [[CrossRef](#)] [[PubMed](#)]
57. Ge, L.; Villinger, S.; Mari, S.A.; Giller, K.; Griesinger, C.; Becker, S.; Müller, D.J.; Zweckstetter, M. Molecular Plasticity of the Human Voltage-Dependent Anion Channel Embedded Into a Membrane. *Structure* **2016**, *24*, 585–594. [[CrossRef](#)]
58. Villinger, S.; Briones, R.; Giller, K.; Zachariae, U.; Lange, A.; de Groot, B.L.; Griesinger, C.; Becker, S.; Zweckstetter, M. Functional dynamics in the voltage-dependent anion channel. *Proc. Natl. Acad. Sci. USA* **2010**, *107*, 22546–22551. [[CrossRef](#)]
59. Peng, W.; Wong, Y.C.; Krainc, D. Mitochondria-lysosome contacts regulate mitochondrial Ca<sup>2+</sup> dynamics via lysosomal TRPML1. *Proc. Natl. Acad. Sci. USA* **2020**, *117*, 19266–19275. [[CrossRef](#)]
60. Schredelseker, J.; Shimizu, H.; Huang, J.; Lin, B.; Chen, J.-N. Regulation of Voltage-Dependent Anion Channel 2 at Glutamate 73 is Critical for its Role in Cardiac Calcium Handling. *Biophys. J.* **2012**, *102*, 312a. [[CrossRef](#)]
61. Bera, A.K.; Ghosh, S. Dual mode of gating of voltage-dependent anion channel as revealed by phosphorylation. *J. Struct. Biol.* **2001**, *135*, 67–72. [[CrossRef](#)]
62. Banerjee, J.; Ghosh, S. Phosphorylation of rat brain mitochondrial voltage-dependent anion as a potential tool to control leakage of cytochrome c. *J. Neurochem.* **2006**, *98*, 670–676. [[CrossRef](#)]
63. Gupta, R.; Ghosh, S. Phosphorylation of purified mitochondrial Voltage-Dependent Anion Channel by c-Jun N-terminal Kinase-3 modifies channel voltage-dependence. *Biochim. Open* **2017**, *4*, 78–87. [[CrossRef](#)]
64. Gatliff, J.; East, D.A.; Singh, A.; Alvarez, M.S.; Frison, M.; Matic, I.; Ferraina, C.; Sampson, N.; Turkheimer, F.; Campanella, M. A role for TSPO in mitochondrial Ca<sup>2+</sup> homeostasis and redox stress signaling. *Cell Death Dis.* **2017**, *8*, e2896. [[CrossRef](#)]
65. Baines, C.P.; Song, C.-X.; Zheng, Y.-T.; Wang, G.-W.; Zhang, J.; Wang, O.-L.; Guo, Y.; Bolli, R.; Cardwell, E.M.; Ping, P. Protein kinase Cepsilon interacts with and inhibits the permeability transition pore in cardiac mitochondria. *Circ. Res.* **2003**, *92*, 873–880. [[CrossRef](#)] [[PubMed](#)]
66. Sheldon, K.L.; Maldonado, E.N.; Lemasters, J.J.; Rostovtseva, T.K.; Bezrukov, S.M. Phosphorylation of Voltage-Dependent Anion Channel by Serine/Threonine Kinases Governs Its Interaction with Tubulin. *PLoS ONE* **2011**, *6*, e25539. [[CrossRef](#)] [[PubMed](#)]
67. Rovini, A.; Gurnev, P.A.; Beilina, A.; Queralt-Martín, M.; Rosencrans, W.; Cookson, M.R.; Bezrukov, S.M.; Rostovtseva, T.K. Molecular mechanism of olesoxime-mediated neuroprotection through targeting  $\alpha$ -synuclein interaction with mitochondrial VDAC. *Cell. Mol. Life Sci.* **2020**, *77*, 3611–3626. [[CrossRef](#)] [[PubMed](#)]
68. Crimi, M.; Esposito, M.D. Apoptosis-induced changes in mitochondrial lipids. *Biochim. Biophys. Acta* **2011**, *1813*, 551–557. [[CrossRef](#)]
69. Arbel, N.; Shoshan-Barmatz, V. Voltage-dependent Anion Channel 1-based Peptides Interact with Bcl-2 to Prevent Antiapoptotic Activity. *J. Biol. Chem.* **2010**, *285*, 6053–6062. [[CrossRef](#)] [[PubMed](#)]
70. Huang, H.; Shah, K.; Bradbury, N.A.; Li, C.; White, C. Mcl-1 promotes lung cancer cell migration by directly interacting with VDAC to increase mitochondrial Ca<sup>2+</sup> uptake and reactive oxygen species generation. *Cell Death Dis.* **2014**, *5*, e1482. [[CrossRef](#)]
71. Monaco, G.; Decrock, E.; Arbel, N.; van Vliet, A.R.; La Rovere, R.M.; De Smedt, H.; Parys, J.B.; Agostinis, P.; Leybaert, L.; Shoshan-Barmatz, V.; et al. The BH4 domain of anti-apoptotic Bcl-XL, but not that of the related Bcl-2, limits the voltage-dependent anion channel 1 (VDAC1)-mediated transfer of pro-apoptotic Ca<sup>2+</sup> signals to mitochondria. *J. Biol. Chem.* **2015**, *290*, 9150–9161. [[CrossRef](#)] [[PubMed](#)]
72. Tornero, D.; Posadas, I.; Ceña, V. Bcl-xL Blocks a Mitochondrial Inner Membrane Channel and Prevents Ca<sup>2+</sup> Overload-Mediated Cell Death. *PLoS ONE* **2011**, *6*, e20423. [[CrossRef](#)] [[PubMed](#)]
73. Arbel, N.; Ben-Hail, D.; Shoshan-Barmatz, V. Mediation of the antiapoptotic activity of Bcl-xL protein upon interaction with VDAC1 protein. *J. Biol. Chem.* **2012**, *287*, 23152–23161. [[CrossRef](#)]
74. Tamse, C.; Lu, X.; Mortel, E.; Cabrales, E.; Feng, W.; Schaefer, S. The Peripheral Benzodiazepine Receptor Modulates Ca<sup>2+</sup> Transport through the VDAC in Rat Heart Mitochondria. *J. Clin. Basic Cardiol.* **2008**, *11*, 24–29.
75. Hein, M.Y.; Hubner, N.C.; Poser, I.; Cox, J.; Nagaraj, N.; Toyoda, Y.; Gak, I.A.; Weisswange, I.; Mansfeld, J.; Buchholz, F.; et al. A Human Interactome in Three Quantitative Dimensions Organized by Stoichiometries and Abundances. *Cell* **2015**, *163*, 712–723. [[CrossRef](#)]
76. Viola, H.M.; Adams, A.M.; Davies, S.M.K.; Fletcher, S.; Filipovska, A.; Hool, L.C. Impaired functional communication between the L-type calcium channel and mitochondria contributes to metabolic inhibition in the mdx heart. *Proc. Natl. Acad. Sci. USA* **2014**, *111*, E2905–E2914. [[CrossRef](#)]
77. Min, C.K.; Yeom, D.R.; Lee, K.-E.; Kwon, H.-K.; Kang, M.; Kim, Y.-S.; Park, Z.Y.; Jeon, H.; Kim, D.H. Coupling of ryanodine receptor 2 and voltage-dependent anion channel 2 is essential for Ca<sup>2+</sup> transfer from the sarcoplasmic reticulum to the mitochondria in the heart. *Biochem. J.* **2012**, *447*, 371–379. [[CrossRef](#)] [[PubMed](#)]

78. Liu, Y.; Ma, X.; Fujioka, H.; Liu, J.; Chen, S.; Zhu, X. DJ-1 regulates the integrity and function of ER-mitochondria association through interaction with IP3R3-Grp75-VDAC1. *Proc. Natl. Acad. Sci. USA* **2019**, *116*, 25322–25328. [[CrossRef](#)]
79. D'Eletto, M.; Rossin, F.; Occhigrossi, L.; Farrace, M.G.; Faccenda, D.; Desai, R.; Marchi, S.; Refolo, G.; Falasca, L.; Antonioli, M.; et al. Transglutaminase Type 2 Regulates ER-Mitochondria Contact Sites by Interacting with GRP75. *Cell Rep.* **2018**, *25*, 3573–3581.e4. [[CrossRef](#)] [[PubMed](#)]
80. Israelson, A.; Arbel, N.; Da Cruz, S.; Ilieva, H.; Yamanaka, K.; Shoshan-Barmatz, V.; Cleveland, D.W. Misfolded Mutant SOD1 Directly Inhibits VDAC1 Conductance in a Mouse Model of Inherited ALS. *Neuron* **2010**, *67*, 575–587. [[CrossRef](#)] [[PubMed](#)]
81. Rizzuto, R.; Pinton, P.; Carrington, W.; Fay, F.S.; Fogarty, K.E.; Lifshitz, L.M.; Tuft, R.A.; Pozzan, T. Close contacts with the endoplasmic reticulum as determinants of mitochondrial Ca<sup>2+</sup> responses. *Science* **1998**, *280*, 1763–1766. [[CrossRef](#)] [[PubMed](#)]
82. Csordás, G.; Renken, C.; Várnai, P.; Walter, L.; Weaver, D.; Buttler, K.F.; Balla, T.; Mannella, C.A.; Hajnóczky, G. Structural and functional features and significance of the physical linkage between ER and mitochondria. *J. Cell Biol.* **2006**, *174*, 915. [[CrossRef](#)] [[PubMed](#)]
83. Sharma, V.K.; Ramesh, V.; Franzini-Armstrong, C.; Sheu, S.-S. Transport of Ca<sup>2+</sup> from Sarcoplasmic Reticulum to Mitochondria in Rat Ventricular Myocytes. *J. Bioenerg. Biomembr.* **2000**, *32*, 97–104. [[CrossRef](#)] [[PubMed](#)]
84. Brdiczka, D.G.; Zorov, D.B. Mitochondrial contact sites: Their role in energy metabolism and apoptosis. *Biochim. Biophys. Acta Mol. Basis Dis.* **2006**, *1762*, 148–163. [[CrossRef](#)] [[PubMed](#)]
85. Szabadkai, G.; Bianchi, K.; Várnai, P.; De Stefani, D.; Wieckowski, M.R.; Cavagna, D.; Nagy, A.I.; Balla, T.; Rizzuto, R. Chaperone-mediated coupling of endoplasmic reticulum and mitochondrial Ca<sup>2+</sup> channels. *J. Cell Biol.* **2006**, *175*, 901–911. [[CrossRef](#)] [[PubMed](#)]
86. Xu, H.; Guan, N.; Ren, Y.-L.; Wei, Q.-J.; Tao, Y.-H.; Yang, G.-S.; Liu, X.-Y.; Bu, D.-F.; Zhang, Y.; Zhu, S.-N. IP3R-Grp75-VDAC1-MCU calcium regulation axis antagonists protect podocytes from apoptosis and decrease proteinuria in an Adriamycin nephropathy rat model. *BMC Nephrol.* **2018**, *19*, 140. [[CrossRef](#)] [[PubMed](#)]
87. Santin, Y.; Fazal, L.; Sainte-Marie, Y.; Sicard, P.; Maggiorani, D.; Tortosa, F.; Yücel, Y.Y.; Teyssedre, L.; Rouquette, J.; Marcellin, M.; et al. Mitochondrial 4-HNE derived from MAO-A promotes mitoCa<sup>2+</sup> overload in chronic postischemic cardiac remodeling. *Cell Death Differ.* **2020**, *27*, 1907–1923. [[CrossRef](#)]
88. Caterino, M.; Ruoppolo, M.; Mandola, A.; Costanzo, M.; Orrù, S.; Imperlini, E. Protein-protein interaction networks as a new perspective to evaluate distinct functional roles of voltage-dependent anion channel isoforms. *Mol. Biosyst.* **2017**, *13*, 2466–2476. [[CrossRef](#)]
89. Anflous, K.; Armstrong, D.D.; Craigen, W.J. Altered mitochondrial sensitivity for ADP and maintenance of creatine-stimulated respiration in oxidative striated muscles from VDAC1-deficient mice. *J. Biol. Chem.* **2001**, *276*, 1954–1960. [[CrossRef](#)]
90. Raghavan, A.; Sheiko, T.V.; Graham, B.H.; Craigen, W.J. Voltage-dependant anion channels: Novel insights into isoform function through genetic models. *Biochim. Biophys. Acta Biomembr.* **2012**, *1818*, 1477–1485. [[CrossRef](#)]
91. Amodeo, G.F.; Scorciapino, M.A.; Messina, A.; De Pinto, V.; Ceccarelli, M. Charged Residues Distribution Modulates Selectivity of the Open State of Human Isoforms of the Voltage Dependent Anion-Selective Channel. *PLoS ONE* **2014**, *9*, e103879. [[CrossRef](#)] [[PubMed](#)]
92. Cheng, E.H.Y.; Sheiko, T.V.; Fisher, J.K.; Craigen, W.J.; Korsmeyer, S.J. VDAC2 inhibits BAK activation and mitochondrial apoptosis. *Science* **2003**, *301*, 513–517. [[CrossRef](#)] [[PubMed](#)]
93. Abu-Hamad, S.; Sivan, S.; Shoshan-Barmatz, V. The expression level of the voltage-dependent anion channel controls life and death of the cell. *Proc. Natl. Acad. Sci. USA* **2006**, *103*, 5787–5792. [[CrossRef](#)]
94. Sasaki, K.; Donthamsetty, R.; Heldak, M.; Cho, Y.-E.; Scott, B.T.; Makino, A. VDAC: Old protein with new roles in diabetes. *Am. J. Physiol. Physiol.* **2012**, *303*, C1055–C1060. [[CrossRef](#)] [[PubMed](#)]
95. Feng, Y.; Madungwe, N.B.; Imam Aliagan, A.D.; Tombo, N.; Bopassa, J.-C. Liproxstatin-1 protects the mouse myocardium against ischemia/reperfusion injury by decreasing VDAC1 levels and restoring GPX4 levels. *Biochem. Biophys. Res. Commun.* **2019**, *520*. [[CrossRef](#)]
96. Yuan, J.; Zhang, Y.; Sheng, Y.; Fu, X.; Cheng, H.; Zhou, R. MYBL2 guides autophagy suppressor VDAC2 in the developing ovary to inhibit autophagy through a complex of VDAC2-BECN1-BCL2L1 in mammals. *Autophagy* **2015**, *11*, 1081–1098. [[CrossRef](#)]
97. Weisthal, S.; Keinan, N.; Ben-Hail, D.; Arif, T.; Shoshan-Barmatz, V. Ca<sup>2+</sup>-mediated regulation of VDAC1 expression levels is associated with cell death induction. *Biochim. Biophys. Acta Mol. Cell Res.* **2014**, *1843*, 2270–2281. [[CrossRef](#)]
98. Allouche, M.; Pertuiset, C.; Robert, J.L.; Martel, C.; Veneziano, R.; Henry, C.; el dein, O.S.; Saint, N.; Brenner, C.; Chopineau, J. ANT-VDAC1 interaction is direct and depends on ANT isoform conformation in vitro. *Biochem. Biophys. Res. Commun.* **2012**, *429*, 12–17. [[CrossRef](#)]
99. Zaid, H.; Abu-Hamad, S.; Israelson, A.; Nathan, I.; Shoshan-Barmatz, V. The voltage-dependent anion channel-1 modulates apoptotic cell death. *Cell Death Differ.* **2005**, *12*, 751–760. [[CrossRef](#)]
100. Bobba, A.; Amadoro, G.; La Piana, G.; Petragallo, V.A.; Calissano, P.; Atlante, A. Glucose-6-phosphate tips the balance in modulating apoptosis in cerebellar granule cells. *FEBS Lett.* **2015**, *589*, 651–658. [[CrossRef](#)]
101. Dubey, A.K.; Godbole, A.; Mathew, M.K. Regulation of VDAC trafficking modulates cell death. *Cell Death Discov.* **2016**, *2*, 16085. [[CrossRef](#)] [[PubMed](#)]

102. Cárdenas, C.; Müller, M.; McNeal, A.; Lovy, A.; Jaña, F.; Bustos, G.; Urrea, F.; Smith, N.; Molgó, J.; Diehl, J.A.; et al. Selective Vulnerability of Cancer Cells by Inhibition of  $\text{Ca}^{2+}$  Transfer from Endoplasmic Reticulum to Mitochondria. *Cell Rep.* **2016**, *14*, 2313–2324. [[CrossRef](#)] [[PubMed](#)]
103. Ge, Y.; Yan, D.; Deng, H.; Chen, W.; An, G. Novel Molecular Regulators of Tumor Necrosis Factor-Related Apoptosis-Inducing Ligand (TRAIL)-Induced Apoptosis in NSCLC Cells. *Clin. Lab.* **2015**, *61*. [[CrossRef](#)] [[PubMed](#)]
104. Simamura, E.; Shimada, H.; Ishigaki, Y.; Hatta, T.; Higashi, N.; Hirai, K.-I. Bioreductive activation of quinone antitumor drugs by mitochondrial voltage-dependent anion channel 1. *Anat. Sci. Int.* **2008**, *83*, 261–266. [[CrossRef](#)]
105. Grills, C.; Jithesh, P.V.; Blayney, J.; Zhang, S.-D.; Fennell, D.A. Gene Expression Meta-Analysis Identifies VDAC1 as a Predictor of Poor Outcome in Early Stage Non-Small Cell Lung Cancer. *PLoS ONE* **2011**, *6*, e14635. [[CrossRef](#)]
106. Rimessi, A.; Patergnani, S.; Bonora, M.; Wieckowski, M.R.; Pinton, P. Mitochondrial  $\text{Ca}^{2+}$  Remodeling is a Prime Factor in Oncogenic Behavior. *Front. Oncol.* **2015**, *5*, 143. [[CrossRef](#)]
107. Koren, I.; Raviv, Z.; Shoshan-Barmatz, V. Downregulation of voltage-dependent anion channel-1 expression by RNA interference prevents cancer cell growth in vivo. *Cancer Biol. Ther.* **2010**, *9*, 1046–1052. [[CrossRef](#)]
108. Arif, T.; Krelm, Y.; Nakdimon, I.; Benharroch, D.; Paul, A.; Dadon-Klein, D.; Shoshan-Barmatz, V. VDAC1 is a molecular target in glioblastoma, with its depletion leading to reprogrammed metabolism and reversed oncogenic properties. *Neuro. Oncol.* **2017**, *19*, 951–964. [[CrossRef](#)]
109. Chaanine, A.H.; Gordon, R.E.; Kohlbrenner, E.; Benard, L.; Jeong, D.; Hajjar, R.J. Potential Role of BNIP3 in Cardiac Remodeling, Myocardial Stiffness, and Endoplasmic Reticulum. *Circ. Hear. Fail.* **2013**, *6*, 572–583. [[CrossRef](#)]
110. Pan, M.; Han, Y.; Basu, A.; Dai, A.; Si, R.; Willson, C.; Balistreri, A.; Scott, B.T.; Makino, A. Overexpression of hexokinase 2 reduces mitochondrial calcium overload in coronary endothelial cells of type 2 diabetic mice. *Am. J. Physiol. Physiol.* **2018**, *314*, C732–C740. [[CrossRef](#)]
111. Miyamae, M.; Camacho, S.A.; Weiner, M.W.; Figueredo, V.M. Attenuation of postischemic reperfusion injury is related to prevention of  $[\text{Ca}^{2+}]_m$  overload in rat hearts. *Am. J. Physiol.* **1996**. [[CrossRef](#)] [[PubMed](#)]
112. de J García-Rivas, G.; Carvajal, K.; Correa, F.; Zazueta, C. Ru360, a specific mitochondrial calcium uptake inhibitor, improves cardiac post-ischaemic functional recovery in rats in vivo. *Br. J. Pharmacol.* **2006**, *149*, 829–837. [[CrossRef](#)] [[PubMed](#)]
113. Liao, Z.; Liu, D.; Tang, L.; Yin, D.; Yin, S.; Lai, S.; Yao, J.; He, M. Long-term oral resveratrol intake provides nutritional preconditioning against myocardial ischemia/reperfusion injury: Involvement of VDAC1 downregulation. *Mol. Nutr. Food Res.* **2015**, *59*, 454–464. [[CrossRef](#)] [[PubMed](#)]
114. Gomez, L.; Thiebaut, P.-A.; Paillard, M.; Ducreux, S.; Abrial, M.; Crola Da Silva, C.; Durand, A.; Alam, M.R.; Van Coppenolle, F.; Sheu, S.-S.; et al. The SR/ER-mitochondria calcium crosstalk is regulated by GSK3 $\beta$  during reperfusion injury. *Cell Death Differ.* **2016**, *23*, 313–322. [[CrossRef](#)] [[PubMed](#)]
115. Rieusset, J.; Fauconnier, J.; Paillard, M.; Belaidi, E.; Tubbs, E.; Chauvin, M.-A.; Durand, A.; Bravard, A.; Teixeira, G.; Bartosch, B.; et al. Disruption of calcium transfer from ER to mitochondria links alterations of mitochondria-associated ER membrane integrity to hepatic insulin resistance. *Diabetologia* **2016**, *59*, 614–623. [[CrossRef](#)] [[PubMed](#)]
116. Thivolet, C.; Vial, G.; Cassel, R.; Rieusset, J.; Madec, A.-M. Reduction of endoplasmic reticulum- mitochondria interactions in beta cells from patients with type 2 diabetes. *PLoS ONE* **2017**, *12*, e0182027. [[CrossRef](#)]
117. Tubbs, E.; Chanon, S.; Bendridi, N.; Bidaux, G.; Chauvin, M.-A.; Ji-Cao, J.; Durand, C.; Gauvrit-Ramette, D.; Vidal, H.; et al. Disruption of Mitochondria-Associated Endoplasmic Reticulum Membrane (MAM) Integrity Contributes to Muscle Insulin Resistance in Mice and Humans. *Diabetes* **2018**, *67*, 636–650. [[CrossRef](#)] [[PubMed](#)]
118. Dia, M.; Gomez, L.; Thibault, H.; Tessier, N.; Leon, C.; Chouabe, C.; Ducreux, S.; Gallo-Bona, N.; Tubbs, E.; Bendridi, N.; et al. Reduced reticulum-mitochondria  $\text{Ca}^{2+}$  transfer is an early and reversible trigger of mitochondrial dysfunctions in diabetic cardiomyopathy. *Basic Res. Cardiol.* **2020**, *115*, 74. [[CrossRef](#)]
119. Joo, H.K.; Lee, Y.R.; Lim, S.Y.; Lee, E.J.; Choi, S.; Cho, E.J.; Park, M.S.; Ryoo, S.; Park, J.B.; Jeon, B.H. Peripheral benzodiazepine receptor regulates vascular endothelial activations via suppression of the voltage-dependent anion channel-1. *FEBS Lett.* **2012**, *586*, 1349–1355. [[CrossRef](#)]
120. Thai, P.N.; Daugherty, D.J.; Frederich, B.J.; Lu, X.; Deng, W.; Bers, D.M.; Dedkova, E.N.; Schaefer, S. Cardiac-specific Conditional Knockout of the 18-kDa Mitochondrial Translocator Protein Protects from Pressure Overload Induced Heart Failure. *Sci. Rep.* **2018**, *8*, 16213. [[CrossRef](#)]
121. Paillusson, S.; Stoica, R.; Gomez-Suaga, P.; Lau, D.H.W.; Mueller, S.; Miller, T.; Miller, C.C.J. There's Something Wrong with my MAM; the ER-Mitochondria Axis and Neurodegenerative Diseases. *Trends Neurosci.* **2016**, *39*, 146–157. [[CrossRef](#)]
122. Basso, V.; Marchesan, E.; Ziviani, E. A trio has turned into a quartet: DJ-1 interacts with the IP3R-Grp75-VDAC complex to control ER-mitochondria interaction. *Cell Calcium* **2020**, *87*, 102186. [[CrossRef](#)] [[PubMed](#)]
123. Wang, X.; Petrie, T.G.; Liu, Y.; Liu, J.; Fujioka, H.; Zhu, X. Parkinson's disease-associated DJ-1 mutations impair mitochondrial dynamics and cause mitochondrial dysfunction. *J. Neurochem.* **2012**, *121*, 830–839. [[CrossRef](#)] [[PubMed](#)]
124. Lee, S.; Wang, W.; Hwang, J.; Namgung, U.; Min, K.-T. Increased ER-mitochondria tethering promotes axon regeneration. *Proc. Natl. Acad. Sci. USA* **2019**, *116*, 16074–16079. [[CrossRef](#)] [[PubMed](#)]

## Acknowledgement

This dissertation was completed in the working group of PD PhD Johann Schredelseker at the Walther-Straub-Institute of Pharmacology and Toxicology at the faculty of medicine of the LMU Munich, headed by Prof. Thomas Gudermann.

Many people have supported my efforts without whose support this work would not have been feasible. At this point I would like to express my deepest appreciation to them.

Above all, I would like to express my special gratitude to Johann Schredelseker, who gave me the opportunity to do my research under his guidance and who has always supported and encouraged me and my work. Our journey over the past years, the shared ambitions and the exchange he made possible with other excellent researchers have greatly contributed to me becoming the scientist that I am today.

My special thank also goes to Thomas Gudermann, firstly for the opportunity to do my doctoral thesis at the Walther Straub Institute, but also for the continuously improving technical equipment during my time at the Institute, especially the acquisition of the confocal microscope and the support with our publications.

Without really good teamwork, many things would not have been possible and, above all, would have been less fun, which is why I would like to express my tremendous appreciation to the entire Schredelseker working group - especially to Fabiola Wilting, Anna Schedel, Kira Steinhorst and Brigitte Mayerhofer. But also I would like to sincerely thank all the other PhD students, technical assistants, Master's students and interns for our valuable work together.

Outside our working group, several other group leaders gave helpful advice, for which I would especially like to thank Annette Nicke and Andreas Breit at our institute. I would particularly like to thank the Nicke lab - especially Anna Durner and Yves Haufe, who were always there to give advice and support.

Outside our institute, I would like to thank our collaborative labs and partners - the Perocchi Lab at the Helmholtz Center in Munich, the Drakos Lab at the University of Utah, the Dendorfer Lab at the Walter Brendel Center in Munich, the Sedej Lab at the Medical University of Graz, the Hansen Lab at the UKE Hamburg and all other collaborative partners for their support with experimental as well as intellectual expertise.

At the end, because scientifically they have contributed absolutely nothing to my work, I would like to thank my friends and my family for the wonderful distractions, the endless support and the patience they gave me throughout the occasionally challenging time.